Phosphorylation and dephosphorylation regulate the Fanconi anaemia DNA repair pathway

DPhil Candidate: Di Yang

Supervisor: Associate Professor Martin Cohn

Brasenose College, Department of Biochemistry

Trinity 2021

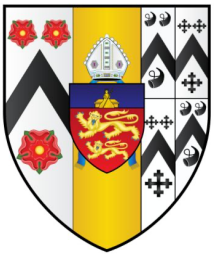

Acknowledgements

First of all, I would like to appreciate my family, especially my parents, for their unwavering support and encouragement throughout my academic journey. Without their love, dedication and sacrifice, I would not have been able to reach this milestone. I am immensely grateful for their financial support, which enabled me to pursue my studies without having to worry about living problem. From a young age, my parents instilled in me a deep appreciation for education and the value of hard work. They have always been my biggest “cheerleaders”, celebrating my successes and providing comfort, strength and emotional support during my struggles throughout the journey. To my dear parents, I cannot thank you enough for all that you have done for me. I hope this thesis is a small token of my gratitude for you, and I hope I have made both of you proud.

Secondly, I would like to sincerely appreciate my supervisor, Associate Professor Martin Cohn, for his guidance and support throughout my DPhil research. His expertise in the field helped me to navigate the challenges of my research and has been instrumental in my development as a PhD student. I am truly grateful for the time and effort he has invested in me throughout my DPhil journey!

I would like to express my deepest gratitude to my college advisor, Professor Elspeth Garman, who is truly an amazing lady that has provided me with invaluable support, encouragement and guidance. Although Elspeth is working in a different field, her willingness to lend an ear and her generosity to share her time, wise counsel and resources during my moments of uncertainty or doubt were a significant source of strength and reassurance. I appreciate her invaluable time and effort in shaping my thesis before the submission. Besides, her positive and lively personality outside the academic setting have impressed me as well! I have always enjoyed the college formals we had together, where her humour and positive energy would light up the room. I feel fortunate and blessed to have had the opportunity to get to know her.

Next, I would like to acknowledge and convey my boundless thanks to Dr David Lopez-Martinez, for his remarkable intellect and brilliant insights in creating the project that forms the basis of this DPhil thesis. I am particularly thankful for his unfailing patience and insight in answering my continuous stream of questions and providing me with careful trainings. From the very beginning of my DPhil study, David generously shared his precious time, extensive knowledge and expertise to offer me with the vital skills necessary to tackle complex research questions. Despite leaving the university during my second year, his exceptional talent and keen eye for details have inspired me throughout my DPhil studies, and I also feel incredibly fortunate to have had the opportunity to work with him.

Last but not least, I would like to extend my deepest appreciation to my lovely colleagues/friends, and a special thank you to my boyfriend, Dr. Li-Yao Huang. Your presence has made the long hours in the lab and the stressful moments of writing more pleasant with some laughter. I would like to thank Dr. Kelvin Yaprianto and Dr. Colette Lipp for the wonderful company and interesting discussions over the past years. You have made the time we spent together more enjoyable, and your contributions to our conversations have enriched my thinking and understanding. I am truly grateful for the opportunity to engage with such great colleagues like you and for the friendship we have developed. Previous lab members Dr. Anna Motnenko and Dr. Marian Kupculak, I appreciate all the things you have shown me. I am indebted for your willingness to share your knowledge and expertise. Especially Marian, thank you so much for popping up at my farewell, it was a big surprise! I would also like to thank Dr. Ai Murata, Fengxiang Bai, Hannan Xu, Sujun Li, Lily Cao, Xinhui Lan and Dr. Qiang Luo for your willingness to lend a hand when I needed it, I really appreciate your help and support during my professional journey.

Abstract

Interstrand crosslink (ICL) is a highly deleterious form of DNA damage as crosslinked DNA double strands block DNA replication, transcription machinery and prevent chromosome segregation. One of the major pathways for resolving DNA ICL damage is the Fanconi anaemia (FA) pathway, of which recruitment of the FANCD2/FANCI complex to sites of ICL damage is crucial for its repair by the FA pathway. The activity of FANCD2/FANCI complex is tightly regulated by post-translational modifications. Monoubiquitination of the FANCD2/FANCI complex lead to their retention on chromatin, which is essential for subsequent repair events to occur. However, it is believed that ubiquitination takes place after the recruitment of the FANCD2/FANCI complex to DNA, thus how recruitment of the complex is regulated still remain to be investigated. Our group reported a previously unknown kinase CK2 dependent phosphorylation event on FANCD2 at a six-residue cluster spanning from residue 882-898, which reduces the activity of FANCD2/FANCI complex, hence blocking subsequent events in the FA pathway. Phosphorylation of FANCD2 by CK2 restrains not only recruitment of FANCD2/FANCI complex to DNA but also FANCD2 monoubiquitination, pointing to an inhibitory effect on the function of the complex to prevent cells from spurious activation of repair in unperturbed conditions. We speculated that an unknown phosphatase may antagonize the effect of CK2 and promote the repairing function of FANCD2/FANCI complex during ICL repair. Here we identified one of the members belonging to the protein serine/threonine phosphatase PP2A family, PPP2R3A/PP2A, as the major phosphatase that specifically dephosphorylates and therefore activates CK2-phosphorylated FANCD2 during ICL repair. Silencing the catalytic activity of PPP2R3A/PP2A led to reduced recruitment and ubiquitination of FANCD2 upon induction of ICL damage. Importantly, cells lacking active PPP2R3A/PP2A displayed a deficient activation of the FA pathway, including increased sensitivity to ICL inducing reagent MMC. Our results describe a novel regulatory mechanism in which the function of FANCD2/FANCI complex is tightly regulated by the dynamic phosphorylation and dephosphorylation events mediated by CK2 and PP2A. In addition, PPP2R3A/PP2A that activates FANCD2 could serve as a potential druggable target to overcome

chemotherapy resistance to ICL inducing reagents such as cisplatin, as the major mechanism of developing drug resistance is via an over-activated FA pathway.

Table of Contents

Abbreviations

ALDH	aldehyde dehydrogenases
ALDH2	aldehyde dehydrogenase 2
Alt-EJ	alternative NHEJ
ATM	ataxia telangiectasia mutated
ATRIP	ATR-interacting protein
BER	base excision repair
BLM	bloom syndrome protein
BMF	bone marrow failure
BRCT	BRCA1 C-terminal repeat
BTR	BLM helicase-TopoisomeraseIIIα-RMI1-RMI2
Cal-A	calyculin A
CDK	cycle-dependent kinase
Cisplatin	cis-Diamminedichloroplatinum
CK2	casein Kinase 2
CPDs	cyclobutane pyrimidine dimers
CSB	cockayne syndrome protein B
CtIP	CtBP-interacting protein
cyro-EM	cryo-electron microscopy
DDR	DNA damage response
dHJ	double Holliday junction
D-loop	displacement loop
DNA-PKc	DNA-dependent protein kinase catalytic subunit
dRP	5’ -deoxyribosephosphate
DSBs	double strand breaks
ERCC1	excision repair cross-complementation group 1
EXO1	exonuclease 1
FA	Fanconi anaemia

FAAP100	FA-associated protein of 100
FAAP24	Fanconi anaemia core complex-associated protein 24
FACS	fluorescence-Activated Cell Sorting
FEN1	flap endonuclease 1
FHA	forkhead-associated
GG-NER	genome NER
HR	homologous recombination
HU	to hydroxyurea
ICLs	interstrand crosslink
LP-BER	long-patch BER
MDA	malondialdehyde
MLH	MutL homologue complex
MMC	mitomycin C
MMEJ	microhomology-mediated end joining’
MMR	mismatch repair
MMs	DNA mismatches
MRN	MRE11-RAD50-NBS1
MSH	MutS homologues complexes
NER	nucleotide excision repair
NHEJ	non-homologous end joining
NO	nitric oxide
OA	okadaic acid
OGG1	8-oxoguanine glycosylase 1
PARP1	poly (ADP-ribose) polymerase 1
PARylation	the poly (ADP-ribosyl) ation
PCNA	proliferating cell nuclear antigen
PME-1	PP2A methyl esterase 1
Pol β	polymerase β
Pol δ	polymerase δ

PPM	metal (Mg2+/Mn2+) dependent protein phosphatase
PPP	aspartate-based phosphatase and phosphoprotein phosphatase
PUVA	psoralen-UVA
6-4PPs	6-4 pyrimidine-pyrimidine dimers
RFC	replication factor C
RNA Pol II	RNA Polymerase II
ROS	reactive oxygen species
RPA	replication protein A
SP-BER	short-patch nucleotide BER
SSA	single strand annealing
SSBs	single strand breaks
ssDNA	single strand DNA
TC-NER	transcription-coupled NER
TFIIH	transcription initiation factor IIH
TLS	translesion DNA synthesis
TMP	4,5',8 trimethylpsoralen
UV	ultraviolet light
UV-DDB	UV-damage-binding proteins
UVSSA	UV-stimulated scaffold protein A
XLF	XRCC4-like factor
XRCC1	X-ray repair cross complementing 1
λPP	lambda protein phosphatase

Chapter 1. Introduction

1.1 DNA damage and repair pathways

1.1.1 Sources and types of DNA damage

The maintenance of genome integrity is vital for survival for all types of organisms. However, DNA in our genome is constantly under attack and highly susceptible to a myriad of endogenous and exogenous damaging factors, which account for a variety of different DNA lesions that potentially threaten the genome integrity. If left unattended, these errors might be converted to stable mutations that are incorporated into the genome DNA, and potentially give rise to deleterious double strand breaks (DSBs) that can lead to chromosomal rearrangement and cancer development. It has been estimated that spontaneous DNA damage arise 10^4–10^5 times per cell per day (Bont & Larebeke, 2004). To counteract this, cells have evolved to equip with intricate DNA damage response (DDR) and repair systems, which together ensure sufficient time to signal the presence and mediate the repair or tolerance of the DNA lesion by specific pathways.

Figure 1-1 summarises the endogenous and exogenous origins of representative types of DNA damage as well as the DNA repair pathways that are specifically involved (Figure 1-1, adapted from (Chatterjee & Walker, 2017). Most of endogenous DNA lesions come from inherent hydrolytic and oxidative reactions taking place between the DNA molecule with reactive oxygen species (ROS), reactive electrophiles that are generated as reaction intermediates or by-products during normal physiological processes such as aerobic metabolism in mitochondria (for example, superoxide $O_2^{\cdot -}$ and hydrogen peroxide H_2O_2) (Chatterjee & Walker, 2017; Marnett *et al*, 2003; Lin *et al*, 2019). Overload of these reactive species can cause a total of more than 100 different base lesions and modifications (Bjelland & Seeberg, 2003; Cadet *et al*, 2010). For example, 8-oxo-guanine and thymine glycol are two major types of oxidative base lesions that both have the potential to miscode and cause base transitions, adding mutational load to the whole genome (Figure 1-1) (Cheng *et al*, 1992;

Cathcart *et al*, 1984). In addition, not only DNA bases but also the backbone can be compromised by reactive radicals, which results in single strand breaks (SSBs) straight away that might turn into more deleterious DSBs if left unrepaired (Chatterjee & Walker, 2017; Lee *et al*, 2016). Other endogenous DNA damage originates from mutagenesis as a result of random replication errors induced by polymerases, spontaneous base deamination, abasic sites generation and DNA methylation. These events happen constantly at certain rates, burdening cells with potential inherent threats to the genome integrity.

On the other hand, exogenous DNA damage occurs when cells are exposed to environmental DNA damaging agents, typically UV and ionizing irradiation (IR), alkylating and aromatic compounds, and DNA crosslinking agents (Figure 1-1) (Chatterjee & Walker, 2017). Exposure to these external agents causes a plethora of different genomic lesions, from all kinds of base modifications to intra- and inter-strand crosslinks, as well as SSBs and DSBs (Figure 1-1) (Chatterjee & Walker, 2017; Vítor *et al*, 2020). Additionally, there are other external factors that can lead to an elevated level of intracellular ROS hence compromising DNA backbone and causing exogenous oxidative DNA damage; examples include tobacco smoke and heavy metals (Lin *et al*, 2019; Bhattacharyya *et al*, 2014). Among the exogenous threats, DNA crosslinking agents are a class of substance that can react with and covalently link two nucleotides of DNA together, forming highly toxic DNA crosslink lesions. Crosslinking can occur between nucleotides within the same strand (intrastrand crosslinks) or on opposite strands (interstrand crosslinks). However the latter forms are even more harmful to cells as they compromise DNA replication and transcription by preventing strand separation. The origins and repair of DNA interstrand crosslink (ICLs) will be discussed in more detail in Chapter 1.2.

DDR in response to DNA damage involves the instigation of DNA repair/tolerance pathways that are specifically activated by a particular type of lesion, allowing the removal of the damage in a substrate dependent manner. In mammalian cells, this comprehensive cellular response is mainly governed by three related kinases: ATM (ataxia telangiectasia mutated) that is recruited to DNA by the MRE11-RAD50-NBS1 (MRN) complex in response to DSB; ATR

(ATM and Rad3-related) recruited through ATRIP (ATR-interacting protein) to ssDNA and DNA-PKc (DNA-dependent protein kinase catalytic subunit), which is activated and recruited to DSBs by the protein Ku (Blackford & Jackson, 2017; Menolfi & Zha, 2020). At least seven DNA repair pathways have been identified: mismatch repair (MMR), base excision repair (BER), nucleotide excision repair (NER), DNA interstrand crosslink repair pathways – the NEIL3 and the Fanconi anaemia (FA) pathways, homologous recombination (HR) and non-homologous end joining (NHEJ). These repair pathways orchestrate to act as a safety guard to prevent cells from genetic instability. A dysregulated DDR is associated with elevated genome instability and mutagenesis, thereby promoting carcinogenesis. It has been found that DNA repair/tolerance pathways are highly disrupted in many cancer cell lines. Besides, failure in these processes is also linked to some neurodegenerative disorders and genetic diseases, such as FA caused by mutations in FA genes that mediate DNA ICL repair, which will be discussed in more detail in Chapter 1.2.

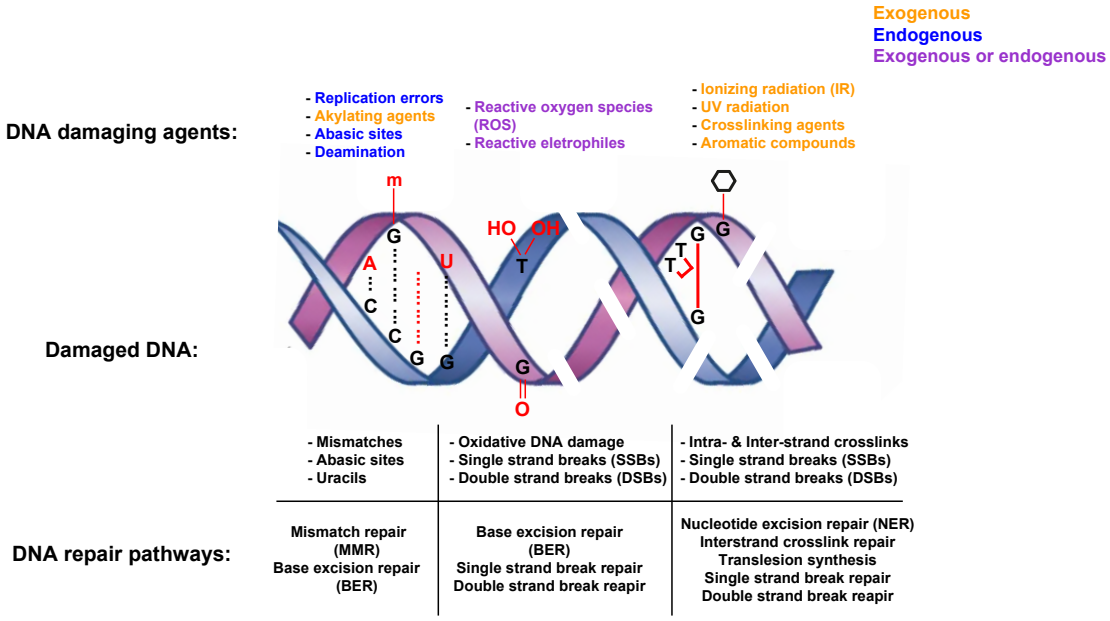

Figure 1-1 Schematic of the endogenous and exogenous origins of DNA damage and the DNA repair pathways involved. Plenty of factors can lead to different types of DNA damage, which provoke specific DNA repair pathways. DNA damaging agents are shown at the top panel: exogenous sourced in orange, endogenous sourced in blue, exogenous and endogenous sourced in purple. The middle panel shows representative DNA damage caused by corresponding damage agents. The bottom panel lists specific repair pathways triggered. Adapted from (Chatterjee & Walker, 2017).

1.1.2 Base excision repair (BER), mismatch repair (MMR) and nucleotide excision repair (NER)

Undesirable modifications to DNA bases resulting from oxidative DNA damage, alkylation reactions, base deamination and hydrolysis caused abasic sites are dealt by a highly conserved multienzyme DNA repair process, the BER pathway. There are at least 30 proteins involved in BER, which have been characterised into two sub-pathways according to the length of the repair patch; short-patch or one nucleotide BER (SP-BER) that only the single damaged base is removed; and long-patch BER (LP-BER) where 2-10 nucleotides are synthesised to displace the repair area (Grundy & Parsons, 2020; Beard *et al*, 2019). The first step of BER is the recognition and excision of the damaged base by a substrate specific glycosylase (Jacobs & Schär, 2012). In human cells, there are 11 DNA glycosylases identified and they can be categorised into three groups: monofunctional, bifunctional and endonuclease VIII-like (NEIL family) glycosylases (Grundy & Parsons, 2020). Monofunctional glycosylases, such as uracil DNA glycosylase (UNG), only excise out the damaged base and leave an apurinic/apyrimidinic (AP) site with non-cleaved phosphodiester backbone (Dizdaroglu *et al*, 2017). In contrast, bifunctional glycosylases associated with an AP-lyase activity, such as 8-oxoguanine glycosylase 1 (OGG1) not only remove the base but also introduce a nick to the phosphodiester bond on the 3' side of the damaged base via β-elimination, creating an SSB with a 3'-α, β-unsaturated aldehyde (Dizdaroglu *et al*, 2017; Parsons & Dianov, 2013). Additionally, NEIL DNA glycosylases can cleave on either side of the removed lesion via a β, δ-elimination reaction, giving rise to an SSB with a nucleotide gap and a phosphate group attached to both the 5'- and 3'- ends of the broken strand (Dizdaroglu *et al*, 2017; Grundy & Parsons, 2020; Wallace, 2013). Next, the enzyme apurinic/apyrimidinic endonuclease 1 (APE1) cleaves the DNA backbone on the 5' side to the AP created by monofunctional glycosylases, forming an SSB with a 5' -deoxyribosephosphate (dRP) and 3'-OH ends (Grundy & Parsons, 2020; Robson & Hickson, 1991; Demple *et al*, 1991); or removes the 3'-α, β-unsaturated aldehyde following β-elimination catalysed by bifunctional glycosylases and leaves a 3'-OH group (Chen *et al*, 1991;

Dizdaroglu *et al*, 2017). The 3'-P left by NEIL DNA glycosylases associated β, δ-elimination is removed by polynucleotide kinase phosphatase (PNKP) (Dizdaroglu *et al*, 2017; Wiederhold *et al*, 2003). Now the DNA is processed into a one nucleotide gap product suitable for DNA polymerase action. On the formation of an SSB, poly (ADP-ribose) polymerase 1 (PARP1) is engaged to catalyse the poly (ADP-ribosyl)ation (PARylation) of itself as well as other proteins such as histones (Woodhouse *et al*, 2008; Eustermann *et al*, 2011), which facilitate the recruitment of DNA repair proteins including a complex formed by X-ray repair cross complementing 1 (XRCC1), polymerase β (Pol β) and DNA Ligase III (Demin *et al*, 2021; Breslin *et al*, 2015). XRCC1 subsequently displaces PARP1 from the lesion therefore allowing the access of Pol β to the SSB, filling the one nucleotide gap and catalysing a lyase reaction to remove the 5'-dRP that might originate from APE1-mediated digestion (Grundy & Parsons, 2020; Matsumoto & Kim, 1995; Sobol *et al*, 1996). The repair process that only involves a single nucleotide extension is called short-patch BER (SP-BER), which is predominantly initiated by a bifunctional or NEIL DNA glycosylase (Fortini *et al*, 1999). However, there are occasions in which the 5' -dRP in the one nucleotide gap is rather a weaker substrate for the lyase activity for Pol β, such as adenylated dRP. Under these circumstances, either Pol β or other polymerases (e.g., Pol δ and Pol ε) will carry out gap filling with addition of nucleotides past the AP site and displace the adjacent strand by generating a polynucleotide overhang with the 5'-dRP residue attached (5' flap) (Beard *et al*, 2019; Sattler *et al*, 2003). To complete the BER, the 5'-flap overhang created during this repair mode is removed by flap endonuclease 1 (FEN1), ending up with a nick ready for DNA ligation (Lieber, 1997; Prasad *et al*, 2000). This sub-pathway is termed long-patch BER (LP-BER). Finally, the remaining nick is sealed by DNA Ligase I or XRCC1/DNA Ligase III complex (Beard *et al*, 2019; Parsons & Dianov, 2013; Wallace, 2014).

Another main source of genome instability arises from DNA mismatches (MMs) occurring during regular DNA replication when an incorrect base is incorporated into the newly synthesised strand. If left unrepaired, it can be converted to stable mutations that might alter normal cellular function and cause disease (Li, 2008; Ijsselsteijn *et al*, 2020). To avoid such deleterious consequence, cells have evolved to possess multiple repair pathways to deal with

DNA MMs, including the most crucial DNA mismatch repair (MMR) pathway. MMR corrects spontaneous base-base mispairs and small nucleotide insertion and deletions, contributing more than 100-fold to replication fidelity as it can correct the incorrect bases that are accidently added by replicative polymerases but which escaped proofreading (Fishel & Lee, 2016; Kunkel, 2004; Pećina-Šlaus *et al*, 2020). The DNA repair of mismatched bases is initiated by checking and recognising the lesion by two MutS homologues (MSH) complexes, named MSH2-MSH6 (MutSα) and MSH2-MSH3 (MutSβ) respectively (Pećina-Šlaus *et al*, 2020; Reyes *et al*, 2015). It has been shown that MSH6 is expressed 10 times more than MSH3 therefore the MutSα complex dominates in human cells. Upon loading to DNA, MSH complexes exchange their bound ADP to ATP and convert to a clamp that slides until it reaches the lesion, promoting the recruitment of the MutL homologue (MLH) complex that is endowed with endonuclease activity to the mismatched base (Brown *et al*, 2016; Liu *et al*, 2017). In human cells, the MLH protein involved in MMR is called MutLα which is a dimer consisting of MLH1 and PMS2. At the same time, other repairing factors such as proliferating cell nuclear antigen (PCNA), replication factor C (RFC) and exonuclease 1 (Exo1) are also recruited to the lesion, together introducing strand scission either 5' or 3' to the mismatch with the excision tract extending to non-specific area adjacent to the mismatched base and leading to an SSB (Martín-López & Fishel, 2013; Kolodner, 1996; Modrich & Lahue, 1996). After removal of the mismatch, MutLα physically interacts with DNA polymerase delta (Pol δ) and brings the enzyme to the site of nucleotide gap where the missing bases are re-synthesised (Prindle & Loeb, 2012). To finish up the MMR, the DNA strand is sealed by DNA ligase 1 (Fishel & Lee, 2016; Modrich & Lahue, 1996).

Nucleotide excision repair (NER) is the DNA repair pathway for removing helix-distorting bulky adducts, such as intra-strand crosslinks including thymidine dimers, cyclobutane pyrimidine dimers (CPDs) and 6-4 pyrimidine-pyrimidine dimers (6-4PPs) induced by ultraviolet light (UV), cisplatin and other toxins. Although the general process of NER is conserved through evolution, different proteins are employed to NER in prokaryotes and eukaryotes (Vaughn & Sancar, 2020; Sancar, 2016). In human cells, NER is classified into two

distinct mechanisms: the global genome NER (GG-NER) and the transcription-coupled NER (TC-NER). GG-NER is the transcription independent pathway that removes bulky adducts in non-transcribed regions, while TC-NER couples with DNA transcription and repairs lesions present on the transcribed strand in active genes (Leyns & Gonzalez, 2012). In the case of GG-NER, repair is initiated with damage recognition XPC-HR23B and UV-damage-binding proteins (UV-DDB) complexes (Kusakabe *et al*, 2019; Marteijn *et al*, 2014). Whereas in TC-NER, repair is triggered by stalling of RNA Polymerase II (RNA Pol II) that stabilise the transient interaction with several proteins including Cockayne syndrome protein B (CSB), Cockayne syndrome WD repeat protein A (CSA), UV-stimulated scaffold protein A (UVSSA) and ubiquitin specific processing protease 7 (USP7) (Marteijn *et al*, 2014; Lans *et al*, 2019). In both cases, transcription initiation factor IIH (TFIIH) complex, XPA and replication protein A (RPA) are recruited to the lesion to conduct further verifications, promoting the loading of the XPF and excision repair cross-complementation group 1 (ERCC1) complex (XPF/ERCC1) (Schärer, 2013). XPG is subsequently recruited through the interaction to TFIIH, facilitating the endonuclease activity of XPF/ERCC1. Next, XPF/ERCC1 make the incision at the 5' side and XPG induces another one 3' downstream of the lesion, then the single strand gap is filled by DNA polymerase δ ε and κ. The nick left after DNA polymerisation is sealed by XRCC1/DNA Ligase III or DNA ligase I (Leyns & Gonzalez, 2012; Spivak, 2015; Fousteri & Mullenders, 2008).

1.1.3 Double strand break (DSB) repair: non-homologous end joining (NHEJ) and homologous recombination (HR)

DSBs are less common however the most cytotoxic DNA lesion, they arise as a result of a direct exposure to IR, strand attack by ROS or SSBs induced to two separate but close points on opposite strands (e.g., consequence of the attempted repair of UV radiation-induced base damage). They pose an immediate threat to genome stability as they might provoke chromosomal rearrangements, jeopardising chromosomal structure and function (Scully *et al*,

2019; Vítor *et al*, 2020). Therefore, repair of DSBs requires the triggering of even more sophisticated cellular damage responses and repair pathways. DSBs are mainly removed by two principal mechanisms, depending on whether the homologous DNA strand is used as the template for repair or not: 'classical' non-homologous end-joining (cNHEJ) and homologous recombination (HR). Besides, additional pathways of DSB repair are also recognised, including microhomology-mediated end joining' (MMEJ), synonymously with alternative NHEJ (Alt-EJ) as well single strand annealing (SSA).

cNHEJ is able to join the two ends of DSB together without utilising a homologous strand as the template, which operates throughout the vertebrate cell cycle (Rothkamm *et al*, 2003). DSBs can be fast and efficiently repaired by this mechanism, however it tends to be error prone as small base deletions or insertions are likely to be introduced into the break point. Occasionally, two irrelevant DSBs from different chromosomes can be accidently joined together during cNHEJ, leading to chromosomal rearrangements that may cause cancer (Ghezraoui *et al*, 2014; Scully *et al*, 2019). cNHEJ starts with recognition and protection of the free ends by the protein Ku (Ku70 and Ku80) heterodimer, which prevents end resection favouring HR and also serve as a scaffold for other repairing factors, including the DNA-dependent protein kinase catalytic subunit (DNA-PKcs), DNA Ligase IV and the associated scaffolding factors XRCC4, XRCC4-like factor (XLF) and paralogues of XRCC4 and XLF (PAXX) (McElhinny *et al*, 2000; Ahnesorg *et al*, 2006). XRCC4 in complex with Ligase IV is required for its activity and stability, while XLF and PAXX lie redundant scaffolding functions (Zha *et al*, 2011; Kumar *et al*, 2016). The two free ends are brought in proximity and closely aligned by a synaptic reaction requiring the kinase activity of DNA-PKcs and the presence of XLF (Blackford & Jackson, 2017). Several proteins participate in the end-processing prior to end-joining, including the endonuclease Artemis that is recruited and phosphorylated by DNA-PKcs, which ensures the capability of the two DSB ends (Stinson *et al*, 2020). With the support of XLF and PAXX, the two free ends of DSB are finally ligated by XRCC4/Ligase IV (Lescale *et al*, 2016).

Unlike cNHEJ which occurs throughout the cell cycle, HR is mainly restricted to the S

and G2 phases of the cell cycle due to the regulation of the DSB pathway choice by 5' end resection. In S and G2 phase, the MRE11/RAD50/NBS1 (MRN) complex is activated by increased activity of cell cycle-dependent kinase (CDK) and recruited to the free ends of DSB breaks. At the same time, the multi-functional DNA damage signalling kinase ATM is employed by the MRN complex, and it phosphorylates a variety of downstream proteins including the DSB-associated histone H2AX. Phosphorylated H2AX is named γH2AX, which is a hallmark of DSB activated DDR. γH2AX, together with other proteins recruited, employs the E3 ligase RNF168, which can monoubiquitinate the lysine 13 or 15 on H2A and lead to the formation of mUb-H2A (Scully & Xie, 2013; Ciccia & Elledge, 2010). The BRCA-P complex, which comprises of BRCA1, BARD1, PALB2, BRCA2, and RAD51, is recruited by mUb-H2A and accumulates at the site of DSB. Local accumulation of the BRCA-P complex has been implicated in a crucial role in DSB repair pathway choice. BRCA1 within the BRCA-P complex activates the CtBP-interacting protein (CtIP) that is recruited to the lesion in an MRN and ATM-dependent manner, and CtIP activates the nuclease activity of MRE11 within the MRN complex to stimulate end resection (Scully *et al*, 2019; Ciccia & Elledge, 2010). In addition to mUb-H2A, another transient marker, the unmethylated lysine 20 on histone H4 (H4K20me0), has also been identified to recruit the BRCA-P complex (via interaction between H4K20me0 and BARD1). As H4K20me0 is only present on newly replicated DNA strands, it adds another layer of regulation to ensure that end resection dependent HR is favoured within the S and G2 (Saredi *et al*, 2016; Becker *et al*, 2021). MRE11 activated by CtIP subsequently initiates a "short-range" end resection by employing its 3′–5′ exonuclease activity (Limbo *et al*, 2007; Sartori *et al*, 2007). This initial resection process results in the formation of a short 3' overhang, which is thought to facilitate the displacement of the Ku70–Ku80 complex from the DSB ends (Langerak *et al*, 2011). The "short-range" resection is then converted to a "long-range" resection where more enzymes, including EXO1, helicase Bloom syndrome protein (BLM) and endonuclease DNA2 are employed to further progress the strand digestion in the 5' to 3' direction, extending the 3' single stranded overhang for strand invasion (Mimitou & Symington, 2008; Nimonkar *et al*, 2011; Daley *et al*, 2017). The single-stranded overhang is rapidly coated with the ssDNA binding heterotrimeric complex replication protein A (RPA), which is subsequently exchanged

for the recombinase RAD51 in the presence of the recombination mediator BRCA2 (Scully *et al*, 2019; Yang *et al*, 2005). RAD51-bound ssDNA, which is named as RAD51 nucleoprotein filament, now mediates the homology search by invading the sister chromatid duplex DNA and promoting base-pairing with the complementary homologous DNA sequences. After locating the homologous sequence, the 3' end of the invading strand extends using the complementary sequence as template and a displacement loop (D-loop) intermediate structure is formed when the other strand of the invaded molecule is displaced (Heijden *et al*, 2008; Trenner & Sartori, 2019). Capturing the 3' overhang of the second DNA end by the displaced ssDNA of the D-loop followed by more DNA synthesis result in the formation of another intermediate structure, termed double Holliday junction (dHJ), which are resolved by BLM helicase-TopoisomeraseIIIα-RMI1-RMI2 (BTR) complex or specific nucleases such as the SLX1-SLX4-MUS81-EME1 (SLX-MUS) complex in either a cross-over that involves exchange of genetic information between the two sister chromatids, or a non-cross manner (Punatar *et al*, 2017; Wyatt *et al*, 2013; Castor *et al*, 2013).

Importantly, the choice of DNA repair between the error-prone cNHEJ and error-free HR pathways is highly dependent on cell cycle and regulated by two key effectors: 53BP1 in cNHEJ and BRCA1 in HR. In G1 phase, the recruitment of 53BP1 to sites of DNA damage promotes cNHEJ while antagonizes the recruitment of BRCA1 by binding to a G1-specfic histone modification (H4K20me2/3) and the DNA damage-induced H2AK15Ub marker. In the contrast, during S and G2 phase, BRCA1-BARD1 complex removes 53BP1 at DNA damage sites to direct HR by binding to a post replication histone modification (H4K20me0) and DNA damage-induced H2AK15Ub marker (Nakamura *et al*, 2019; Becker *et al*, 2021)

In addition to the cNHEJ and HR there are several DSB repair pathways have been identified. Alternative NHEJ (Alt-EJ), which is a PARP-1 dependent error-prone NHEJ pathway that repairs DSBs when cNHEJ is not functional. Alt-EJ involves the using of a short microhomology region at the two ends of the breakpoint exposed by CtIP-activated MRN mediated end resection, therefore the pathway is also termed microhomology-mediated end

joining (MMEJ) (Yan *et al*, 2007; Ranjha *et al*, 2018). Another DSB repair pathway identified recently is single strand annealing (SSA), which is similar to Alt-EJ yet it requires a more extensive resection catalysed by nucleases, such as EXO1, to expose a longer homology region that is usually longer than 25bp. Annealing of the complementary single strand DNA ends in SSA is directed by Rad51 and Rad52, while in Alt-EJ the shorter microhomology region is annealed by DNA polymerase θ (Pol θ) (Bhargava *et al*, 2016).

1.2 DNA interstrand crosslink (ICL) repair

1.2.1 Origin of ICLs

As was mentioned in section 1.1.1, DNA ICLs are highly cytotoxic lesions that covalently join the two strands of the DNA double helix together. Defective ICL repair compromises DNA replication and transcription as it prevents strand separation, which might give rise to devastating outcomes such as bone marrow failure linked diseases like FA, or cancer predisposition syndromes. ICLs can be introduced by both exogenous and endogenous agents. In fact, exogenous ICL inducing agents have been widely used as therapeutic anticancer and chemotherapeutic drugs due to their extremely high cytotoxicity. They may kill cancer cells by damaging their DNA and stopping them from dividing. They can react with DNA at specific sequences and generate various DNA lesions, including DNA mono-adducts, intrastrand crosslinks and ICLs, which distort the double helix to different extent by introducing a bend and twist in the helical structure (Muniandy *et al*, 2009). The chemical structure of the main crosslinking agents and the ICLs they form are summarised in Figure 1-2 (adapted from Lopez-Martinez *et al*, 2016).

Nitrogen mustards, such as cyclophosphamide and chlorambucil, are the earliest small bifunctional alkylating compounds identified and synthesised. They usually react with the N7 of guanine, although reactions with the N3 and N7 atoms of adenine have also been

documented (Balcome *et al*, 2004). However, nitrogen mustards only give rise to 5% ICL products (95% DNA monoadduct) when reacting with DNA, and introduce an unwinding of 2-6° plus a bend of 10° to the double helix (Figure 1-2 A) (Semlow & Walter, 2021; Lopez-Martinez *et al*, 2019; Lopez-Martinez, 2018). Mitomycin C (MMC), a natural present compound produced by the actinobacteria *Streptomyces caespitosus*, has been widely used in the clinic as a chemotherapeutic drug and a laboratory cross-linking agent (Muniandy *et al*, 2009). This compound must be enzymatically reduced at its quinone ring by oxidoreductases *in vivo* before it reacts with the N2 exocyclic amine of the two guanines in the sequence CG at 5'CpG sites, yielding either a monoadduct in the minor groove or an ICL (Figure 1-2 B) (Sartorelli *et al*, 1994; Warren *et al*, 1998). Lesions introduced by MMC only impose minimal disruption on the DNA duplex with no bending or twist (Rink *et al*, 1996). Another ICL inducing compound that has received extensive use in chemotherapy is cis-Diamminedichloroplatinum (cisplatin), with great success against testicular cancer (Muniandy *et al*, 2009). Cisplatin is activated with the displacement of the two chloride ligands by water molecules, to form the active form $[Pt(NH3)_2(H2O)_2]^{2+}$ that is able to react with a variety of cellular components from proteins and phospholipids to RNA and DNA. The major types of DNA lesions formed by cisplatin are ~65% intrastrand crosslinks occurring at GpG and ~25% at ApG sites. ICLs only occur at a much lower rate (5% - 8%) between N7 of the two guanines at GpC sites (Figure 1-2 C) (Jamieson & Lippard, 1999; Ghosh, 2019). Unlike nitrogen mustards and MMC, cisplatin induces a significant disruption to the DNA helix with an unwinding of 110° and a bending of 47° towards the DNA minor groove. The two cytosines within the GpC sites are both extruded out and point away from the helix axis after modified by cisplatin, due to the large distortion (Malinge *et al*, 1994; Coste *et al*, 1999). Another type of crosslinking agents is psoralens, which are a group of natural chemicals isolated from some plants and fungi (Cimino *et al*, 1985). They are hydrophobic tricyclic planar molecules therefore can access nuclear DNA and intercalate the DNA bases easily by getting across the plasma membrane, yet their reactions with DNA require photoactivation by exposure to UVA (320–400 nm light). In fact, psoralen-UVA (PUVA) therapy is treated as the first-line phototherapy for patients with psoriasis (Grundmann-Kollmann *et al*, 2004). They preferentially intercalate into the sequence TA and form covalent bonds

between the two thymidines, giving rise to a more significant proportion of ICLs (around 40%) compared to other crosslinking agents (Lopez-Martinez *et al*, 2016). Either the furan or pyrone ring within the psoralen molecule react with the thymidine to form a furan or a pyrone monoadduct. Unlike the pyrone monoadduct that is unable to react further, the furan monoadduct may react with the other thymine on the opposite strand and form a crosslink. 4,5',8 trimethylpsoralen (TMP), which is extensively used in this study, is modified to largely favour crosslink formation and it can give rise to 98% ICLs (Huang *et al*, 2013; Lopez-Martinez *et al*, 2019). Generally, psoralen crosslinked DNA molecule is not bent and unwinds only at a minor degree around 25° (Figure 1-2 D).

More importantly, endogenous by-products of metabolic processes also induce ICLs, which suggests ICLs can be generated intrinsically and might explain the reason that cells have evolved to equip with complex repair mechanisms to combat with these toxic lesions. Reactive aldehydes are one of the major sources of endogenous DNA crosslinks. Despite massive efforts have been input to identify intrinsic source of DNA crosslinks, di(N2-guanosyl) methane cross-link formed by the endogenous metabolic by-product of purine and amino acid synthesis, formaldehyde, is the only endogenous ICL reported to be detected in tissues (Semlow & Walter, 2021; Lu *et al*, 2010). A recent study defined an excision-independent repair pathway specifically dealing with ICLs caused by the endogenous and alcohol-derived metabolite, acetaldehyde, in *Xenopus* egg extract (Hodskinson *et al*, 2020). In fact, acetaldehyde has been suggested as a main source of endogenous ICL DNA damage, despite that it can be efficiently processed into non-toxic carboxylic acids by aldehyde dehydrogenases (ALDH). In addition, other metabolic aldehyde by-products such as malondialdehyde (MDA) and crotonaldehyde produced during lipid peroxidation have also been shown to induce endogenous ICLs (Semlow & Walter, 2021; Langevin *et al*, 2011; Pang & Andreassen, 2009). Aldehydes induced ICLs are generally formed in CpG sequences via targeting guanine, and they are located in the minor groove with no disruption of the Watson–Crick helix (Figure 1-2 E) (Cho *et al*, 2007). Endogenously generated nitric oxide (NO) is another potential source of ICL. Similarly, the reaction happens between two guanines within the CpG sequence (Figure 1-2 F) without introducing significant distortion to the DNA structure.

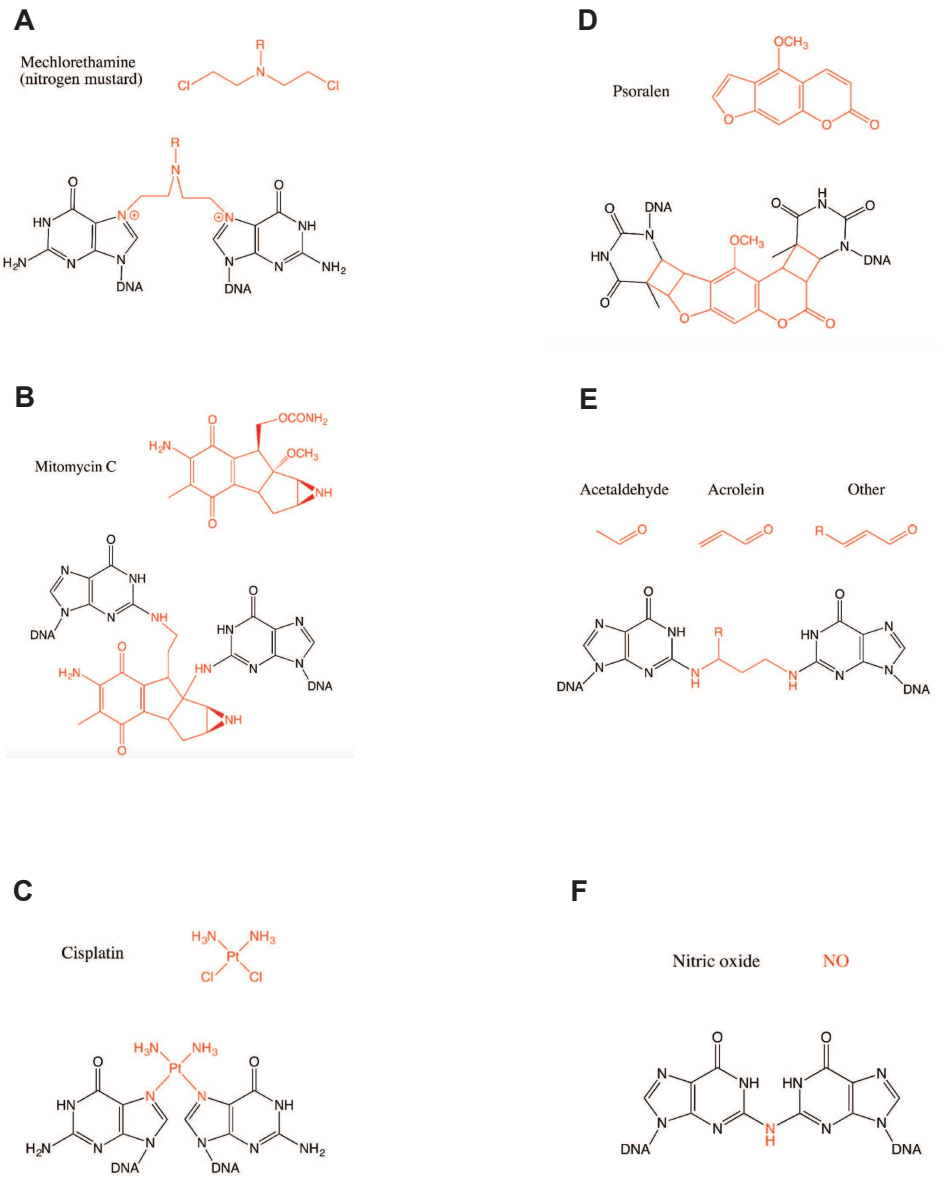

Figure 1-2 Chemical structures of common crosslinking agents and the ICLs they create. (A) Mechlorethamine (example of nitrogen mustard). (B) Mitomycin C. (C) Cisplatin. (D) Psoralen. (E) Aldehydes (acetaldehyde, acrolein and others). (F) Nitric oxide. Crosslinking agents are drawn in red. Adapted from Lopez-Martinez *et al*, 2016.

1.2.2 Fanconi anaemia (FA), replication dependent ICL repair and the FA pathway

FA is a rare autosomal recessive disease affecting around 1 in 200,000 to 400,000 people in the general population (Dong *et al*, 2015). Although it can affect and induce abnormities to multiple body systems including the skin, hematologic, urogenital and central nervous systems, FA is characterised by the most common symptom: early bone marrow failure (BMF), which usually leads to aplastic anaemia (Moreno *et al*, 2021; Lopez-Martinez *et al*, 2016). The patients are prone to develop various type of cancers, especially acute myelogenous leukaemia (AML). However, later they were found to be highly susceptible to chemotherapeutic drugs. Indeed, FA patient derived hematopoietic stem cells are hypersensitive to ICL-forming agents such as MMC, and this phenotype has been used to diagnose FA for more than two decades (Moreno *et al*, 2021; Auerbach, 2009). The FA-associated BMF phenotype has been suggested to be driven by the accumulation of endogenously produced aldehydes, as loss of the aldehyde-catalysing enzyme aldehyde dehydrogenase 2 (*ALDH2*) gene together with *FANCD2* have been linked to the occurrence of severe BMF in mouse models (Garaycoechea *et al*, 2012; Hodskinson *et al*, 2020). Nevertheless, the root cause of FA phenotypes still remains controversial and needs to be investigated further, as most of the FA patients do possess normal aldehydes metabolism except a small group of Japanese patients carrying mutated *ALDH2*, and there has not been clear evidence demonstrating that ICLs are accumulated in FA patient derived cells (Hira *et al*, 2013).

ICLs are prone to induce replication fork stalling that can impede DNA replication and lead to a catastrophic result; it is therefore not surprising that stalled DNA replication forks facilitate ICL repair. The majority of ICL repair pathways identified are DNA replication-dependent - including the FA pathway, NEIL3 pathway and the recently discovered alcohol-derived ICL repair pathway (Figure 1-3) (Amunugama & Walter, 2020). Activation of all of the three pathways requires a convergence of the two replication forks at the ICL lesion. The NEIL3

and the alcohol-derived pathways are both DNA incision independent. Specifically, after the two replication forks encounter and undergo convergence at the ICL lesion, the glycosylase NEIL3, or a still unknown protein that is involved in the alcohol-derived pathway, is recruited to the damage site. Recruited NEIL3 unhooks the ICL by inducing a cleavage event around one of the two N-glycosyl bonds forming the crosslink (Semlow *et al*, 2016), while the unknown protein involved in the alcohol-derived pathway incises the bond formed between one of the two bases and the ICL (Hodskinson *et al*, 2020) generating either an AP site (NEIL3 pathway) or an SSB (alcohol-derived pathway), as well as a nucleotide adduct that are subsequently processed by related downstream pathways (Figure 1-3). Nevertheless, the FA pathway involves incision of the phosphodiester backbone adjacent to the lesion and hence creating a double-strand break intermediate (Figure 1-3), potentially leading to chromosomal translocations and other genome instabilities.

In *Xenopus* and mammalian cells, the newly identified pathway is specifically activated by acetaldehyde induced ICLs. The 33 pathway is the choice for the repair of psoralen and AP ICLs, while the FA pathway can repair any ICLs, including MMC and cisplatin induced ICLs, that cannot be removed by NEIL3 (Li *et al*, 2020; Hodskinson *et al*, 2020; Amunugama & Walter, 2020; Hoogenboom *et al*, 2017). In other words, the NEIL3 pathway is favoured over the FA pathway during ICL repair. In fact, the choice between the NEIL3 and FA pathway is regulated by the E3 ligase TRAIP (Wu *et al*, 2019; Amunugama & Walter, 2020). DNA helicase CMG (the complex of CDC45, MCM2–7 and GINS) stalled by ICL can be ubiquitinated by TRAIP and short ubiquitination chains on CMG are sufficient to recruit NEIL3, which is capable of unhooking the ICL in the presence of CMG (Semlow *et al*, 2016). If it encounters ICL that cannot be processed – as in the case of cisplatin ICLs, the ubiquitination chains continue to grow which facilitates the unloading of CMG helicase by the p97 ATPase, allowing processing the ICL by the FA pathway (Wu *et al*, 2019; Räschle *et al*, 2008; Fullbright *et al*, 2016). On the other hand, replication independent ICL repair must take place outside of S phase to maintain genome integrity in non-dividing cells, such as neurons. ICLs can be recognised and removed by the NER protein XPC and XPF/ERCC1, or the MMR factor MutSα/MutLα in the absence of

replication fork (Bessho *et al*, 1997; Kato *et al*, 2017). Translesion DNA synthesis (TLS) and gap filling machinery involving the DNA polymerase κ and ζ are subsequently carried out to fill the single-stranded gap resulting from NER or MMR mediated ICL removal (Roy & Schärer, 2016; Williams *et al*, 2012).

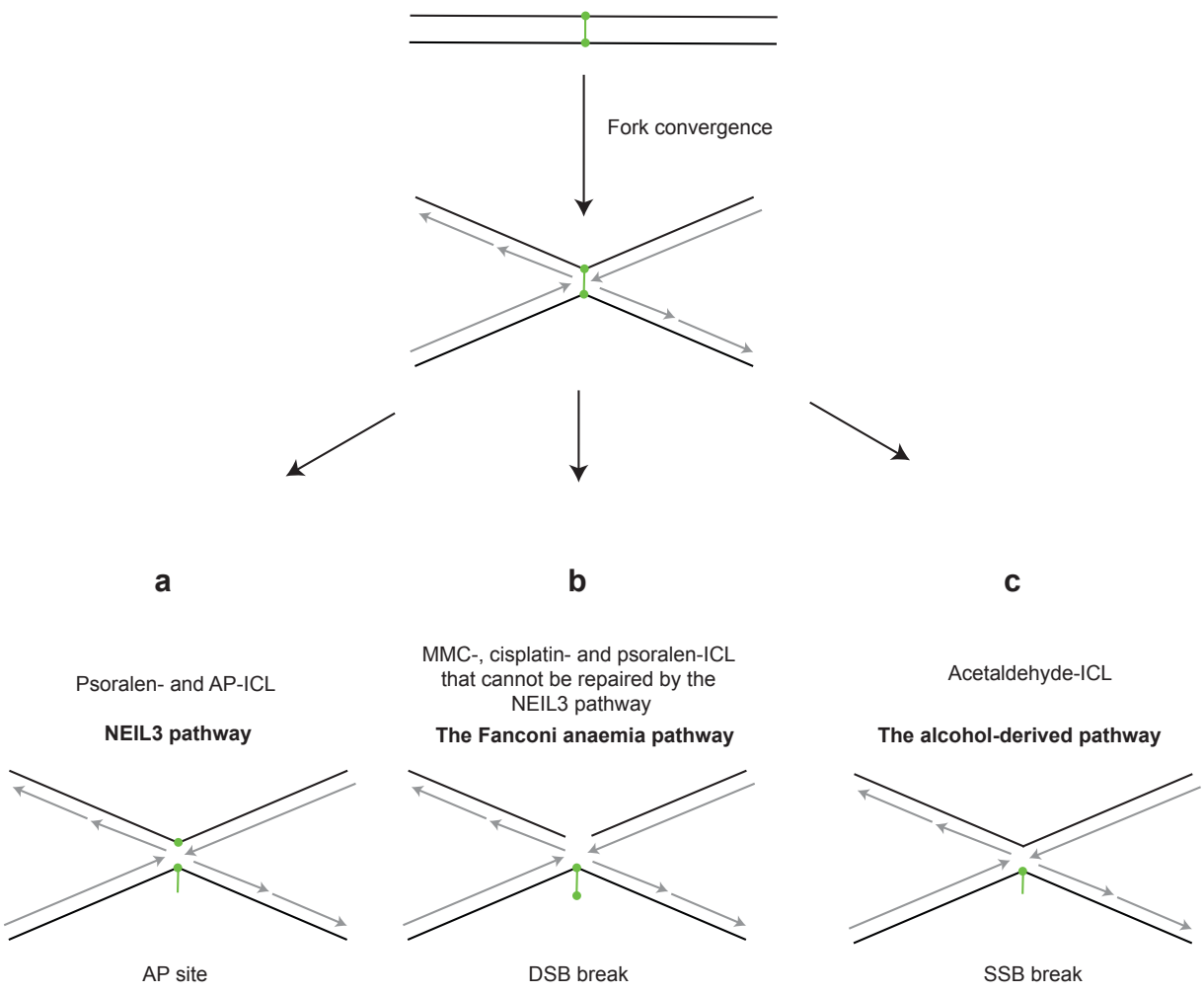

Figure 1-3 DNA replication dependent ICL repair pathways. a Psoralen and AP induced ICLs are repaired by the NEIL3 pathway which incises around the glycosyl bond forming the ICL, creating an AP site and an ICL adduct in each strand respectively. **b** The FA pathway deals with MMC, cisplatin induced and psoralen induced ICLs that cannot be fixed by the NEIL3 pathway through dual incisions in the phosphodiester backbone on one of the strands, therefore resulting in a DSB. **c** Acetaldehyde ICLs, which are usually formed between two guanines are removed by a newly discovered repair pathway (Hodskinson *et al*, 2020). After cleavage it generates a guanine in one strand and a propanoguanine in the other strand. Adapted from (Amunugama & Walter, 2020).

To date, there are 22 genes whose mutations have been associated with FA disease, which can be classified into 4 functional groups (Table 1-1) (Semlow & Walter, 2021; Wang & Smogorzewska, 2015). The first step of the FA pathway is detection of the ICL lesion, which was initially found to be associated with the first group protein, the ATPase FANCM, as well as its interacting partners, Fanconi anaemia core complex-associated protein 24 (FAAP24) and the histone fold proteins MHF1 and MHF2 (Figure 1-4, 1) (Basbous & Constantinou, 2019; Ciccia *et al*, 2007; Wang *et al*, 2013; Singh *et al*, 2010). The FANCM/FAAP24 or FANCM/MHF1/MHF2 complexes display high affinity towards branched DNA structures, and are therefore recruited to protect the replication fork stalled at the ICL lesion (Gari *et al*, 2008a, 2008b). Besides, FANCM can also drive fork traverse through the ICL when the second replication fork is absent, which actually accounts for 60% of the total fork stalling events (Figure 1-4, 1) (Liang *et al*, 2016; Huang *et al*, 2013; Yan *et al*, 2010b; Zhao *et al*, 2014). Notably, despite its important role played in replication fork protection and traverse, whether it recognises the stalled replication fork or the ICL independently of replication still remain unclear. In fact, its defection just weakly correlates with FA phenotypes as only a minor group of the FA patients carry mutated FANCM (Table 1-1, 0.1%). It turned out later that the patient who carried the original FANCM mutations was apparently also FANCA deficient (Singh *et al*, 2009), so the status of it being a FA gene has been questioned and is still controversial. Additionally, the non-FA protein UHRF1 and UHRF2, were recently reported to be ICL sensors whose recruitments are required for efficient FANCD2 accumulation at the ICL lesion (Figure 1-4, 2) (Alcón *et al*, 2020; Liang *et al*, 2015; Motnenko *et al*, 2018; Tian *et al*, 2015).

Our current understanding of ICL repair comes from research widely carried out in an *in vitro* cell free system based on *Xenopus* egg extract where the mechanism of ICL repair has been studied in a replication dependent manner (Räschle *et al*, 2008; Knipscheer *et al*, 2012). In this system, a single ICL is introduced to a plasmid that has been designed to allow each repair step of that single ICL to be monitored specifically. Using this setup, it was found that the two replication forks converge at the damage site when encounter the ICL (Zhang *et al*, 2015), and the CMG helicase is unloaded from DNA due to TRAIP mediated poly-ubiquitination

(Figure 1-4, 3) (Wu *et al*, 2019). In addition, one of the replication forks might undergo fork reversal, although further research is required to conclude the mechanical significance of this step. The second and third group proteins, FANCD2/FANCI complex and the FA core complex - which is a large E3 ligase, are subsequently recruited to the chromatin upon fork convergence and CMG unloading (Table 1-1, Figure 1-4, 4). The FA core complex is a megadalton multiprotein that comprises two copies of a central core structure of FANCB and FA-associated protein of 100 kDa (FAAP100), flanked by two copies of the E3 ligase FANCL that mediates the monoubiquitination of FANCD2 and FANCI respectively together with UBE2T (FANCT). The remaining six subunits, FANCA, C, E, F, G and FAAP20 assemble to the core structure, giving rise to an extended asymmetric structure (Shakeel *et al*, 2019; Wang *et al*, 2021). Although subunits in the FA core complex account for around 85% of patient mutants (FANCA 64 %, FANCC 12 %, FANCG 8 % and etc.), the exact functions of each subunit other than FANCL still remain to be investigated (Wang & Smogorzewska, 2015).

Importantly, monoubiquitination of FANCD2/FANCI by the FA core complex is the keystone and is indispensable for the activation of the FA pathway. FANCD2 itself is unable to interact with DNA. It interacts with FANCI, giving rise to a heterodimer that does interact with DNA (Alcón *et al*, 2020). Several studies performed *in vitro* suggest that the monoubiquitination reaction is largely enhanced by addition of DNA, which points to the reaction takes place on chromatin after the complex is recruited (Sato *et al*, 2012; Longerich *et al*, 2014; Twest *et al*, 2017). Recently one of our colleagues reported a group of previously unknown serine/threonine kinase Casein Kinase 2 (CK2) dependent phosphorylation events happening on FANCD2, which keep the FANCD2/FANCI complex away from chromatin by lowering its affinity for DNA in the absence of ICL damage (Lopez-Martinez *et al*, 2019; Lopez-Martinez, 2018). In theory, FANCD2 needs to be dephosphorylated by a still unidentified phosphatase before being recruited to chromatin where it gets monoubiquitinated (Figure 1-4, 5).

Monoubiquitination of FANCD2/FANCI is promoted by ATR and also other kinases such

as Chk1, and it locks the complex on chromatin by converting it into a sliding clamp that can slide away from the initial site of ICL, allowing the act-on of downstream repair factors (Figure 1-4, 6) (Alcón *et al*, 2020; Wang *et al*, 2020; Park *et al*, 2005; Tan *et al*, 2020; Rennie *et al*, 2020). Monoubiquitinated FANCD2/FANCI subsequently recruits members in group 4, including the scaffolding protein SLX4 (FANCP), nucleases such as XPF(FANCQ)/ERCC1, as well as other components involved in HR repair: BRCA2 (FANCD1), BRCA1 (FANCS), RAD51C (FANCO), RAD51 (FANCR), XRCC2 (FANCU), PALB2 (FANCN), RFWD3 (FANCW) and BRIP1 (FANCJ) (Table 1-1). XPF/ERCC1 together with the scaffolding protein SLX4 unhook the ICL lesion by incising around the proximity, leading to a DSB and an SSB with the unhooked ICL adduct attached (Figure 1-4, 7) (Yuan *et al*, 2009; Klein Douwel *et al*, 2014; Douwel *et al*, 2017; Yamamoto *et al*, 2011). TLS, then bypass the ICL adduct via the action of Rev1 and Rev7 (FANCV) associated Pol ζ, who are capable to fill the ICL adduct containing gap for their ability to accommodate bulky DNA (Figure 1-4, 8) (Bezalel-Buch *et al*, 2020; Budzowska *et al*, 2015; Garcia-Higuera *et al*, 2001). The DSB ends are resected by nucleases such as CtIP, EXO1 and DNA2 recruited by FANCD2 (Figure 1-4, 8) and subsequently subjected to RAD51-directed HR (Figure 1-4, 9-11) (Yamamoto *et al*, 2011; Klein Douwel *et al*, 2014; Douwel *et al*, 2017; Murina *et al*, 2014; Unno *et al*, 2014; Roques *et al*, 2009). Strand invasion mediated by RAD51 is followed by resolution of the Holliday junction proceed by the SLX4/SLX1/MUS81 complex, and finally the remaining ICL adduct is removed by BER or NER (Kuraoka *et al*, 2000; Mouw & D'Andrea, 2014; Wood, 2010; Slyskova *et al*, 2018; Zheng *et al*, 2003). After the repair is finished, the FANCD2/FANCI clamp is deubiquitinated by USP1/UAF1 to be able to dissociate from DNA, which is essential for the completion of ICL repair (Figure 1-4, 12) (Kuraoka *et al*, 2000; Cohn *et al*, 2007; Nijman *et al*, 2005; Oestergaard *et al*, 2007).

No	Group	Name	Other names	Patient frequency	Protein Functions
1	1	FANCM	-	0.1%	DNA translocase, fork traverse
2	2	FANCA	-	64%	FA core complex
3	2	FANCB	-	2%	FA core complex
4	2	FANCC	-	12%	FA core complex
5	2	FANCE	-	1%	FA core complex
6	2	FANCF	-	2%	FA core complex
7	2	FANCG	-	8%	FA core complex
8	2	FANCL	-	0.4%	FA core complex, E3 ubiquitin ligase
9	2	FANCT	UBE2T	-	FA core complex, E2 ubiquitin-conjugating enzyme
10	3	FANCD2	-	4%	ID2 complex, ubiquitinated by FANCL and recruit downstream proteins
11	3	FANCI	-	1%	ID2 complex, ubiquitinated by FANCL and recruit downstream proteins
12	4	FANCJ	BRIP1, BACH1	2%	Homologous recombination, 5’ - 3’ DNA helicase
13	4	FANCN	PALB2	0.7%	Homologous recombination
14	4	FANCO	RAD51C	0.1%	Homologous recombination
15	4	FANCP	SLX4, BTBD12	0.5%	Scaffold of XPF/ERCC1
16	4	FANCQ	ERCC4, XPF	0.1%	Part of the unhooking nuclease
17	4	FANCR	RAD51	-	Homologous

					recombination
18	4	FANCS	BRCA1	0.1%	Homologous recombination
19	4	FANCD1	BRCA2	2%	Homologous recombination
20	4	FANCU	XRCC2	-	Homologous recombination
21	4	FANCV	REV7	-	Translesion synthesis
22	4	FANCW	RWD3	-	E3 ligase

Table 1-1 The lists of the 22 currently known FA pathway genes. The 22 FA genes are classified into 4 groups according to their functions in this table, which are highlighted with different colours. The mutation frequency of each gene among FA patients is also listed. Adapted from Wang & Smogorzewska, 2015.

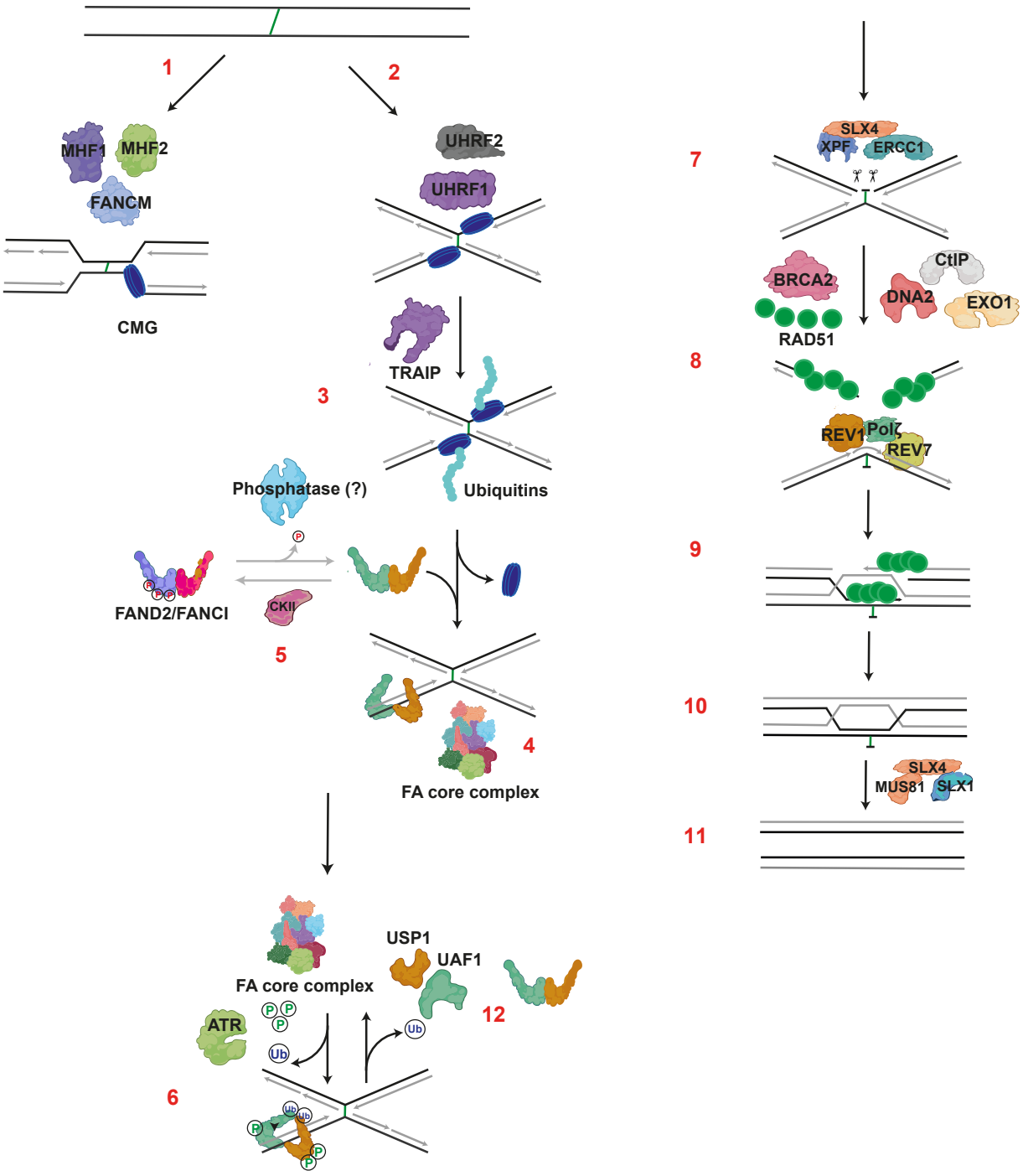
1
2
MHF1
MHF2
FANCM
CMG
UHRF2
UHRF1
TRAIP
3
Ubiquitins
Phosphatase (?)
FAND2/FANCI
CKII
5
4
FA core complex
USP1
UAF1
FA core complex
ATR
12
6
7
SLX4
XPF
ERCC1
BRCA2
CtIP
DNA2
EXO1
RAD51
8
REV1
Polζ
REV7
9
10
SLX4
MUS81
SLX1
11

Figure 1-4 The FA ICL repair pathway. (1) FANCM can recognise the ICL and mediate fork traverse when the second replication fork is absent. (2) ICL can also be sensed by non-FA sensor proteins, such as UHRF1 and UHRF2. (3) The two replication forks convergence at the ICL, and CMG helicases are subsequently unloaded in a TARIP dependent manner. (4) The FA core complex containing the E3 ligase FANCL is recruited. (5) CK2 phosphorylated FANCD2 needs to be dephosphorylated by a still unidentified phosphatase prior to DNA recruitment. (6) Upon chromatin binding, the FANCD2/FANCI complex is fully activated by undergoing further post-translational modifications, including ATR mediated phosphorylation and monoubiquitination by the FA core complex. The monoubiquitination event converts the complex into a sliding clamp and locks it on the DNA. (7) Monoubiquitinated FANCD2/FANCI recruit nucleases such as the SLX4/XPF/ERCC1 complex, which incises around and unhooks the ICL. (8) Other HR related repairing factors are also recruited by monoubiquitinated FANCD2. Unhook of the ICL leads to an SSB on one of the sister chromatids and a DSB on the other. The DSB ends are resected by nucleases such as CtIP, EXO1 and DNA2 and subsequently covered with Rad51 in a BRCA2 dependent manner. The ICL adduct containing gap is filled by Rev1 and Rev7 (FANCV) associated Pol ζ mediated TLS. (9) to (11) Rad51 deposition promotes strand invasion and the resulting double Holliday junction is resolved by the SLX4/SLX1/MUS81 complex. Finally, the remanent crosslink adduct is removed by BER or NER. (12) After the repair is completed, FANCD2/FANCI is deubiquitinated by USP1/UAF1 and dissociates from DNA. Adapted from Lopez-Martinez *et al*, 2016.

1.3 Role of protein phosphorylation and dephosphorylation in DNA damage response (DDR)

1.3.1 Protein phosphorylation, dephosphorylation and DDR

As already mentioned, the DDR is composed of a substantial number of proteins involved in various mechanisms that sense and signal the induction of DNA damage, to coordinate DNA repair with other damage elicited cellular processes, such as cell cycle arrest. The DDR signal, which initiates from the lesion on chromatin, is driven primarily by changes in protein-protein interactions, localisations and post-translational modifications including phosphorylation/dephosphorylation, ubiquitination/deubiquitination, acetylation, SUMOylating and etc. (Huen & Chen, 2008; Freeman & Monteiro, 2010). Among all the types of modifications, protein phosphorylation and dephosphorylation events, mainly on serine and threonine residues, constitute the primary transducers in the signalling cascade via concerted action of activating/deactivating a variety of downstream effectors to combat the genomic damage.

The signal transduction pathways involved in DDR are primarily driven by protein phosphorylation (Maréchal & Zou, 2013). DDR related kinases usually act upstream of DNA damage where they are triggered directly by sensing proteins that recognize aberrant DNA structures. Studies carried out in yeast and mammalian cells have identified a set of evolutionarily conserved DDR activated kinases, including ATM (ataxia-telangiectasia mutated), ATR and DNA-dependent protein kinase (DNA-PKcs) that all belong to the phosphatidylinositol 3' kinase (PI3K)-related kinase (PIKK) family (Allen *et al*, 1994; Carr, 1995; Savitsky *et al*, 1995; Lempiäinen & Halazonetis, 2009; Lovejoy & Cortez, 2009). They act as the master transducers of the DDR signal, which phosphorylate and transduce the DNA damage signal to more than 700 effectors participating in a wide spectrum of cellular pathways from cell cycle arrest and DNA repair to apoptosis and senescence (Matsuoka *et al*, 2007). ATM and

ATR can also induce a second wave of phosphorylation by phosphorylating other kinases, such as Chk1, Chk2, and MK2 protein kinases (Matsuoka *et al*, 1998; Reinhardt *et al*, 2007). Given the important role played by protein phosphorylation in response to DNA damage, it is not surprising that a proportion of these phosphorylation events transduce DDR signal via regulating protein-protein interactions. In fact, the DNA damage signals are timely propagated through a concerted action between kinase dependent phosphorylation and sequence-specific recognition of the phosphorylated proteins - which is evidenced by the identification of conserved phospho-binding motifs in DDR related proteins, the BRCA1 C-terminal repeat (BRCT) and forkhead-associated (FHA) domains (Yu *et al*, 2003; Manke *et al*, 2003; Durocher *et al*, 1999). For example, BRCA1 harbouring tandem BRCT repeats is an important player especially in mediating DSB repair. It has been shown to interact with CtIP in a phosphorylation-dependent manner to promote end resection and HR (Yu & Chen, 2004; Kim *et al*, 2007). In addition, proteins containing the FHA motif, such as Chk2, have been implicated in DDR triggered cell cycle regulation and DNA repair. Upon DNA damage, ATM phosphorylates Chk2 creating a binding site for Chk2 FHA motif, which results in its homo-oligomerization via the interaction of one Chk2 FHA with another phosphorylated Chk2. This facilitates the full activation of Chk2 kinase activity through auto-phosphorylation on the activation-loop of Chk2, and it is important for its role in maintaining cell cycle arrest (Schwarz *et al*, 2003; Ahn *et al*, 2002).

Temporal and spatial activation of kinase activity is necessary for transducing the DDR signal. On the other hand, fine-tuning of phosphorylation events by phosphatases is essential for efficient DNA damage repair to avoid over-activation of the DDR at the late stage. Whereas the functions of kinases involved in the DDR have been well documented, our knowledge of the complicated roles of protein phosphatases still remains rudimentary (Harper & Elledge, 2007; Shimada & Nakanishi, 2013). Historically, it is believed that protein phosphatases only contribute to shutting off DDR induced phosphorylation when the repair is complete – for example, PP4 and a PP2A have been shown to dephosphorylate and reverse ATM induced γH2AX in response to DSBs, which is required for the completion of DNA repair (Chowdhury *et*

al, 2005, 2008). However, it was found by a proteomic study that immediately after DSB damage more than 300 sites among 750 phosphorylation sites on almost 400 proteins are modified by phosphatases (Bensimon *et al*, 2010; Zheng *et al*, 2015). Given that protein dephosphorylation plays important role in shutting off damage induced phosphorylation at the late stage of DDR, results from this proteomic analysis point to the existence of potential functions of phosphatases in facilitating DDR, rather than just switching it off. Actually, in the recent years several studies have revealed that phosphatases are also capable of directly facilitating the DDR at the repair level, which altered the perspective of the role that protein dephosphorylation played in response to DNA damage (Ramos *et al*, 2019). For example, protein phosphatase PP4C dephosphorylates 53BP1 hence allowing the formation of 53BP1 foci that promotes NHEJ mediated DSB repair during G1 (Lee *et al*, 2010). The serine/threonine protein phosphatase-1 (PP1) has also been documented to have a role in directly modulating DNA repair through dephosphorylating Chk2 phosphorylated BRCA1, which is essential for the completion of the HR mediated DSB repair (Moorhead *et al*, 2007; Kurimchak & Grana, 2012). Also, BLM helicase is sequestered from DNA through Chk1 mediated phosphorylation and is dephosphorylated by putative phosphatases in response to DSBs, allowing its localisation to the site of lesion where it catalyses the dissolution of dHJ before the completion of HR directed repair (Dutertre *et al*, 2002).

1.3.2 Protein phosphatase 2 (PP2A) and DDR

Since most of the DDR signal is propagated by phosphorylation/dephosphorylation events on serine/threonine residues, it is not surprising that protein serine/threonine phosphatases play vital roles in regulating these processes. Protein serine/threonine phosphatases are classified into three subfamilies based on their sequence, structure and biological properties: metal (Mg^{2+}/Mn^{2+}) dependent protein phosphatase (PPM), aspartate-based phosphatase and phosphoprotein phosphatase (PPP) (Nematullah *et al*, 2018). The mammalian genome encodes around 400 serine threonine phosphatases and yet only about

40 serine/threonine phosphatases catalytic subunits (Moorhead *et al*, 2007). This can be explained by the capacity to form specific phosphatase complexes *in vivo* by associating distinct protein subunits that recognise different substrates. In this thesis, we identified that one of the protein phosphatase 2A (PP2A), which is a group of ubiquitously expressed and highly conserved serine/threonine phosphatases belonging to the PPP family, is involved in mediating the activation of the FA pathway via dephosphorylating FANCD2 upon ICL damage. PP2A has been relatively well characterised compared to other protein phosphatases, and approximately 70 PP2A heterotrimers have been identified in mammalian cells (Ding *et al*, 2003). It can act on a wide range of cellular pathways, including cell cycle progression, DNA replication and gene transcription/translation, via its multifarious holoenzymes. Each holoenzyme is composed of a catalytic (C), scaffold (A) and a regulatory (B) subunit (Figure 1-5) (Janssens & Goris, 2001; Jeong & Yang, 2013; Hunt, 2013). While the catalytic subunits and scaffold subunits are only encoded by two genes respectively (*PPP2CA* and *PPP2CB* for the catalytic, *PPP2R1A* and *PPP2R1B* for the scaffold subunits), PP2A regulatory subunits are encoded by 15 different genes that alternatively splice to 26 distinct transcripts. They are split into 4 families: the B (PR55), B′ (PR56), B′′ and B′′′ (Striatin) (Figure 1-5), which are expressed in a tissue specific manner to mediate the localisation, substrate specificity and activity of the holoenzymes (Schönthal, 2001; Eichhorn *et al*, 2009). It is known that PP2A dephosphorylates over 300 proteins involved in cell cycle regulation via the action of diverse holoenzymes. It participates in fine-tuning most of pathways of cell cycle initiation and checkpoints (Wlodarchak & Xing, 2016), among which the Greatwall-ENSA-PP2A/PR55 mediating G2 to mitosis transition & mitosis exit is highly conserved and one of the most important pathways. Immediately before mitosis in later G2, PP2A/PR55 is inhibited by Greatwall kinase phosphorylated Endosulfine proteins, ARPP-19 and ENSA, which bind to PP2A/PR55 and block the complex from Cdk1/CyclinB substrates (Gharbi-Ayachi *et al*, 2010; Mochida *et al*, 2010). Consequently, mitosis is promoted through maximised phosphorylation of Cdk1/CyclinB substrates. At the metaphase to anaphase transition, the activity of Greatwall decreases due to PP1 mediated dephosphorylation hence releasing ENSA and ARPP-19 from PP2A/PR55, which leads to normal mitotic exit. In addition to directly regulating Cdk1/CyclinB substrates

by PP2A/PR55, PP2A/PR56 dephosphorylates and inhibits the Cdk1 activator, the Cdc25C phosphatase (Forester *et al*, 2007), hence promoting mitotic exit due to a lowered Cdk1 activity.

The enzymatic activity of PP2A depends upon the stability and half-life of the functional monomeric subunits, and the ability of interaction with each other to form trimeric holoenzymes (Seshacharyulu *et al*, 2013). For example, PP2A/PR56 regulatory subunits that also mediate the whole process of mitosis are constantly shuttling between nucleus and cytoplasm during interphase to provide spatial substrate specificity for the enzymes (Flegg *et al*, 2010).

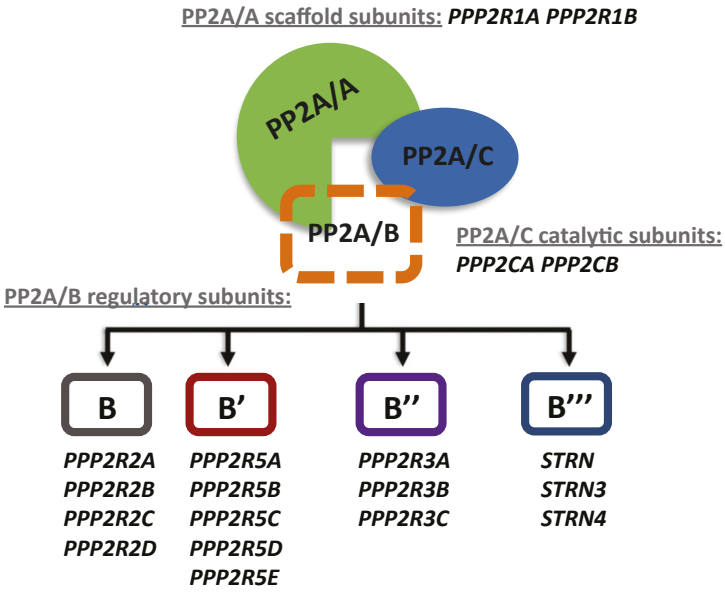

Figure 1-5 The heterotrimeric PP2A holoenzyme. Each PP2A holoenzyme comprises a scaffold, a catalytic and a regulatory subunit. While the scaffold and catalytic subunits are only encoded by 2 genes respectively, the regulatory subunits are encoded by 15 different genes that are categorised into 4 distinct families. Adapted from (Kurimchak & Grana, 2012)

PP2A takes part in and is indispensable for most of the cellular pathways. Its activity is required for embryogenesis, as PPP2CA -/- (catalytic subunit α knockout) mice are embryonically lethal (Götz *et al*, 1998). It is not surprising that PP2A plays a role in DDR and

DNA repair. In fact, it not only contributes to shutting off DDR by regulating the activity of primary (ATM, ATR, DNA-PK) and secondary (Chk1 and Chk2) kinases, but also directly involves in facilitating DNA repair. It has been suggested that PP2A mediated dephosphorylation of DNA-PK stimulates NHEJ *in vitro* (Douglas *et al*, 2001). In addition, in response to hydroxyurea (HU) induced replication fork collapse, PP2A dephosphorylated ATM/ATR phosphorylated RPA32 at the end of repair which is required for the completion of the repair process (Feng *et al*, 2009). Consistent with a general role for PP2A in the DDR, it is considered to be a tumour suppressor and is functionally inhibited in cancer (Seshacharyulu *et al*, 2013). Complete inhibition of its activity and loss of its functional subunits are characteristics of neoplastic transformation. Treating mice with the PP2A inhibitor okadaic acid (OA) leads to skin cancers, which was subsequently found out to be caused by the activation of multiple cancer-prone pathways (Suganuma *et al*, 1988, 1990; Fujiki & Suganuma, 1993; Schönthal, 2001). Specifically, while there has barely been any reports of alterations of the PP2A catalytic subunits in any cancer types, mutations and aberrant expression of PP2A scaffold and regulatory subunits have been observed in various types of human malignant tumours – such as lung (PPP2R1A/B, PPP2R2C, PPP2R5C), breast (PPP2R1A/B, PPP2R5E) and colon cancers (PPP2R1B) (Calin *et al*, 2000; Banerjee *et al*, 2007; Dupont *et al*, 2010). Some studies have pointed to the targeting of PP2A phosphatases to combat cancer, which focus on development of direct or indirect PP2A reactivating compounds. For instance, the drug bortezomib that activates PP2A indirectly by inhibiting the PP2A inhibitor CIP2A has been utilised to treat triple negative breast cancer cells (Tseng *et al*, 2012).

Chapter 2. Dephosphorylation of FANCD2 by PP2A activates the FANCD2/FANCI complex in human cells

2.1 Introduction

As alluded previously, the central component of the FA pathway is the FANCD2/FANCI heterodimer that is recruited to the site of damage on DNA, where the complex is subsequently monoubiquitinated by the FA core complex and hence activating the FA pathway (Liang *et al*, 2016; Alcón *et al*, 2020). The complex is considered to act as an intermediate that bridges the early detection of the ICL to repair events that happen downstream. Monoubiquitinated FANCD2/FANCI can interact and recruit several repair proteins to the ICL, such as BRCA1 (Garcia-Higuera *et al*, 2001) and nucleases XPF/ERCC1 (Douwel *et al*, 2017; Kuraoka *et al*, 2000) together with the scaffolding protein SLX4 (Yamamoto *et al*, 2011; Klein Douwel *et al*, 2014), which unhook the ICL by incising the DNA around the lesion and hence generating a DSB. Considering the crucial role of the FANCD2/FANCI complex in ICL repair, it is not surprising that strict regulatory mechanisms are in place to ensure an efficient and accurate activation/deactivation of this complex to avoid illicit events happening on chromosomes. It has been found that FANCD2/FANCI can directly bind to DNA (Park *et al*, 2005; Wang *et al*, 2020; Yuan *et al*, 2009) and monoubiquitination by the FA core complex increases its affinity to DNA by transforming the complex into a locked DNA clamp (Alcón *et al*, 2020; Wang *et al*, 2020; Tan *et al*, 2020; Rennie *et al*, 2020). However, these results do not provide information for regulated DNA binding by FANCD2/FANCI in response to ICL damage. Therefore, mechanistic insight into how the complex is recruited to DNA is needed.

Some light has been shed on this question: according to results from studies conducted *in vitro* with cell free extracts from *Xenopus eggs* where the ICL repair has mainly been studied in a replication dependent manner, the recruitment of FANCD2/FANCI and subsequent monoubiquitination on DNA by the FA core complex occur after fork convergence and CMG

unloading (Zhang *et al*, 2015; Long *et al*, 2014). In addition, ATR is found to be one of the master regulators of the FA pathway (Andreassen *et al*, 2004; Pichierri & Rosselli, 2004). It directly phosphorylates several components of the FA pathway, including the FANCD2/FANCI complex, resulting in promotion of its monoubiquitination, and activation of the FA pathway (Cheung *et al*, 2017; Ishiai *et al*, 2008; Zhi *et al*, 2009). As mentioned in 1.2.2, Our colleagues Lopez-Martinez *et al.* recently described a novel mechanism that switches the FA pathway on and off by regulating the DNA binding affinity of the FANCD2/FANCI complex (Lopez-Martinez *et al*, 2019; Lopez-Martinez, 2018). They reported previously unknown phosphorylation events of FANCD2 at a six-residue cluster spanning residues 882-898 mediated by the serine/threonine kinase CK2 (Figure 2-1 A) (Lopez-Martinez *et al*, 2019; Lopez-Martinez, 2018), and phosphorylation of these sites reduces the affinity of the FANCD2/FANCI complex for DNA, hence blocking subsequent events in the pathway, including FANCD2 monoubiquitination on DNA. In fact, CK2 appears as a tetramer composed of two catalytic subunits (α and α') and two regulatory subunits (β). The catalytic subunits α and α' are encoded by two different genes respectively, which are highly conserved across different species. While the regulatory subunit β has only one isoform in mammalian cells (Litchfield, 2002). The CK2 features a target sequence with a serine or threonine followed by an acidic residue (aspartic acid, D or glutamic acid, E), or another phosphorylated serine or threonine at position +1 or +3 (Lopez-Martinez, 2018). The 6 serine/threonine residues found within the FANCD2 882-898 cluster match the target prediction of CK2, and are well-conserved among species (Figure 2-1 A) (Lopez-Martinez *et al*, 2019; Lopez-Martinez, 2018).

We assume that this CK2 dependent phosphorylation event acts like a safeguard to avoid spurious activation of DNA repair pathways in the absence of genomic stress, through prevention loading of the FANCD2/FANCI complex on DNA (Lopez-Martinez *et al*, 2019; Lopez-Martinez, 2018). Since CK2 constitutively phosphorylates FANCD2 and keeps it in an inactive state in the absence of DNA damage, the model implies that FANCD2 must be dephosphorylated by a still unidentified phosphatase, prior to DNA loading and monoubiquitination in response to DNA damage. Dephosphorylation of the 882-898 cluster

on FANCD2 should precede the recruitment of FANCD2 by creating a facultative active form of the FANCD2/FANCI complex with higher affinity for DNA, which can now be loaded onto DNA to undergo further modifications such as monoubiquitination by the FA core complex and ATR mediated activating phosphorylation (Lopez-Martinez *et al*, 2019; Lopez-Martinez, 2018).

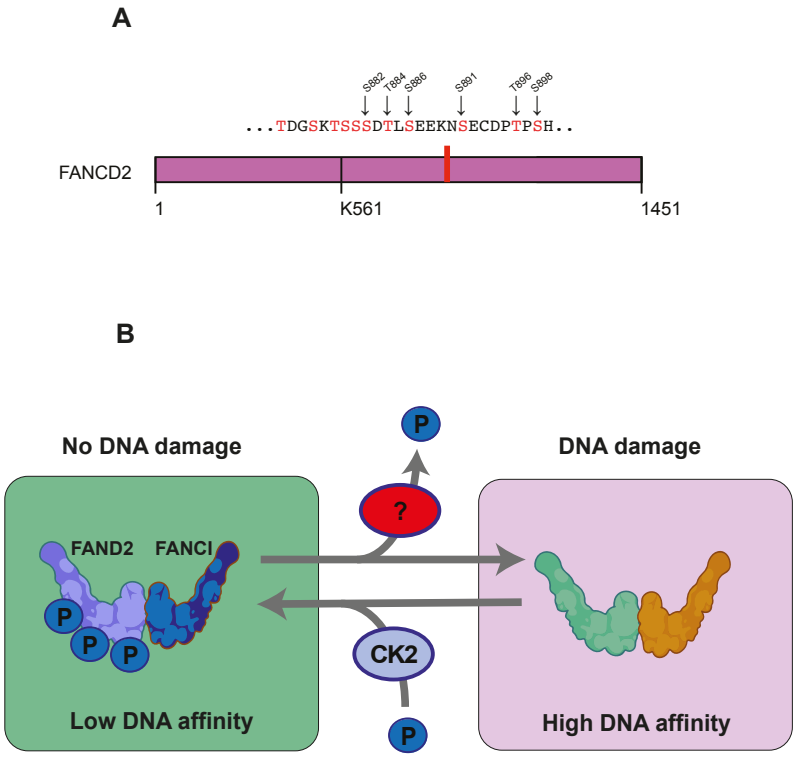

Figure 2-1 FANCD2 needs to be dephosphorylated before chromatin recruitment. (A) Schematic representation of the 882-898 CK2 cluster on FANCD2. The K561 monoubiquitinaiton site is also highlighted. (B) FANCD2 is constantly phosphorylated by CK2 and kept at a low DNA affinity in the absence of DNA damage. In response to ICL, FANCD2 needs to be dephosphorylated by a still unknown phosphatase and converted to a state with higher DNA affinity prior to chromatin recruitment.

In order to identify the putative phosphatase responsible for this event, we conducted preliminary screening for serine/threonine phosphatases using family wide inhibitors and assessed the reduction in FANCD2 recruitment to chromatin upon induction of ICL (Lopez-Martinez, 2018). We observed that HeLa cells treated with Sanguinarine (PPM and PP2C family wide inhibitor) and Calyculin A (Cal-A, PP1 and PP2A family inhibitor) displayed a significantly

affected FANCD2 recruitment to DNA after ICL induction, which indicated that the phosphatase could be a member of PPM/PP2C or the PP2A-like family (Lopez-Martinez, 2018). In the light of these data, we performed further screening using siRNA mediated gene silencing, and assessed the defect in FANCD2 ubiquitination in response to ICL induction. Cells transfected with siRNAs that target the catalytic subunits of different phosphatases in the PP2A-like family were treated with 4, 5', 8-Trimethylpsoralen (TMP), which is a chemical reagent that only generates ICLs in combination with UVA irradiation (Lopez-Martinez *et al*, 2016; Lai *et al*, 2008), at 72 h post transfection. Cells incubated with TMP were irradiated with UVA to introduce the ICL damage and then they were analysed by Western blot. Among all siRNAs tested silence of both PP2A catalytic subunits (siPPP2CA+B, α and β subunits) showed the highest level of reduction in FANCD2 ubiquitination, as well as in FANCI ubiquitination (Figure 2-2, lane 9). These experiments suggest that the dephosphorylation of the 882-898 cluster on FANCD2 upon DNA damage is potentially catalysed by the serine/threonine phosphatase PP2A.

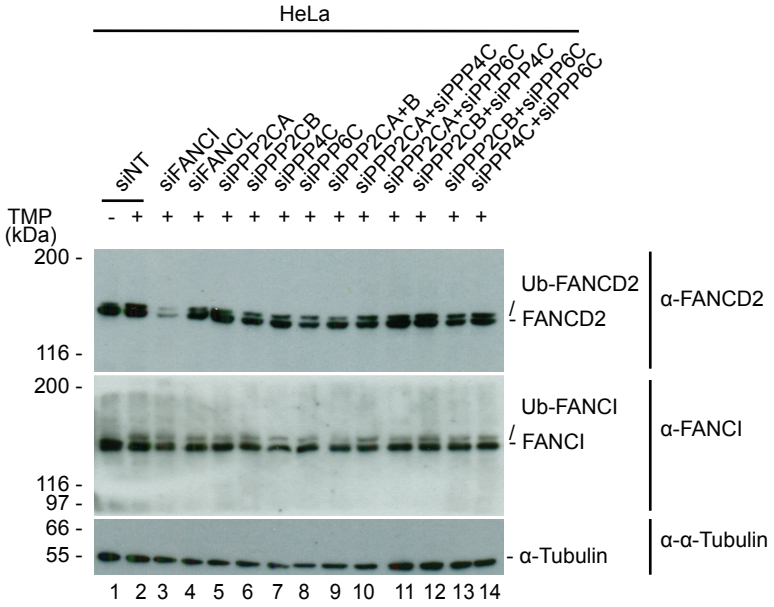

Figure 2-2 Western blot of the siRNA screening for phosphatases responsible for dephosphorylating FANCD2. ICLs were induced by treatment with TMP (2 μg/ml) and UVA (50 mJ/cm^2). Cells transfected with a non-targeting siRNA were used as the control. Data produced by Lopez-Martinez.

2.2 Effect of PP2A inhibition on FANCD2 monoubiquitination

First, we validated the result of the screening experiments by assessing FANCD2 monoubiquitination in PP2A inhibited cells. HeLa cells were separately treated with two types of PP1/PP2A inhibitors, Cal-A and OA. Both compounds are isolated from marine sponges and have been described as potent tumour promoters (Ishihara *et al*, 1989; Suganuma *et al*, 1988, 1990). Cal-A inhibits PP2A and PP1 *in vitro* with approximately equal potency (IC50 0.5-2 nM) whereas OA has about a hundred fold higher specificity for PP2A (IC50 2 nM) than for PP1 (IC50 300 nM) *in vitro* (Resjö *et al*, 1999; Ishihara *et al*, 1989). The concentration of the inhibitors used in the intact-cell experiment (*in vivo*) is usually higher than *in vitro* (Yan *et al*, 2010a; Resjö *et al*, 1999). Experiments conducted in rat adipocytes and human MCF-7 breast cancer cells showed that incubation with OA at a concentration as high as 1 μM did not significantly affect PP1 activity but blocked PP2A activity by 50% -75%, and incubation with approximately 300 nM Cal-A was sufficient to inhibit both phosphatases completely (Yan *et al*, 2010a; Resjö *et al*, 1999). Therefore OA is the compound more suitable for our purpose to achieve PP2A inhibition without affecting other phosphatases – although both inhibitors were tested. Cells were treated at a concentration that has been described in literatures previously (25 nM for Cal-A and 200 nM for OA) (Chowdhury *et al*, 2005; Garcia *et al*, 2002; Yan *et al*, 2010a; Resjö *et al*, 1999), and then were collected from 1-3 hours post TMP/UVA treatment and lysed for Western blot analysis. As expected, FANCD2 monoubiquitination in response to TMP/UVA caused ICL damage was largely abolished after the enzymatic activity of PP2A was inhibited by either Cal-A or OA, in comparison to non-treated controls (Figure 2-3, A and B), which is in agreement with result from the siRNA screening.

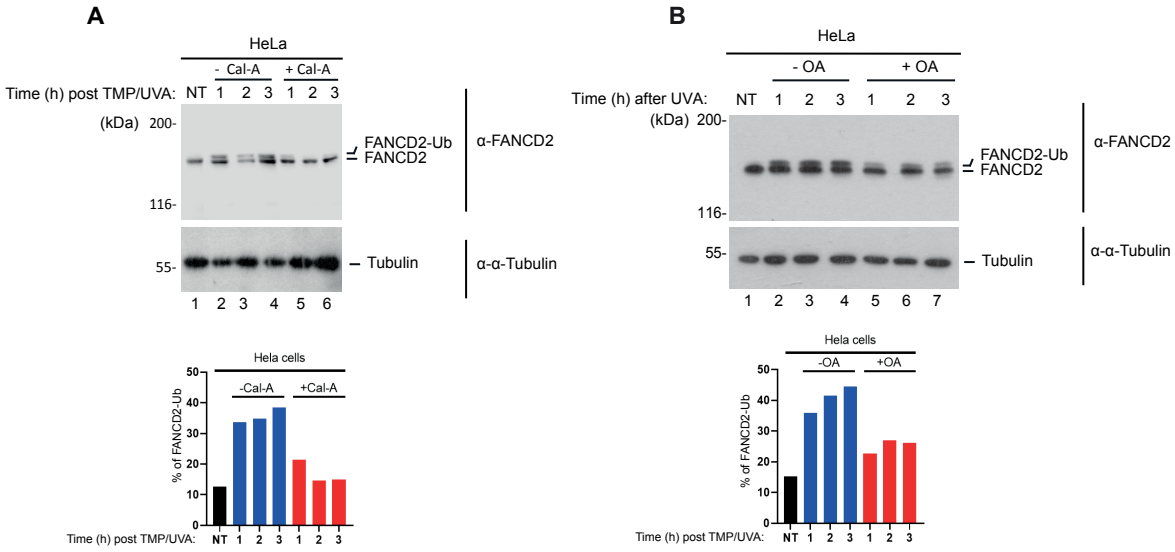

Figure 2-3 Treatment with PP2A inhibitors Cal-A and OA affects FANCD2 monoubiquitination. Representative Western blots and quantification of FANCD2 monoubiquitination in HeLa cells treated with 25 nM Cal-A (A) and 200 nM OA (B). ICLs were induced by treatment with TMP (2 μg/ml) and UVA (50 mJ/cm^2). All the Western blots shown in this thesis represent at least three independent experiments, unless otherwise stated in the figure legend.

The result of the siRNA screening was also validated in another cell line where an EGFP-tag was introduced into the *FANCD2* gene by the CRISPR/Cas9 (clustered regularly interspaced short palindromic repeats) system. The catalytic activity of PP2A was silenced by the same siRNAs targeting the catalytic subunits as shown in Figure 2-2. While a robust monoubiquitination was induced to the EGFP fused FANCD2 in the control cells, cells depleted with both PP2A catalytic subunits displayed a significantly suppressed FANCD2 ubiquitination upon TMP/UVA treatment, to an extent greater than that in cells transfected with siRNAs targeting FANCI (Figure 2-4 A, lane 2, lane 4 and lane 6).

We then tested whether the two catalytic subunits are functionally redundant to each other. In rat, the α subunit mRNA is about 10 times more abundant than the β subunit (Khew-Goodall & Hemmings, 1988). In good agreement, in HeLa cells we observed that solely depletion of the α subunit leads to a greated reduction in FANCD2 ubiquitination, compared to depletion of the β subunit (Figure 2-4 B lane 1 to 8). Silencing both genes markedly

suppressed FANCD2 monoubiquitination after damage compared to control cells (Figure 2-4 B lanes 1-2 and 9-10). However, depletion of the α or β subunit alone only led to partial reduction in FANCD2 monoubiquitination, suggesting that the two catalytic subunits are not functionally redundant with respect to each other in regulating the FA pathway during ICL repair (Figure 2-4 B lane 6, 8 and 10).

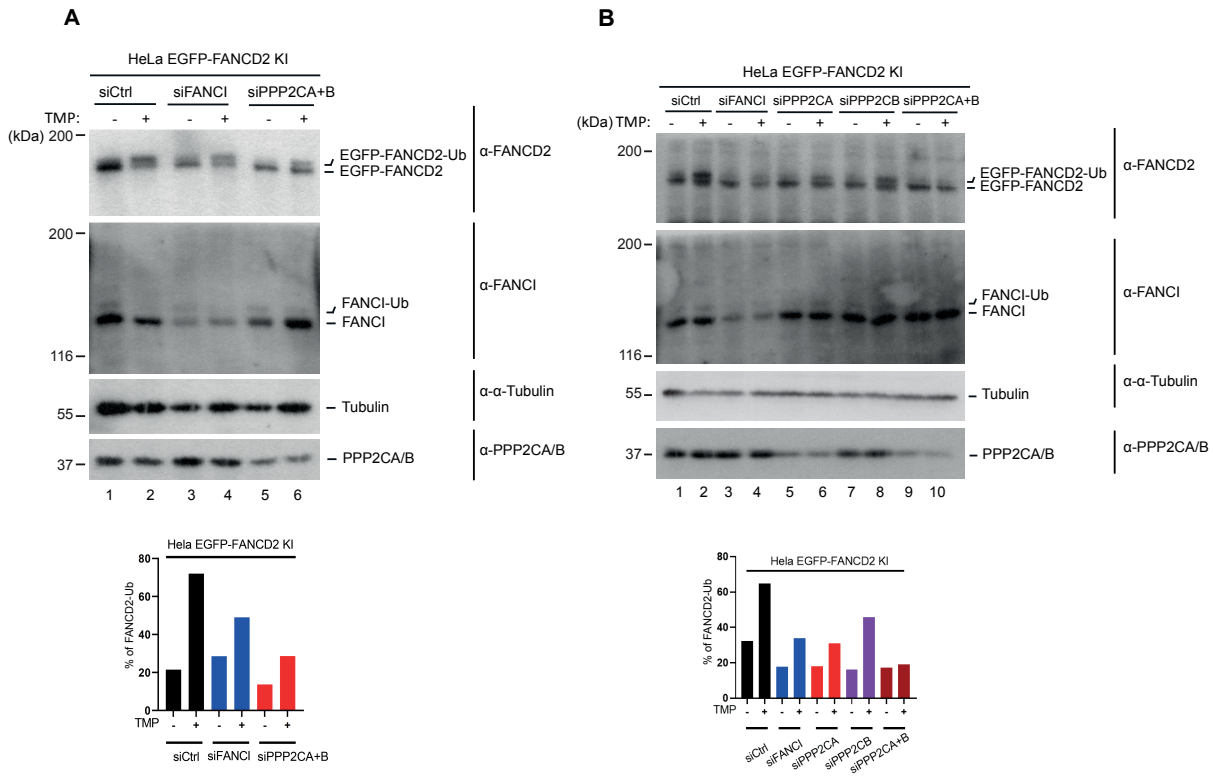

Figure 2-4 Depletion of PP2A catalytic subunits affects FANCD2 monoubiquitination. Representative Western blot and quantification of FANCD2 monoubiqutination in HeLa EGFP-FANCD2 knock-in cells transfected with (A) siRNAs targeting both of the PP2A catalytic subunits, (B) siRNAs targeting either the PP2A catalytic α or β. FANCI depleted cells were used as a positive control. ICLs were induced by treatment with TMP (2 μg/ml) and UVA (50 mJ/cm^2).

Our data show that the cellular ubiquitination of FANCD2 in response to ICL damage is reduced following suppression of PP2A. It is generally believed that DNA binding is likely to precede and promote monoubiquitination during ICL, according to evidence from research conducted both *in vivo* and *in vitro* (Liang *et al*, 2016; Lopez-Martinez, 2018; Sato *et al*, 2012; Longerich *et al*, 2014; Twest *et al*, 2017). We therefore speculated that FANCD2 could not be

recruited to chromatin in PP2A defective cells, which is the defect that directly leads to the observed phenotype of affected FANCD2 monoubiquitination.

2.3 Effect of PP2A inhibition on FANCD2 recruitment to chromatin

To test our hypothesis, we assessed the real-time recruitment of FANCD2 to ICLs in chromosomes in live cells. We took the advantage of a live-cell imaging system where cells stably expressing fluorophore-tagged proteins were treated with TMP, then ICLs were introduced by TMP activated at a "stripe" region that was irradiated by a localised UVA laser (Figure 2-5). By this means we can quantify the targeted protein recruitment to DNA in the stripe with ICL lesions.

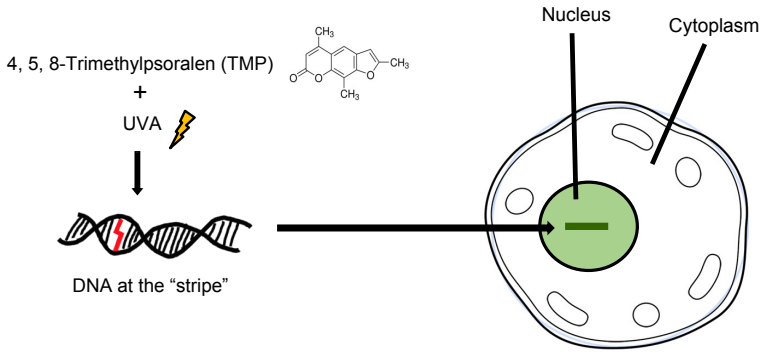

Figure 2-5 Schematic representation of the live-cell imaging system based on laser confocal scanning microscopy. Stable cell lines expressing fluorophore-tagged proteins are treated with TMP and ICLs are subsequently introduced to the nucleus by a localised UVA laser on the microscope.

HeLa cells where *FANCD2* is knocked-out that was previously created using the CRISPR/Cas9 technique were complemented with WT EGFP-FANCD2 to achieve expression at the endogenous level (Lopez-Martinez *et al*, 2019; Lopez-Martinez, 2018). mCherry-UHRF1 was co-expressed in the cell line to act as a control for the introduction of ICLs. We monitored the recruitment of FANCD2 and UHRF1 over time after ICLs were introduced by TMP treatment and microirradiation in either PP2A competent or defective cells. We first tested whether the PP2A inhibitor, OA, influences FANCD2 recruitment. As expected, FANCD2 was recruited

normally to ICLs in control cells, accumulating at the stripe area after ICL introduction (Figure 2-6 A, the top panel). In comparison, the recruitment of FANCD2 was largely supressed in cells treated with OA where the PP2A enzymatic activity was inhibited (Figure 2-6 A, the bottom panel). Meanwhile, mCherry-UHRF1 was recruited promptly in both control and OA-treated cells. Similar results were obtained in cells transfected with the siRNAs targeting the PP2A catalytic subunits, where they showed a defective FANCD2 recruitment to ICLs after the loss of PP2A (Figure 2-6 B). FANCD2 is believed to be recruited to chromatin as a heterodimer with FANCI. Thus, we also assessed FANCI recruitment in PP2A depleted cells and observed that it also was substantially reduced (Figure 2-6 C). Taken together, these data show that the FANCD2/FANCI complex is dependent on PP2A catalytic activity for its proper recruitment to chromatin in response to DNA damage.

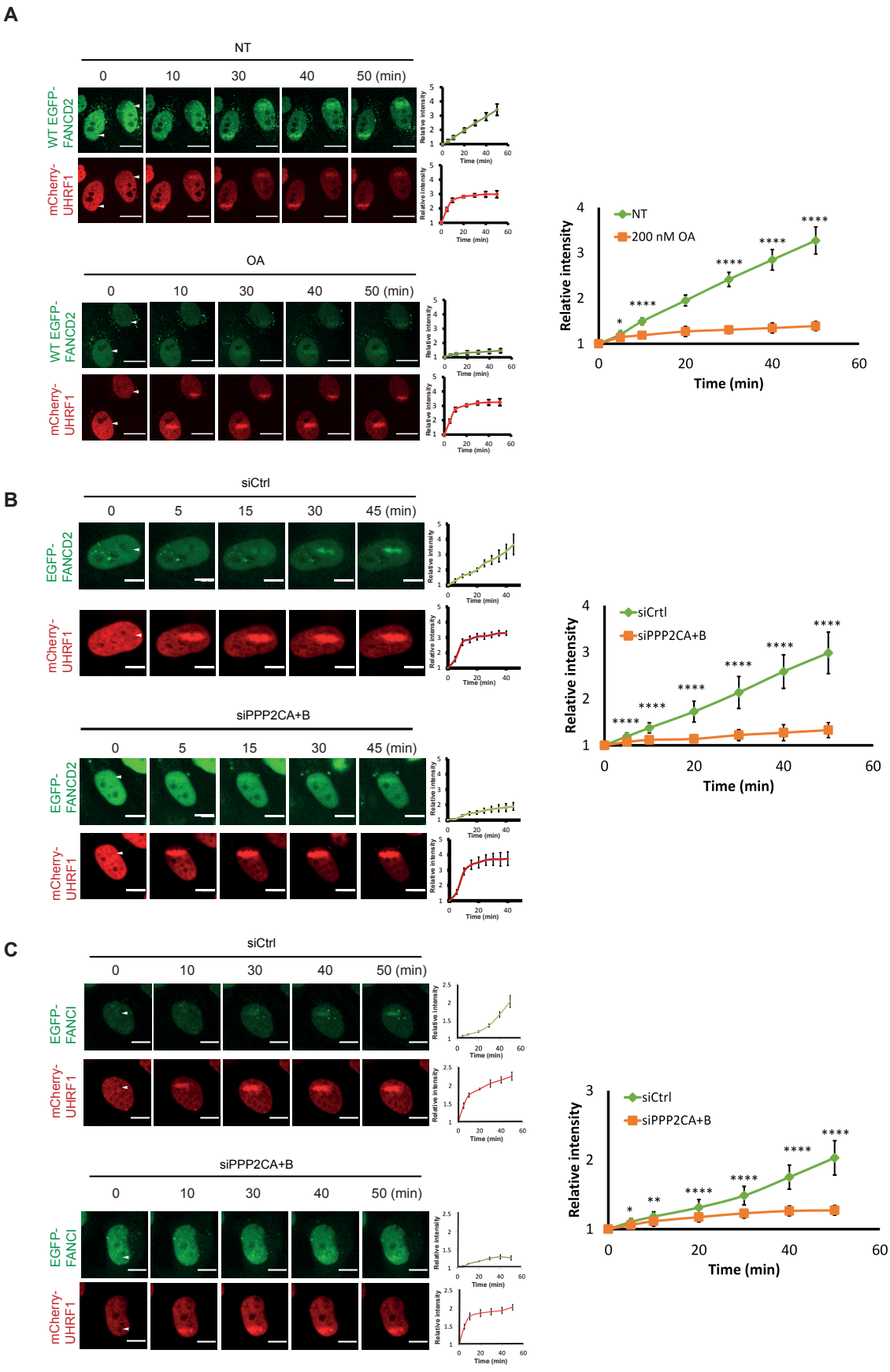
A
NT
0
10
30
40
50 (min)
WT EGFP-FANCD2
mCherry-UHRF1
Relative intensity
Time (min)
OA
NT
200 nM OA
Relative intensity
Time (min)
B
siCtrl
0
5
15
30
45 (min)
EGFP-FANCD2
mCherry-UHRF1
siPPP2CA+B
siCtrl
siPPP2CA+B
Relative intensity
Time (min)
C
siCtrl
EGFP-FANCI
mCherry-UHRF1
siPPP2CA+B
siCtrl
siPPP2CA+B
Relative intensity
Time (min)

Figure 2-6 FANCD2 and FANCI chromatin recruitment is reduced with inhibited PP2A activity *in vivo*. Representative live cell imaging of HeLa FANCD2 -/- complemented with EGFP-FANCD2 treated with PP2A inhibitor OA (A) or transfected with siRNAs targeting both of the PP2A catalytic subunits (B) (C). Cells were treated with 20 μg/ml TMP and micro-irradiated by a 405 nM UVA laser at the indicated areas (white arrows). Images were recorded at the indicated time points post irradiation, the change in recruitment of FANCD2 or FANCI was quantified by calculating the ratio of the fluorescence intensity at the stripe areas to the nucleus background (please see Materials & Methods). Three independent experiments were performed, 5 cells were quantified in each replicate (15 cells for three replicates of each sample). Quantification of the representative data of FANCD2, FANCI and UHRF1 recruitment is shown right next to the microscope images, and quantification of FANCD2 and FANCI recruitment of the three biological replicates are shown at the right of each panel. Mean ± SD, Scale bar: 10 μm. *p<0.05, ** p<0.01, **** p<0.0001.

We hypothesized that the functionally deficient FANCD2 observed in PP2A defective cells is due to the inability of FANCD2 dephosphorylation on the 882-898 six-residue cluster by PP2A, as opposed to be as a result of secondary cellular effects of PP2A inhibition. In order to test this directly, we employed another FANCD2 -/- cell line, into which we reintroduced a mutant derivative of FANCD2 where the six phosphorylation sites in the 882-898 cluster have been mutated to alanine residues that cannot be phosphorylated, named 6A EGFP-FANCD2 (Figure 2-7 A) (Lopez-Martinez *et al*, 2019; Lopez-Martinez, 2018). We speculated that this 6A mutant form of FANCD2 should be immune to PP2A inhibition. Indeed, while WT EGFP-FANCD2 was barely recruited to DNA upon depletion of PP2A, the recruitment of 6A EGFP-FANCD2 was not significantly affected in PP2A depleted cells compared to control cells (Figure 2-7 B and C).

We also evaluated the abilities of WT and 6A EGFP-FANCD2 to be monoubiquitinated in PP2A depleted cells. WT EGFP-FANCD2 was monoubiquitinated equally strongly as the 6A mutant in cells transfected with control siRNA (Figure 2-7 D, left panel lanes 2 and 4). As predicted, the monoubiquitination of 6A EGFP-FANCD2 was barely influenced by PP2A depletion (Figure 2-7 D, left panel lanes 4 and 8) whereas WT EGFP-FANCD2 monoubiquitination was clearly reduced (Figure 2-7 D, left panel lanes 2 and 6). Taken together, our live-cell imaging and molecular biology data suggest that FANCD2 is dysfunctional in PP2A deficient cells. It is not recruited to chromatin and therefore cannot be

ubiquitinated if PP2A is catalytically defective. In response to ICL damage, FANCD2 needs to be dephosphorylated by PP2A on the six CK2 phosphorylated sites in the 882-898 cluster prior to chromatin recruitment.

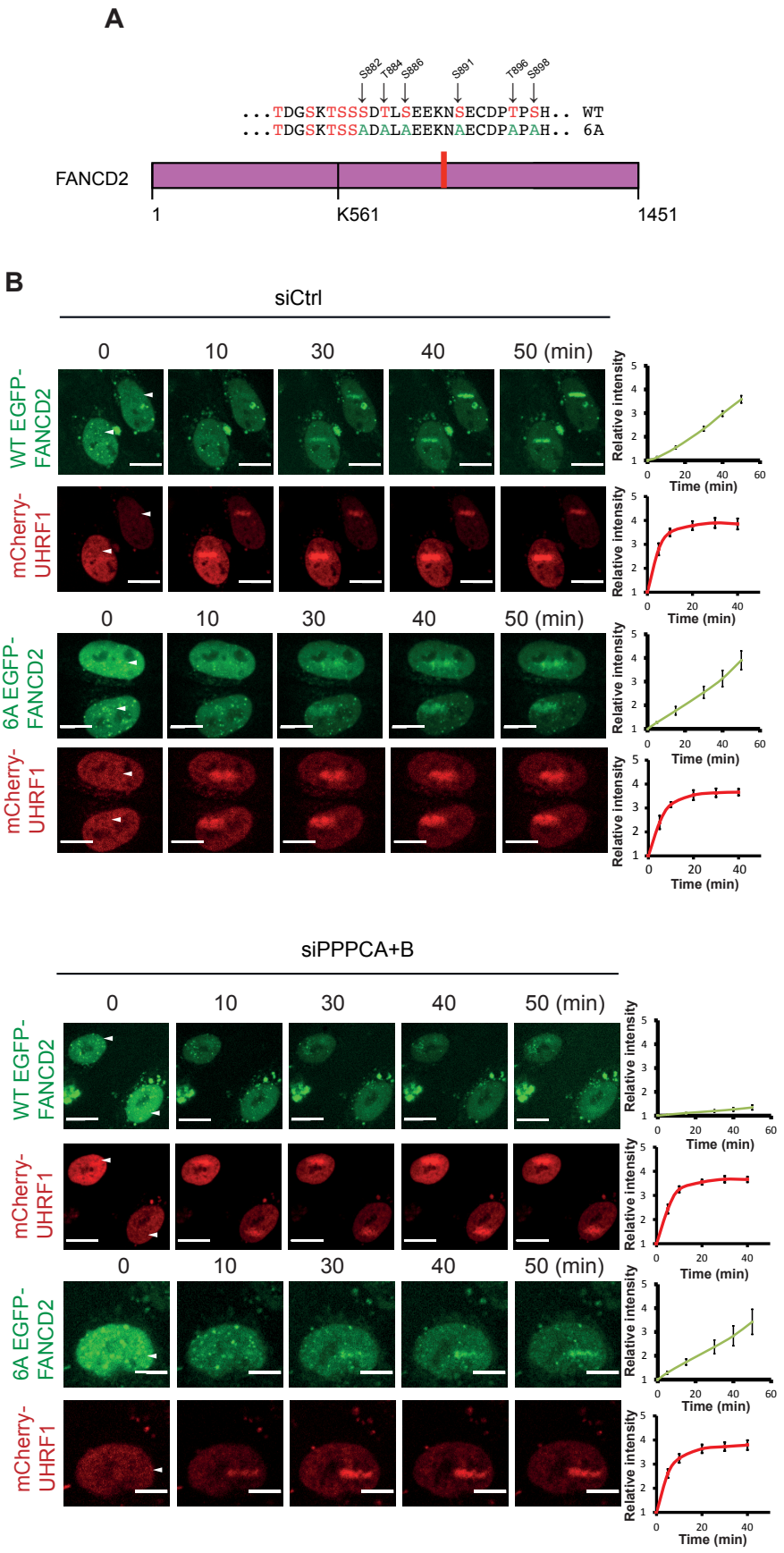
A
S882
T884
S886
S891
T896
S898
...TDGSKTSSSDTLSEEKNSECDPTPSH.. WT
...TDGSKTSSADALAEEKNAECDPAPAH.. 6A
FANCD2
1
K561
1451
B
siCtrl
0
10
30
40
50 (min)
WT EGFP-FANCD2
mCherry-UHRF1
6A EGFP-FANCD2
Relative intensity
Time (min)
siPPPCA+B

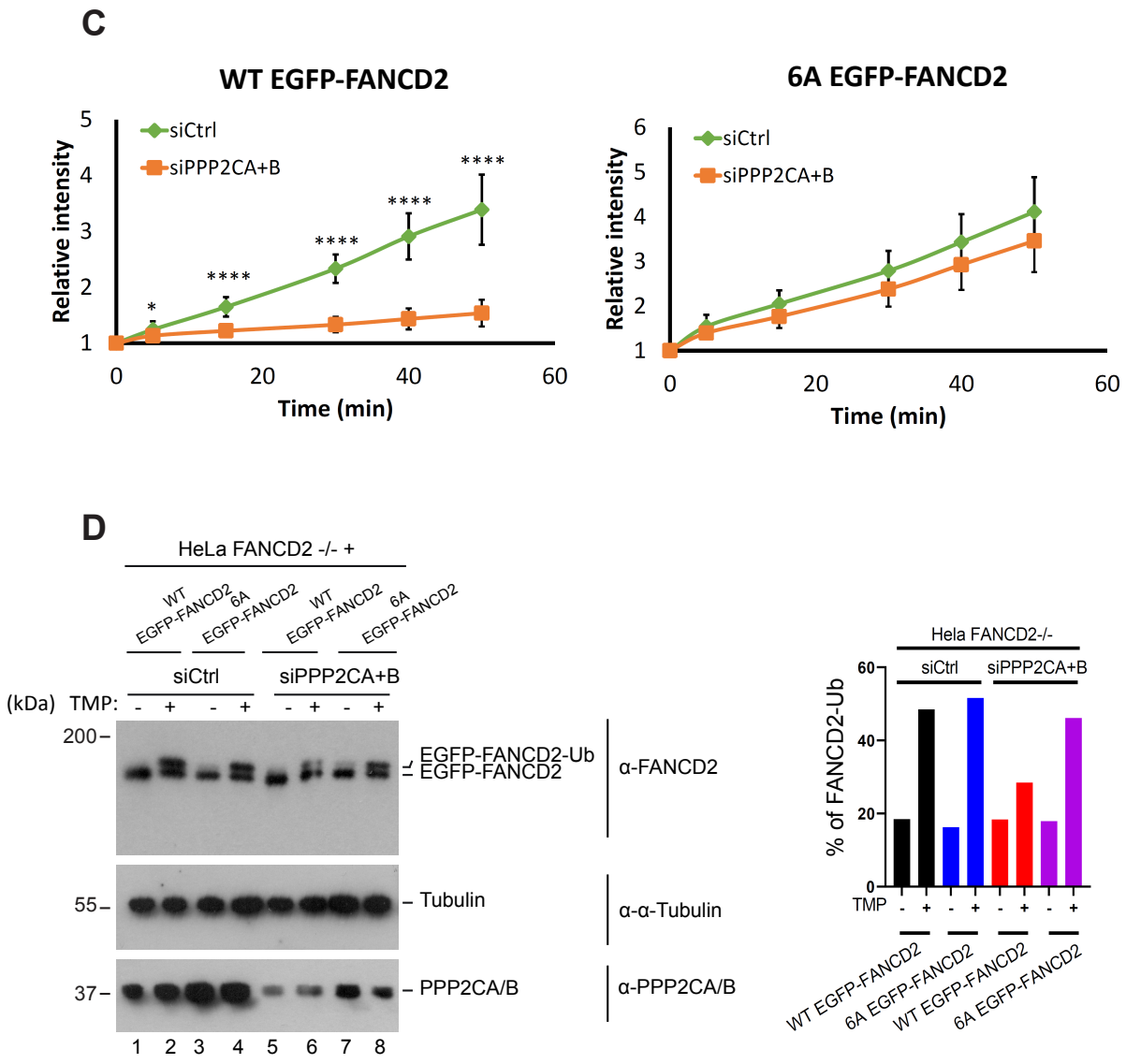

Figure 2-7 The non-phosphorylable 6A FANCD2 mutant is immune to PP2A depletion *in vivo*. (A) Schematic representation of the six mutated serine residues in 6A FANCD2 compared to wild type. (B) Representative live cell imaging and quantification of HeLa FANCD2 -/- complemented with either EGFP-FANCD2 or 6A-EGFP-FANCD2. Cells were irradiated with the same condition in Figure 2-6 at the indicated areas (white arrows). (C) Quantification of FANCD2 recruitment of the three biological replicates in (B). 5 cells were quantified in each replicate (15 cells for three replicates of each sample), Mean ± SD, Scale bar: 10 µm. *p<0.05, **** p<0.0001. (D) Representative Western blot and quantification of HeLa FANCD2 -/- cells complemented with either EGFP-FANCD2 or 6A-EGFP-FANCD2 before and after treatment with TMP (2 µg/ml) and UVA (50 mJ/cm^2).

2.4 Loss of PP2A catalytic subunits results in increased G2 population after MMC treatment

The FA pathway mediated ICL repair is believed to occur primarily in S phase in a replication dependent manner (Zhang *et al*, 2015; Räschle *et al*, 2008; Amunugama *et al*, 2018). PP2A is one of the master regulators of the cell cycle, as it plays important roles in most cell cycle initiation pathways as well as in major checkpoints during the cell cycle progression (Wlodarchak & Xing, 2016; Mochida *et al*, 2009; Zhang *et al*, 2009; Kolupaeva & Janssens, 2013). Therefore, the impact on FANCD2 could just because of a disrupted cell cycle in PP2A deficient cells. Thus, we decided to assess the effect of PP2A inhibition on the cell cycle progression in both unperturbed cells and cells treated with another ICL inducing agent, MMC. HeLa cells were incubated with propidium iodide to stain the DNA, and then were processed through a Fluorescence-Activated Cell Sorting (FACS) system to analyse the cell cycle profile. In unperturbed conditions, depletion of the PP2A catalytic subunits by siRNA hardly altered either the general cell cycle population as well as the percentage of cells in S (Figure 2-8 A and B), which rules out the possibility that the observed phenotype of FANCD2 dysfunction in PP2A depleted cells results from a disrupted cell cycle distribution with decreased S population.

The transition of G2/M in the cell cycle is prolonged in FA cells (Dutrillaux *et al*, 1982; Sala-Trepat *et al*, 2000; Centurion *et al*, 2000), and it is further increased if cells are exposed to DNA cross linking agents, such as MMC. This is actually a well-characterised phenotype of FA patient cells (Kaiser *et al*, 1982; Grompe & D'Andrea, 2001), and is therefore used diagnostically. With the exposure to MMC, whereas only a small increase in the percentage of cells in G2 (4%) could be observed for the non-transfected cells, the loss of PP2A catalytic activity led to an additional 12% G2 arrest in comparison to the control (Figure 2-8 A and C). The HeLa FANCD2 -/- cell line described previously (Lopez-Martinez *et al*, 2019; Lopez-Martinez, 2018) was employed as a positive control, which displayed an additional 35% G2 arrest after MMC exposure (Figure 2-8 A and C). A Western blot was also performed to validate

the siRNA knock down of PPP2CA/B, which is shown in Figure 2-8 D.

Held together, our data demonstrate that the observed phenotype of FANCD2 deficiency was because of PP2A depletion itself, rather than being a side effect of an impacted cell cycle progression. PP2A depleted cells exposed to MMC displayed a significant G2 arrest, which resembles one of the defining phenotypes of FA patient cells.

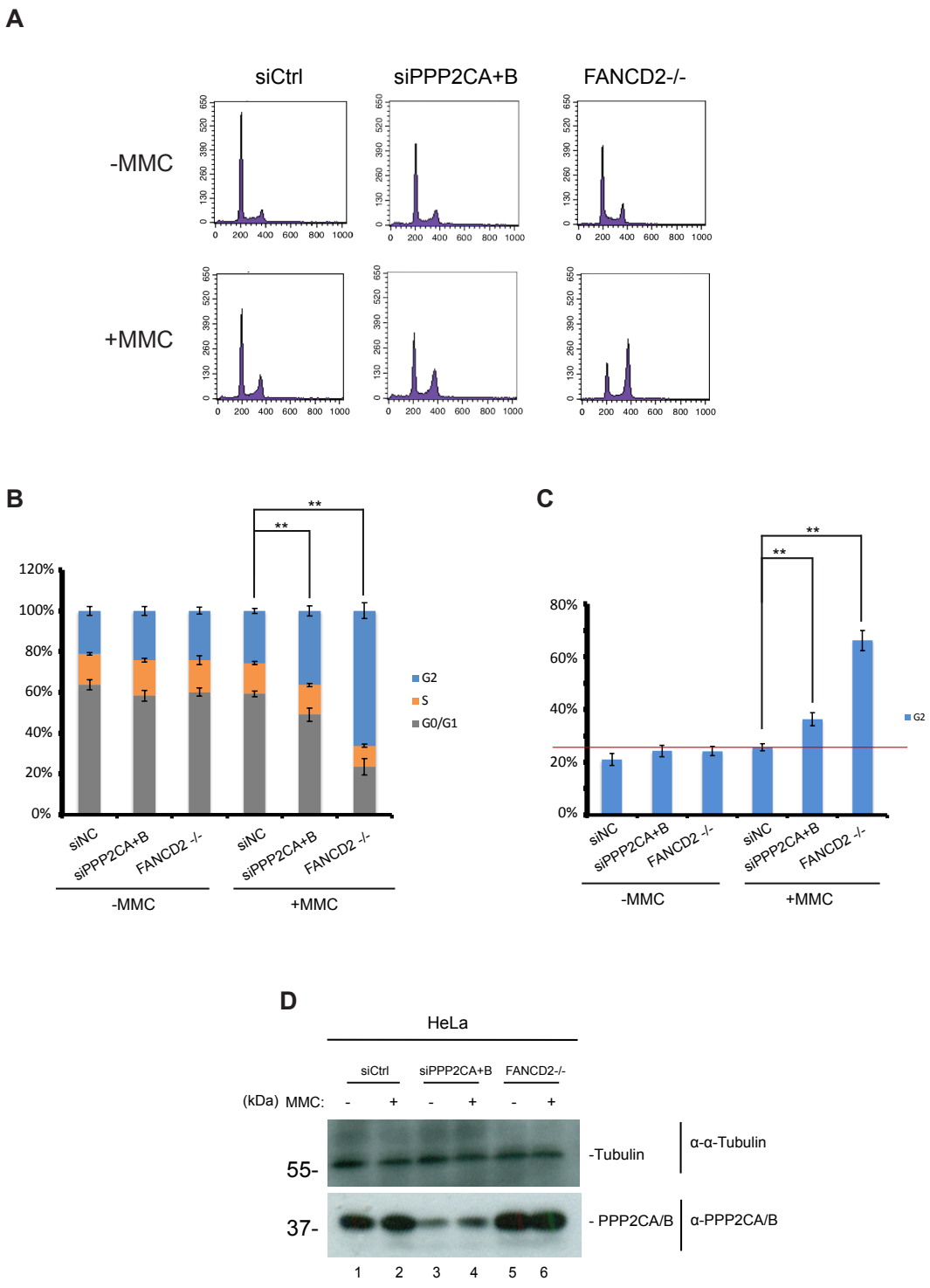
A
siCtrl
siPPP2CA+B
FANCD2-/-
-MMC
+MMC
B
120%
100%
80%
60%
40%
20%
0%
G2
S
G0/G1
siNC
siPPP2CA+B
FANCD2 -/-
-MMC
+MMC
C
80%
60%
40%
20%
0%
G2
D
HeLa
siCtrl
siPPP2CA+B
FANCD2-/-
(kDa) MMC: - + - + - +
55-
37-
-Tubulin
α-α-Tubulin
- PPP2CA/B
α-PPP2CA/B
1 2 3 4 5 6

Figure 2-8 Depletion of PP2A catalytic subunits induces G2 accumulation without affecting S phase population after ICL induction. (A) Cell cycle profiles by DNA content of PP2A catalytic depleted HeLa cells treated with 20 ng/mL MMC for 2 h followed by 24 h recovery. HeLa FANCD2 -/- cells were used as a positive control. (B) (C) Quantification of data shown in (A). Histograms showing the percentage of cells in each cell cycle stage (B) or in G2 (C) after MMC treatment. Mean ± SEM, n = 3, ** $p<0.01$. (D) Western blot of cells used in this experiment, confirming the PP2A catalytic subunits were efficiently reduced.

2.5 Discussion

In mammalian cells, the full repair of ICL lesions is achieved through the coordinated action of several DNA repair pathways. The FA pathway is thought to act at the early stage to bridge the detection of the ICL lesion to downstream repair events mediated by HR, NER and TLS (Lai *et al*, 2008). Thus there is substantial intricate crosstalk existing between the FA pathway and different DNA repair mechanisms during ICL repair. The key event of the FA pathway involves recruitment of the FANCD2/FANCI complex to chromatin, which subsequently orchestrates the recruitment of various DNA repair factors including nucleases that can lead to DSBs. Together these facts emphasise the importance of a strictly regulated FANCD2/FANCI complex. Recently, a new critical layer of regulation on FANCD2 activation mediated through CK2 dependent phosphorylation and dephosphorylation by a still unknow phosphatase was proposed (Lopez-Martinez *et al*, 2019; Lopez-Martinez, 2018). In the absence of ICLs, CK2 constitutively phosphorylates FANCD2 at the 882-898 six-residue cluster (Figure 2-1) keeping the FAND2/FANCI complex inactivate in a state with low DNA affinity to prevent cells from spurious activation of DNA repair. Dephosphorylation thus must take place prior to chromosomal recruitment and monoubiquitination upon ICL induction.

In the light of the data generated previously (Figure 2-2), we discovered that the phosphatase responsible for FANCD2 dephosphorylation is likely to be the serine/threonine phosphatase PP2A. This chapter describes results obtained from cell based *in vivo* experiments suggesting that FANCD2 is kept in an inactive state by CK2 in the absence of DNA damage. Upon DNA damage, the FANCD2/FANCI complex is dephosphorylated by PP2A, thereby licensing its DNA loading. After ICL induction in PP2A deficient cells, the complex is not monoubiquitinated and not recruited to chromatin in response to ICL damage in the absence of catalytically active PP2A (Figure 2-3 to 2-7). Importantly, the catalytic deficiency of PP2A itself did not alter the cell cycle profile in unperturbed conditions. However it led to a significant G2 arrest in cells exposed to the ICL inducing agent MMC, which resembles one of the common clinical features of FA patient cells (Figure 2-8) (Meetei *et al*, 2003; Sharp *et al*,

2020; Kaiser *et al*, 1982). Notably, the recruitment and ubiquitination of non-phosphorylatable 6A EGFP-FANCD2 were immune to PP2A depletion (Figure 2-7). This latter result implies that PP2A acts in response to ICL damage by mediating a direct dephosphorylation of the 882-898 six-residue cluster, thereby controlling the activity of FANCD2.

Overall, these data indicate that PP2A regulates the DNA binding and subsequent activating events of the FANCD2/FANCI complex by mediating the dephosphorylation at the 882-898 CK2 cluster. Lack of the PP2A catalytic activity can result in FA-like phenotypes. Nonetheless as discussed in chapter 1.3.2, the multifarious isoforms of the PP2A regulatory element (B) can form numerous functionally distinct PP2A heterotrimers with other functional subunits, and hence there are plenty variants of PP2A holoenzymes present in nature. Although we have observed that the absence of PP2A catalytic subunits (α and β) caused FA like phenotypes, it is still important to identify which variant of PP2A holoenzyme specifically dephosphorylates FANCD2 and hence regulating the FA pathway during ICL repair. This will be discussed in detail in Chapter 3.

Chapter 3. The PPP2R3A regulatory subunit of PP2A mediates FANCD2 dephosphorylation in response to ICLs

3.1 Introduction

We have found the serine/threonine phosphatase PP2A is potentially the phosphatase that dephosphorylates FANCD2 on the 882-898 six residue cluster and hence activating the FA pathway after ICL induction. Technically, PP2A is a diverse family comprising structurally and functionally distinct trimeric holoenzymes with the substrate specificity and subcellular localisation conferred by a specific regulatory B subunit (Seshacharyulu *et al*, 2013; Eichhorn *et al*, 2009; Ramos *et al*, 2019). To fully understand the role of PP2A played in the regulation of the FA pathway, it is necessary to confirm that the regulatory B subunit is responsible for dephosphorylating FANCD2 during ICL repair.

Although there are only two isoforms present in the catalytic C and scaffold A families, the regulatory B subunit is a much more multifarious family in which at least 26 different transcripts and splice variants encoded by 15 distinct genes are further characterised into four subfamilies (see Chapter 1.3.2). We summarised the names and subcellular distribution of the regulatory subunits based on the literature (Table 3.1) (Eichhorn *et al*, 2009; Seshacharyulu *et al*, 2013). Notably, the phospho-tyrosyl phosphatase activator (PTPA), or PPP2R4, is a special one among the regulatory subunits, as it was found to play important roles in a complicated mechanism that controls PP2A activity and biogenesis (Guo *et al*, 2014; Sents *et al*, 2013; Fellner *et al*, 2003; Hombauer *et al*, 2007). It is actually thought that PP2A catalytic subunits are synthesised *de novo* in an inactive conformation, bound to a negative regulator PP2A methyl esterase 1 (PME-1) (LONGIN *et al*, 2004). PTPA can activate the phospho-seryl/threonyl phosphatase activity of native inactive PP2A complex, by stabilising an active conformation of the PP2A catalytic subunit active site and promoting the loading of catalytic metal ions (Guo

et al, 2014). It also induces conformational change by acting as a peptidyl-prolyl cis/trans isomerase that targets the Pro190 on PP2A catalytic subunits, which facilitates PP2A to be released from the negative regulator PME-1 (Jordens *et al*, 2006). In yeast and mammalian cells, knock down of PTPA resembles a PP2A catalytically deficient state (Sents *et al*, 2013; Fellner *et al*, 2003; Hombauer *et al*, 2007). Therefore, PTPA is regarded as a PP2A activator rather than a specific regulatory subunit with distinct substrate specificity.

This chapter will discuss experiments conducted to identify the specific regulatory B subunit that dephosphorylates FANCD2, and the role that particular subunit plays in activating the FA pathway during ICL repair.

Family	Gene name	Other names	Subcellular distribution
Regulatory (B)	PPP2R2A	PR55α, PP2ABα	Membranes, cytoplasm, microtubules, Golgi complex, endoplasmic reticulum and nucleus
	PPP2R2B	PR55β, PP2ABβ	Cytoplasm
	PPP2R2C	PR55γ, PP2ABγ	Mainly in Cytoskeletal fraction
	PPP2R2D	PR55δ, PP2ABδ	Cytoplasm
Regulatory (B'')	PPP2R3A	PR130, PP2AB''α1 PR72, PP2AB''α2	Centrosome, Golgi complex Cytoplasm and nucleus
	PPP2R3B	PR70, PR48, PP2AB''β	Nucleus
	PPP2R3C	G5PR, G4-1	Nucleus
Regulatory (B')	PPP2R5A	PR56/ 61α, PP2AB'α	Cytoplasm
	PPP2R5B	PR56/ 61β, PP2AB'β	Cytoplasm
	PPP2R5C	PR56/ 61γ, PP2AB'γ	Cytoplasm and nucleus
	PPP2R5D	PR56/ 61δ, PP2AB'δ	Cytoplasm, mitochondria, microsomes and nucleus
	PPP2R5E	PR56/ 61ε, PP2AB'ε	Cytoplasm
_	PPP2R4	PTPA, PR53	Cytoplasm and nucleus
Regulatory (B''')	STRN	Striatin, PR110	Membrane and cytoplasm
	STRN3	SG2NA	Nucleus

Table 3.1 Isoforms of PP2A regulatory subunits. Table showing the gene name, alternative names and subcellular localisation of each isoform. Adapted from (Seshacharyulu *et al*, 2013; Eichhorn *et al*, 2009).

3.2 Identification of the PP2A regulatory B subunit regulating the FA pathway

Similar to the family wide screening performed previously (Figure 2-2), we knocked down each of the candidate regulatory subunits using siRNAs and determined whether they are involved in the activation of FANCD2 in response to ICL damage by assessing the FANCD2 monoubiquitination after TMP/UVA treatment. The 15 genes of regulatory subunits were split into two groups where 11 were tested first (Figure 3-1 A), followed by the last 4 (Figure 3-1 B). As expected, loss of the PP2A catalytic α and β subunits markedly abolished the induction of FANCD2 monoubiquitination (Figure 3-1 A, left panel lane 3), serving as a positive control for the siRNA transfection. Among all the candidates tested, depletion of the PP2A regulatory subunit PPP2R3A substantially and invariably resulted in the attenuation of FANCD2 monoubiquitination (Figure 3-1 A, left panel lane 8 and B, lane 4). Although some of the other subunits, such as PPP2R5A and PPP2R5E, also seemed to attenuate FANCD2 monoubiquitination when they were absent, the results were not reproducible (Figure 3-1 B top left and right panels, lanes 5 and 7). We also created small hairpin RNA (shRNA) constructs against 10 subunits. Generation of stable cell lines using these plasmids showed a similar result, which was that FANCD2 ubiquitination was consistently suppressed in cells where PPP2R3A was depleted (Figure 3-1 C, left panel lane 5). At the same time, it is worth noting that FANCD2 was also far less active in PTPA depleted cells (Figure 3-1 A, left panel lane 13 and C, left panel lane 10), which corresponds with the previous discovery that PTPA deficiency leads to PP2A catalytically defect related phenotypes.

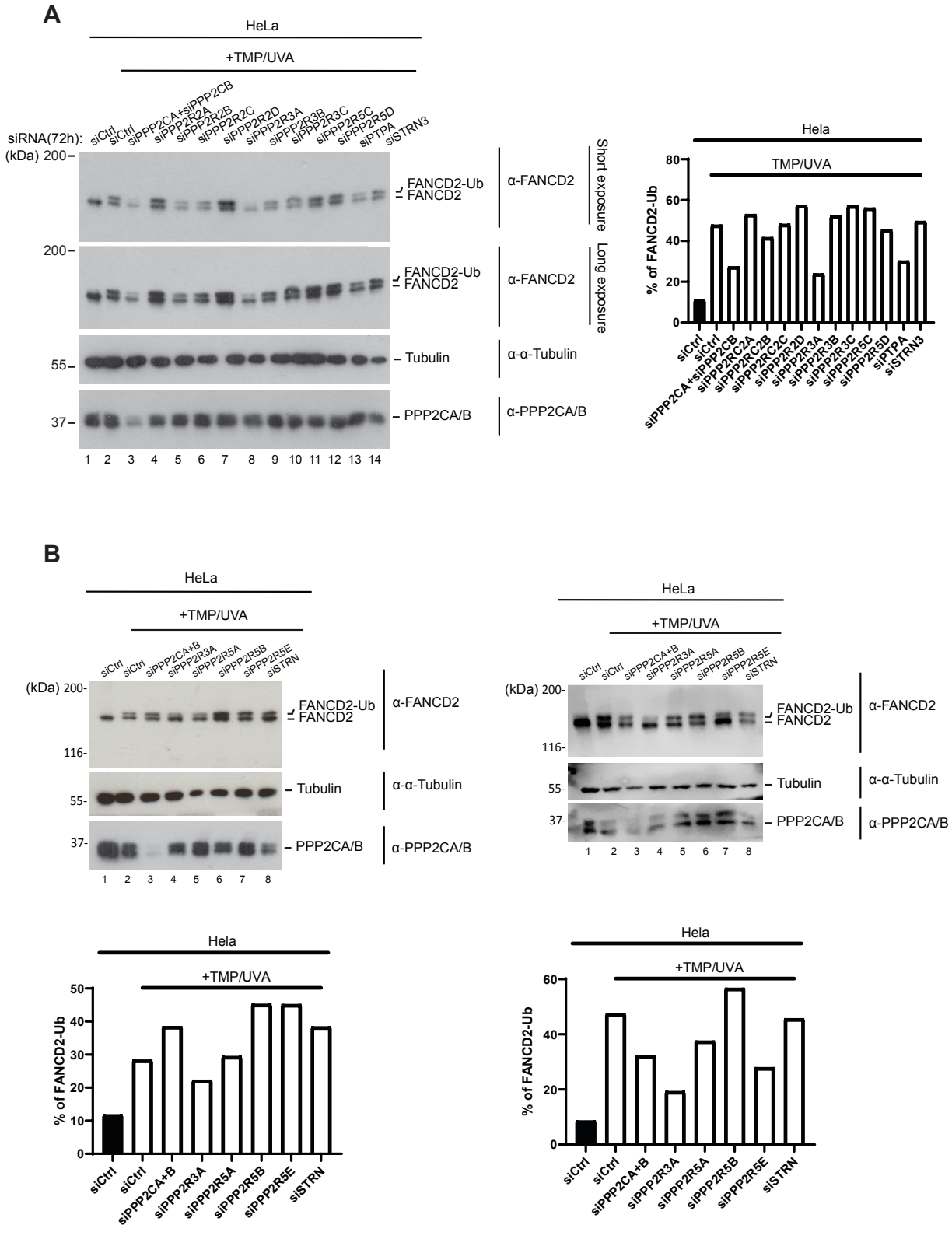
A
HeLa
+TMP/UVA
siRNA(72h):
siCtrl
siCtrl
siPPP2CA+siPPP2CB
siPPP2R2A
siPPP2R2B
siPPP2R2C
siPPP2R2D
siPPP2R3A
siPPP2R3B
siPPP2R3C
siPPP2R5C
siPPP2R5D
siPTPA
siSTRN3
(kDa) 200
200
55
37
FANCD2-Ub
FANCD2
Tubulin
PPP2CA/B
α-FANCD2
α-α-Tubulin
α-PPP2CA/B
Short exposure
Long exposure
1 2 3 4 5 6 7 8 9 10 11 12 13 14
Hela
TMP/UVA
% of FANCD2-Ub
0
20
40
60
80
siCtrl
siCtrl
siPPP2CA+siPPP2CB
siPPP2R2A
siPPP2R2B
siPPP2R2C
siPPP2R2D
siPPP2R3A
siPPP2R3B
siPPP2R3C
siPPP2R5C
siPPP2R5D
siPTPA
siSTRN3
B
HeLa
+TMP/UVA
siCtrl
siCtrl
siPPP2CA+B
siPPP2R3A
siPPP2R5A
siPPP2R5B
siPPP2R5E
siSTRN
(kDa) 200-
116-
55-
37-
FANCD2-Ub
FANCD2
Tubulin
PPP2CA/B
α-FANCD2
α-α-Tubulin
α-PPP2CA/B
1 2 3 4 5 6 7 8
Hela
+TMP/UVA
% of FANCD2-Ub
0
10
20
30
40
50
siCtrl
siCtrl
siPPP2CA+B
siPPP2R3A
siPPP2R5A
siPPP2R5B
siPPP2R5E
siSTRN
Hela
+TMP/UVA
% of FANCD2-Ub
0
20
40
60
siCtrl
siCtrl
siPPP2CA+B
siPPP2R3A
siPPP2R5A
siPPP2R5B
siPPP2R5E
siSTRN

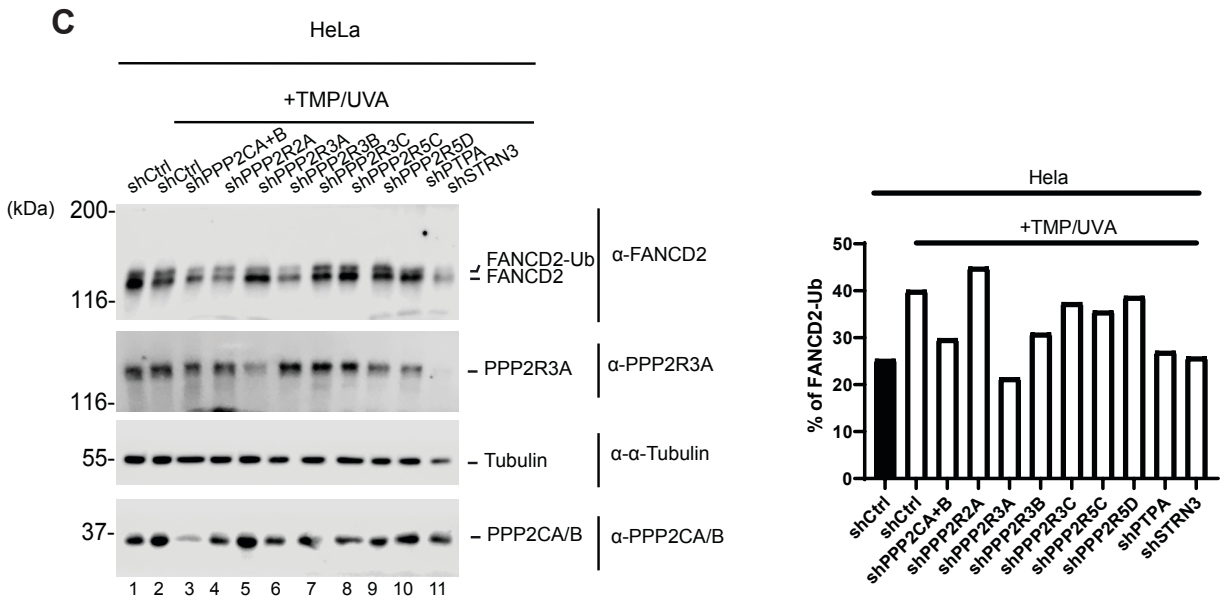

Figure 3-1 Screening for PP2A regulatory subunits activating the FA pathway. (A) (B) Representative Western blots and quantification showing the screening by siRNAs. Cells transfected with a non-targeting siRNA were used as the control. (C) The Western blot and quantification showing the screening by shRNAs. Targeting sequences used are shown in Materials & Methods. Cells transduced with a non-targeting shRNA were used as the control. Depletion of PPP2R3A constantly attenuated FANCD2 monoubiquitination. ICLs were induced by TMP (2 μg/ml) and UVA (50 mJ/cm^2).

PPP2R3A is found in both nucleus and cytoplasm, and it belongs to the PP2A regulatory B'' family that was firstly discovered by yeast two hybrid screening (Seshacharyulu *et al*, 2013). The gene *PPP2R3A* can be transcribed from two different promoters into two variants: PR130 and PR72, which differ at their N-terminal regions where PR130 has a longer stretch of 665 amino acids that is functionally replaced by 44 amino acids in PR72 (Eichhorn *et al*, 2009; Hendrix *et al*, 1993). The two variants display a tissue specific distribution: PR130 is ubiquitously expressed in all tissues and especially abundant in calcium rich tissues such as heart and skeletal muscle, while PR72 is only found in heart and skeletal muscle tissues (Dzulko *et al*, 2020; Zwaenepoel *et al*, 2008; Hendrix *et al*, 1993). HeLa is an immortal human epithelial cell line derived from a cancerous tumour of the cervix. As expected, we could only detect PR130 but not PR72 by Western blot from the HeLa lysate (data not shown). Therefore, the

observed phenotype of FANCD2 deficiency in PPP2R3A disrupted HeLa cells can be attributed to the loss of the PR130 variant.

PPP2R3A (PR130) associated PP2A can dephosphorylate a variety of important proteins, such as ATM, AKT and p53, that are involved in multiple vital signalling pathways regulating cancer related functions, such as cell proliferation, replicative stress response and tumour metastasis (Dzulko *et al*, 2020; Chen *et al*, 2019; Göder *et al*, 2018; Creyghton *et al*, 2006). It has been reported that reduced expression of PPP2R3A resulted in a higher level of the transcription factor p53 in hepatocellular carcinoma cells (Chen *et al*, 2019). To avoid unwanted side effects to the greatest extent potentially be caused by loss of PPP2R3A, we shortened the time of siRNA transfection from 72 h to 24 and 48 h. PPP2R3A protein levels were clearly already reduced 24 h post transfection and a reduced PPP2R3A did not influence p53 levels in HeLa cells (Figure 3-2 A and B, top panel lane 1 and 3, 4 and 6). A clear abrogated FANCD2 monoubiquitination could be observed in PPP2R3A depleted cells as early as 24 h post transfection (Figure 3-2 A, top panel lanes 4 and 6). Altogether, these data imply that FANCD2 cannot be activated, judged by its lack of ubiquitination, when PPP2R3A is absent.

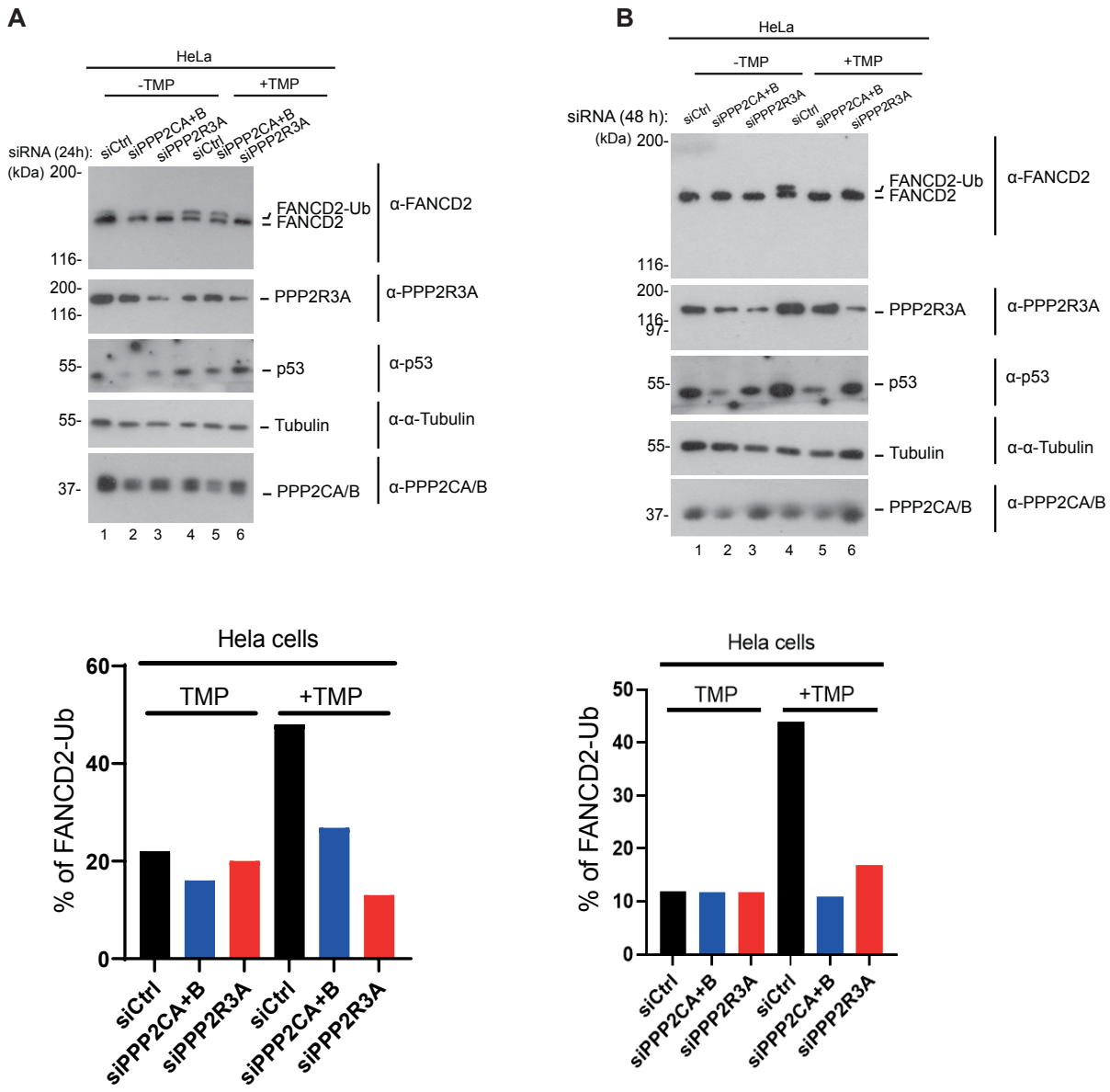

Figure 3-2 FANCD2 ubiquitination was reduced as early as 24h after PPP2R3A depletion *in vivo*. Representative Western blots and quantification of the monoubiquitination of FANCD2 in 24h (A) and 48 h (B) post PPP2R3A depletion. ICLs were induced by TMP (2 μg/ml) and UVA (50 mJ/cm^2).

3.3 Loss of PPP2R3A results in increased G2 population after MMC treatment

We have shown that FANCD2 is not ubiquitinated, and thus cannot be activated, in the absence of PPP2R3A in HeLa cells. Importantly, p53 is not influenced by the loss of PPP2R3A, and therefore the observed phenotype of functionally inactive FANCD2 is not relevant to p53 mediated signalling pathways. However, there is evidence suggesting that PPP2R3A is involved in cell cycle regulation through targeting p-ATM and p-CHK1 (Göder *et al*, 2018). Reduction of PPP2R3A attenuates cell growth of hepatocellular carcinoma cells explained by fewer cells in S and augmented G0/G1 and G2 populations (Chen *et al*, 2019). We therefore assessed whether the loss of PPP2R3A influences cell cycle distribution. Quantification of the FACS data shows that PPP2R3A depletion itself did not alter the cell cycle progression. However, depletion led to an additional 12% G2 arrest after MMC treatment compared to the control cells (Figure 3-3 A and B). Cells depleted for the catalytic subunit α and β, or the FANCD2 -/- cell line, presented with additional 22% and 45% G2 accumulation, respectively. The MMC treatment was generally more potent than that shown in Figure 2-8, as it can be seen from the fact that more G2 arrest was observed in the FANCD2 -/- cells. This might be due to batch variation of the MMC drug used. The knockdown of proteins in cell lines subjected to the FACS was validated by Western blot, which is shown in Figure 3-3 C.

The FACS data demonstrate that the FA pathway is not functional in cells deficient for PPP2R3A, in which a resembled FA phenotype of G2 arrest was observed after MMC exposure. Likewise, the phenotypes of a non-functional FA pathway obtained in cells lacking PPP2R3A were not caused by an impacted cell cycle progression with affected S population, in line with the result obtained in the PP2A catalytic α and β deficient cells (Chapter 2.4).

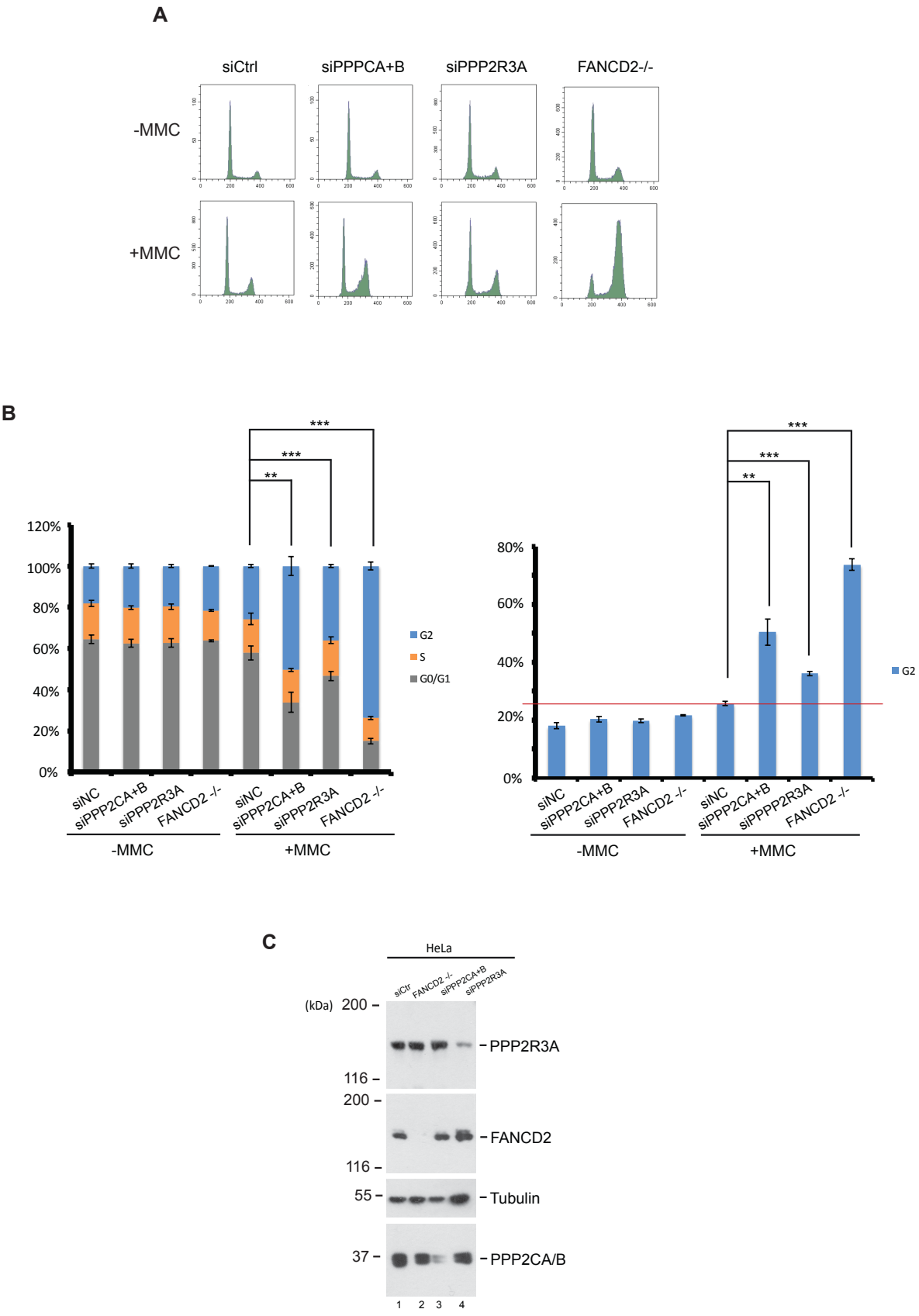
A
siCtrl
siPPPCA+B
siPPP2R3A
FANCD2-/-
-MMC
+MMC
B
120%
100%
80%
60%
40%
20%
0%
G2
S
G0/G1
siNC
siPPP2CA+B
siPPP2R3A
FANCD2 -/-
-MMC
+MMC
80%
60%
40%
20%
0%
G2
C
HeLa
siCtr
FANCD2 -/-
siPPP2CA+B
siPPP2R3A
(kDa)
200
116
200
116
55
37
PPP2R3A
FANCD2
Tubulin
PPP2CA/B
1 2 3 4

Figure 3-3 PPP2R3A depletion induces G2 accumulation without affecting S phase population after ICL induction. (A) Cell cycle profiles by DNA content of PPP2R3A depleted HeLa cells treated with 20 ng/mL MMC for 2 h followed by 24 h recovery. HeLa FANCD2 -/- cells were used as a positive control. (B) (C) Quantification of data in (A). Histograms showing the percentage of cells in each cell cycle stage (B) or in G2 (C) after MMC treatment. Mean ± SEM, n = 3, ** $p<0.01$, *** $p<0.001$. (D) Western blot of cells used in this experiment, confirming that the PPP2R3A was efficiently reduced.

3.4 The role of PPP2R3A in regulating the FA pathway

Since FANCD2 is not ubiquitinated and leads to an inactive FA pathway in the absence of PPP2R3A, we then looked deeper into the functional roles played by PPP2R3A in regulating the activity of FANCD2 during ICL repair.

As discussed in Chapter 2, we speculated that the dephosphorylation of FANCD2 happens at the 882-898 six residue cluster phosphorylated by CK2, and the dephosphorylation must take place prior to the recruitment to chromatin where the complex is further activated by monoubiquitination in response to ICLs. We therefore investigated the real-time accumulation of both WT and 6A EGFP-FANCD2 at ICLs in cells depleted for PPP2R3A using the live-cell imaging system described in Chapter 2.3. As expected, after ICL induction WT EGFP-FANCD2 was efficiently recruited and accumulated at the stripe area in control cells. In contrast, the recruitment was nearly abolished in cells without PPP2R3A (Figure 3-4 A, the first and second panels and B). Meanwhile, recruitment of the non-phosphorylable 6A EGFP-FANCD2 was not affected by the loss of PPP2R3A, which agrees with that observed in PP2A catalytic α and β deficient cells (Figure 3-4 A, the first, second and third panels and B). We also checked the FANCD2 recruitment in PTPA deficient cells that are expected to display a PP2A catalytically deficient phenotype. While recruitment of WT EGFP-FANCD2 largely decreased when PTPA is absent, the 6A mutant was immune to PTPA knock down (Figure 3-4 A, the fourth panel and B), resonating with the observation of a defective FANCD2 ubiquitination shown in Figure 3-1. Thus, as expected, depleting PTPA phenocopies depletion of PPP2R3A.

These live-cell imaging data show that FANCD2 cannot be recruited to chromatin without PPP2R3A. Chromosomal loading of FANCD2 needs to be licensed by the PPP2R3A associated PP2A, via dephosphorylating of FANCD2 at the CK2 phosphorylated 882-898 cluster in response to ICLs.

A

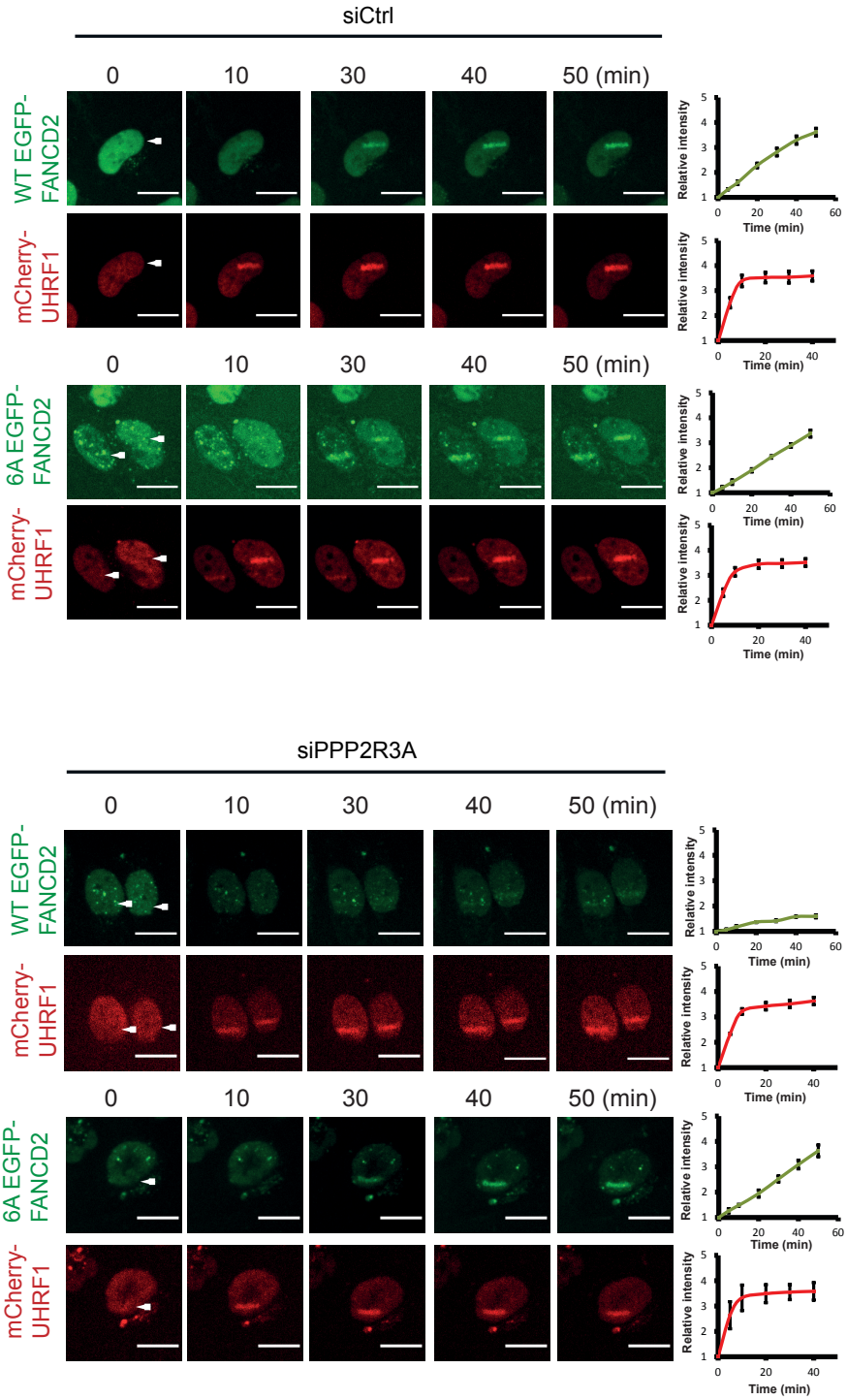
siCtrl
0
10
30
40
50 (min)
WT EGFP-FANCD2
mCherry-UHRF1
6A EGFP-FANCD2
mCherry-UHRF1
Relative intensity
Time (min)
siPPP2R3A
0
10
30
40
50 (min)
WT EGFP-FANCD2
mCherry-UHRF1
6A EGFP-FANCD2
mCherry-UHRF1
Relative intensity
Time (min)

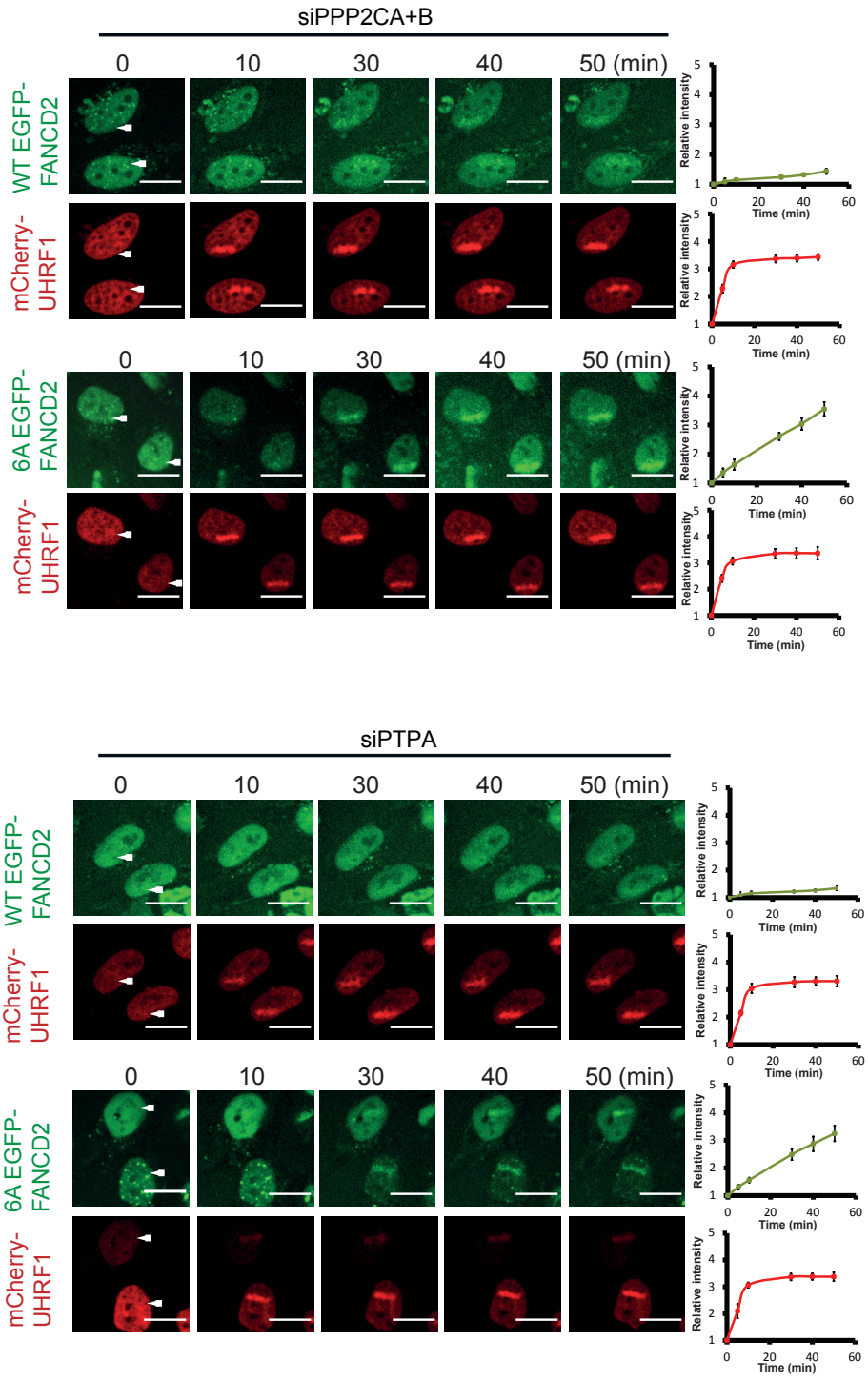
siPPP2CA+B
0
10
30
40
50 (min)
WT EGFP-FANCD2
mCherry-UHRF1
6A EGFP-FANCD2
mCherry-UHRF1
Relative intensity
Time (min)
siPTPA
0
10
30
40
50 (min)
WT EGFP-FANCD2
mCherry-UHRF1
6A EGFP-FANCD2
mCherry-UHRF1
Relative intensity
Time (min)

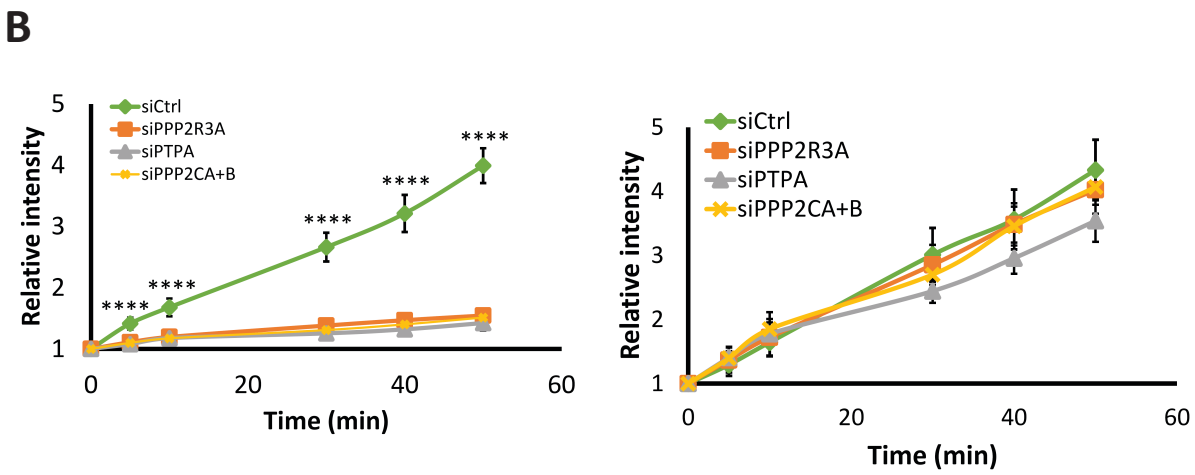

Figure 3-4 Chromatin recruitment of the non-phosphorylable 6A FANCD2 mutant is immune to PPP2R3A depletion *in vivo*. (A) Representative live cell imaging and quantification of HeLa FANCD2 -/- complemented with either EGFP-FANCD2 or 6A-EGFP-FANCD2. Cells were transfected with siRNAs targeting either the PP2A catalytic subunits, PPP2R3A or PTPA (a positive control) respectively. Similarly, cells were treated with 20 µg/ml TMP and micro-irradiated by a 405 nM UVA laser at the indicated areas (white arrows). Images were recorded at the indicated time points post irradiation. (B) Quantification of FANCD2 recruitment of the three biological replicates in (A). 5 cells were quantified in each replicate (15 cells for three replicates of each sample), Mean ± SD, Scale bar: 10 µm. **** $p<0.0001$.

Colleagues in our group have previously shown that the 882-898 CK2 phosphorylation cluster is functionally important for the activity and regulation of the FANCD2/FANCI complex. FANCD2 -/- cells complemented with the mutant derivative where the six phosphorylation sites in the cluster have been mutated to aspartic acid residues to mimic a constitutive phosphorylation (6D FANCD2) and the resulting cell line was subjected to a clonogenic survival assay under increasing concentrations of MMC (Lopez-Martinez *et al*, 2019; Lopez-Martinez, 2018). The 6D FANCD2 was dramatically less functional compared to WT FANCD2, endowing cells with much greater sensitivity after MMC exposure. This indicates that FANCD2 stays in an inactive state as the six-residue cluster remains phosphorylated. We therefore hypothesised that PPP2R3A mediated dephosphorylation is functionally important for the activation of the FANCD2/FANCI complex during ICL repair. In order to test whether PPP2R3A depletion leads to sensitivity to ICL inducing agents, we decided to conduct a clonogenic survival assay with FANCD2 and PPP2R3A deficient cells. In mammalian cells, it has been suggested that the NEIL3 mediated ICL repair pathway is the major pathway that repairs

psoralen- and AP-ICLs, whereas the FA pathway is mainly responsible for clearing MMC and cisplatin induced ICLs (Chapter 1.2.2) (Li *et al*, 2020; Wu *et al*, 2019). To exclude the effect of the NEIL3 pathway, we generated PPP2R3A -/- and FANCD2 -/-, PPP2R3A -/- cell lines by the CRISPR/Cas9 system and performed a similar survival assay under increasing doses of MMC exposure (0.125 – 3 ng/ml).

We first knocked-out *PPP2R3A* in WT HeLa cells to create a PPP2R3A -/- cell line. Clones were screened by Western blot to assess the loss of PPP2R3A expression (Figure 3-5 A). We obtained several positive clones, which we assessed for FANCD2 monoubiquitination following the introduction of ICLs and compared them to WT cells. As expected, cells lacking an intact *PPP2R3A* gene showed a significantly weaker FANCD2 monoubiquitination after ICL induction (Figure 3-5 B). We then knocked-out *PPP2R3A* in FANCD2 -/- cells (Figure 3-5 C) and subjected the FANCD2 -/- + PPP2R3A -/- cell line together with the PPP2R3A -/- cells to the sensitivity assay to assess their ability to survive after the introduction of increasing amounts of MMC. The two PPP2R3A -/- clones we tested were both more sensitive to MMC exposure when compared to control cells (Figure 3-5 D), which is in line with the observed phenotype of a deficient FANCD2 monoubiquitination shown in Figure 3-5 B. Disruption of the *FANCD2* gene itself made cells extremely sensitive to MMC exposure, to a greater extent than that observed in PPP2R3A -/- cells. Importantly, as we knocked-out *PPP2R3A* in FANCD2 -/- cells, we did not observe further sensitization (Figure 3-5 D). Altogether, these data indicated that PPP2R3A plays a role in regulating the repair of MMC induced ICL lesions and suggest a role for PPP2R3A upstream of FANCD2 in the FA pathway.

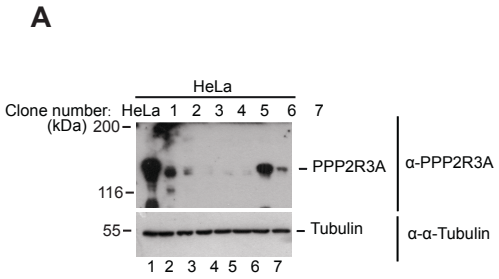
A
HeLa
Clone number: HeLa 1 2 3 4 5 6 7
(kDa) 200
116
55
PPP2R3A
Tubulin
α-PPP2R3A
α-α-Tubulin
1 2 3 4 5 6 7

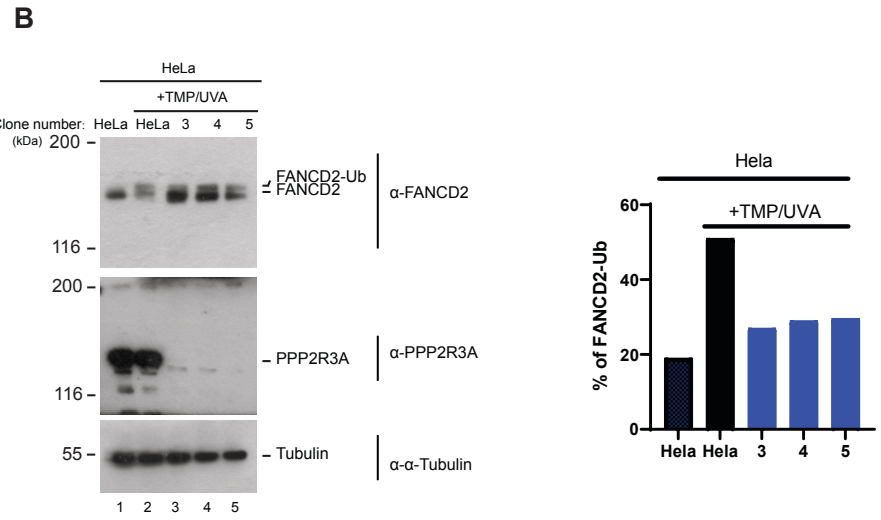
B
HeLa
+TMP/UVA
Clone number: HeLa HeLa 3 4 5
(kDa) 200
116
200
116
55
FANCD2-Ub
FANCD2
PPP2R3A
Tubulin
α-FANCD2
α-PPP2R3A
α-α-Tubulin
1 2 3 4 5
Hela
+TMP/UVA
% of FANCD2-Ub
60
40
20
0
Hela Hela 3 4 5

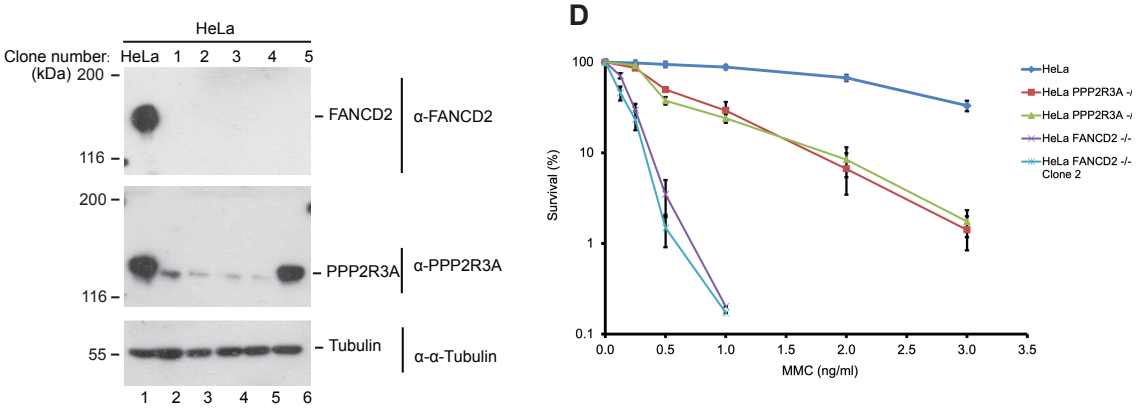
C
HeLa
Clone number: HeLa 1 2 3 4 5
(kDa) 200
116
200
116
55
FANCD2
PPP2R3A
Tubulin
α-FANCD2
α-PPP2R3A
α-α-Tubulin
1 2 3 4 5 6
D
Survival (%)
100
10
1
0.1
0.0 0.5 1.0 1.5 2.0 2.5 3.0 3.5
MMC (ng/ml)
HeLa
HeLa PPP2R3A -/-
HeLa PPP2R3A -/-
HeLa FANCD2 -/-
HeLa FANCD2 -/-
Clone 2

Figure 3-5 Loss of PPP2R3A leads to attenuated FANCD2 ubiquitination and increased MMC sensitivity. (A) Western blot of screening for PPP2R3A -/- clones knocked out with CRISPR/Cas9. (B) Representative Western blot and quantification of FANCD2 ubiquitination in PPP2R3A -/- clones after TMP (2 μg/ml) and UVA (50 mJ/cm^2) treatment. (C) Western blot of screening for FANCD2 -/- + PPP2R3A -/- clones knocked out with CRISPR/Cas9. (D) Clonogenic survival assay of wild type HeLa, HeLa PPP2R3A -/- and HeLa FANCD2 -/- + PPP2R3A -/- clones to MMC added at the indicated concentrations (ng/ml). FANCD2 -/- cells were used as the positive control. Cells were harvested 14 days after treatment. (Mean ± SEM, n=3).

3.5 Discussion

We have characterised the PP2A regulatory subunit PPP2R3A, and to be more precise, PR130 is responsible for dephosphorylating and the activation of FANCD2 in response to ICLs. Cells lacking PPP2R3A displayed a defective FA pathway after ICL induction, reflected by a non-functional FANCD2 with reduced monoubiquitination and chromatin recruitment. Notably, depleting the PP2A catalytic α and β subunits led to greater G2 arrest than depleting PPP2R3A after MMC exposure (Figure 3-3), although they caused a similar reduction in FANCD2 ubiquitination and chromatin recruitment (Figure 3-1, 3-2 and 3-4). This could be explained by the multifarious functions of PP2A. Directly blocking the catalytic activity can potentially affect a variety of other important signalling pathways whose disruption can make the cell more vulnerable to external stress. FANCD2 -/- cells displayed the greatest extent of inhibition of the FA pathway among all the cell lines tested, as it can seen from the FACS and clonogenic data. Considering the amount of FANCD2 protein in the PPP2R3A -/- cells is still normal, as opposed to the FANCD2 -/- cells, perhaps some proteins of FANCD2 escape dephosphorylation or are dephosphorylated by other phosphatase, hence remaining active. Besides, cells subjected to Western blot and live-cell imaging were harvested or analysed within hours after the induction of ICLs by TMP/UVA, while the cell cycle profile was assessed the next day post MMC exposure. So, the timescale was different. There could be functional redundancy existing between PPP2R3A and other regulatory subunits, especially after a long time of losing the PPP2R3A protein. In line with our hypothesis, we could observe an epistatic relationship between PPP2R3A and FANCD2 as depleting PPP2R3A did not further sensitise FANCD2 -/- cells to MMC treatment (Figure 3-5 D), suggesting that PPP2R3A is likely to regulate and act on FANCD2 in the FA pathway.

PP2A is a diverse and multifunctional family in which each phosphatase member regulates very distinct cellular mechanisms. In fact, the cellular functions of PPP2R3A have not been widely studied. There is increasing evidence suggesting that it is a critical mediator of tumour relevant pathways and ontogenetic transformation, and low expression of PPP2R3A

has been linked to elevated p53 level in certain cancer cell lines (Dzulko *et al*, 2020; Chen *et al*, 2019). We could already observe deficient FANCD2 ubiquitination as early as 24 h post RNAi transfection when the protein level of PPP2R3A starts to reduce, without affecting p53 (Figure 3-2) or the cell cycle progression (Figure 3-3), suggesting that the dysfunctional FANCD2 is not a side effect of other disrupted biological processes due to loss of PPP2R3A.

So far, data from several *in vivo* experiments have successfully helped us to elucidate the roles of PPP2R3A/PP2A mediated dephosphorylation at the 882-898 cluster on FANCD2 in controlling the FANCD2/FANCI complex activation. It is clear that PPP2R3A plays an essential role in activating the FA pathway by mediating the chromatin recruitment and hence the monoubiquitination of FANCD2, and that it is functionally important for the cellular survival after exposure to ICL inducing agents. However, in the *in vivo* setting it is difficult to resolve the direct and precise mechanism behind the activating role of PPP2R3A mediated dephosphorylation. We therefore reconstituted an *in vitro* setting that allows us to analyse the dephosphorylation and monoubiquitination more precisely, which will be discussed in Chapter 4.

Chapter 4. Dephosphorylation of FANCD2 by PPP2R3A/PP2A activates the FANCD2/FANCI complex *in vitro*

4.1 Introduction

To obtain more direct evidence for elucidating the precise mechanism behind the activating role of PPP2R3A mediated dephosphorylation on FANCD2, we constituted an in vitro setting with purified recombinant proteins that can help us to recapitulate the in vivo scenario to study the regulation of FANCD2 function. In order to reconstitute the dephosphorylation of FANCD2, we firstly tried to purify the heterotrimeric holo-enzyme of PPP2R3A (PR130)/PP2A as a recombinant protein from Sf9 cells. The levels of PP2A catalytic subunits are strictly regulated at translational and post-translational levels, therefore making massive expression of these proteins is extremely difficult (Baharians & Schönthal, 1998). The successful purification of PP2A has been quite challenging, as the standars of yield, purity and stability required for *in vitro* enzymatic assay are hard to meet (Ikehara et al, 2016). Previously, purification of several distinct variants of PP2A holoenzymes has been reported in different systems. Some were purified from different animal tissues and organisms such as rabbit skeletal muscle and bovine cardiac tissue (Tehrani et al, 1996; ZOLNIEROWICZ et al, 1996; Hendrix et al, 1993b), which requires several kilograms of tissue followed by column chromatography (Ikehara et al, 2006). Transient or stable overexpression and purification of recombinant PP2A have also been reported in mammalian cells, yeast and insect cells (Ikehara et al, 2006; Wadzinski et al, 1992; Evans et al, 1999). However, none of these systems produced recombinant PP2A in high yields. Since the baculovirus system with Sf9 cells has helped us to successfully purify many proteins before, we therefore decided to utilise it first to try to obtain a biologically active recombinant PPP2R3A (PR130)/PP2A.

In mammalian cells, the E3 ligase FANCL is associated with another seven FANC proteins (FANCA, FANCB, FANCC, FANCE, FANCF, FANCG and FAAP100) to form a large protein complex, the FA core complex, which catalyses the monoubiquitination of the FANCD2/FANCI complex (Rajendra et al, 2014; Huang et al, 2014). The core complex comprises a central scaffold formed through the interactions between two dimers of the FANCB and FAAP100 subunits, flanked by two copies of FANCL respectively (Shakeel et al, 2019). This central scaffold formed by the FANCB/FAAP100 dimer assembles the remaining five subunits, resulting in an asymmetric structure that ensures a balanced FANCD2 and FANCI ubiquitination (Twest et al, 2017; Shakeel et al, 2019; Swuec et al, 2017). In cell-free systems, monoubiquitination of FANCD2 can be recapitulated efficiently only in the presence of DNA (Sato et al, 2012; Longerich et al, 2014; Twest et al, 2017; Rajendra et al, 2014). It is generally believed that DNA binding exposes the FANCD2 K561 monoubiquitination site that is buried at the FANCD2/FANCI dimer interface, hence allowing the ubiquitin conjugation (Alcón et al, 2020; Wang et al, 2020). In contrast, while monoubiquitination of FANCD2 is a signal of the FA pathway activation, the importance of FANCI monoubiquitination is disputable. FANCI monoubiquitination is poorly recapitulated in vitro. It can only be mildly monoubiquitinated by purified *Gallus gallus* (Twest et al, 2017; Rajendra et al, 2014) and human FA core complexes (Shakeel et al, 2019; Wang et al, 2020; Alcón et al, 2020). Indeed, the monoubiquitination site mutated FANCI can still largely rescue cell survival after ICL induction (Ishiai et al, 2008; Smogorzewska et al, 2007), suggesting that the dependence of the FA pathway on FANCI ubiquitination is minor.

Initially, the very first in vitro ubiquitination reactions were simply performed with the E1 ubiquitin-activating enzyme UBA1, E2 ubiquitin-conjugating enzyme UBE2T, the E3 ubiquitin- ligase FANCL, ubiquitin, the substrate FANCD2/FANCI complex and DNA (Sato et al, 2012; Longerich et al, 2014). Later it was found that adding the FANCA/G and FANCC/E/F to the FANCB/L/FAAP100 complex could significantly promote FANCD2 monoubiquitination, although the FANCI monoubiquitination remained inefficient (Twest *et al*, 2017; Wang *et al*,

2020). Overall, the reactions taking place in an *in vitro* context can be a useful tool for us to better understand the regulating mechanisms of the FA pathway.

4.2 Purification of PPP2R3A/PP2A holo-enzyme from insect cells

In order to reconstitute the dephosphorylation reaction *in vitro*, we aimed to purify the PPP2R3A/PP2A as a recombinant trimeric protein complex. In fact, the scaffold subunit PPP2R1A is ubiquitously expressed and is typically 10-100% more abundant than the PPP2R1B in cells (ZHOU et al, 2003), and the catalytic α subunit PPP2CA is about 10 times more abundant than the β PPP2CB (Khew-Goodall & Hemmings, 1988). We therefore decided to clone the His-PPP2R1A/Flag-PPP2CA/HA-PPP2R3A genes into the MultiBac baculovirus expression vector system and co-express them in insect Sf9 cells. We firstly checked whether the PPP2R3A (PR130)/PP2A trimer can be stably overexpressed in Sf9 cells. Four independent recombinant bacmids were selected using blue/white selection (see Materials & Methods) and transfected into Sf9 cells to generate recombinant baculovirus respectively. We tested them by Western blot and observed that all of the three subunits were expressed (Figure 4-1). The baculovirus produced from bacmid 1 was selected to transduce Sf9 cells for the large-scale protein purification.

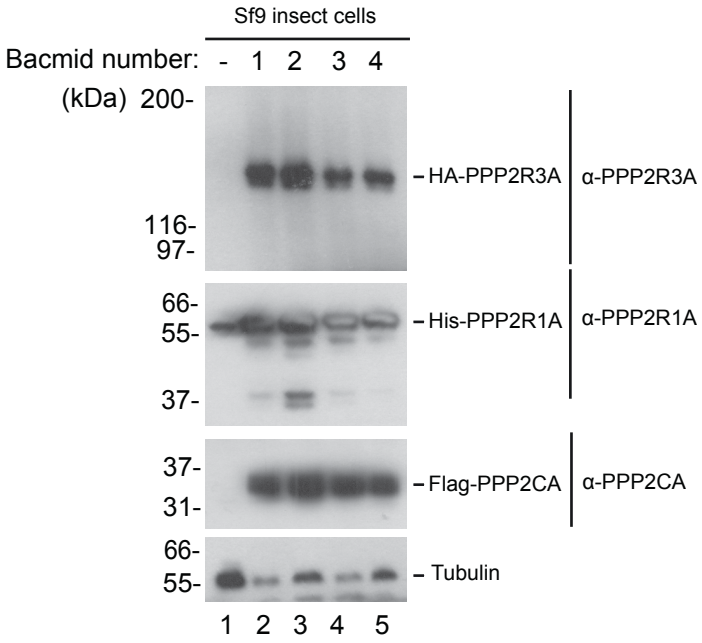

Figure 4-1 The PPP2R3A/PP2A subunits are stably expressed in Sf9 cells. Western blot confirming that all of the three subunits (with different tags) of PPP2R3A/PP2A holoenzyme can be stably over-expressed in Sf9 cells transfected with the MultiBac™ bacmids.

The purification process is summarised in Figure 4-2. We firstly purified the complex by an anti-Flag M2 agarose. Thereafter, the complex was further purified by gel-filtration (Superdex® 200) and an anion-exchange (Mono QTM) column. Finally, the sample was concentrated by PEG dialysis.

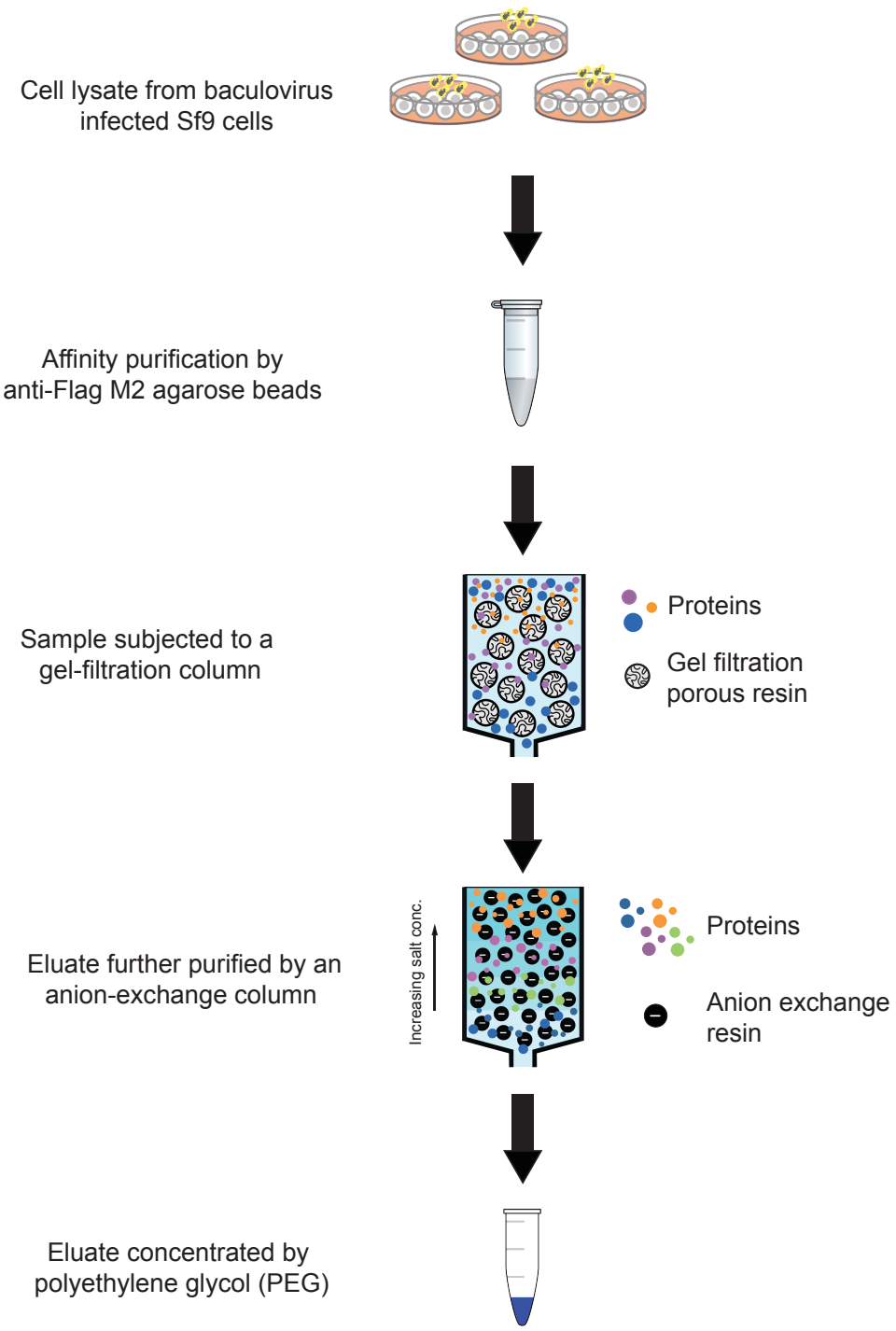

Figure 4-2 Schematic representation of the PPP2R3A holoenzyme purification process. Sf9 insect cells were infected with the PPP2R3A holoenzyme (His-PPP2R1A, Flag-PPP2CA and HA-PPP2R3A) baculovirus generated by the MultiBac™ expression system described in Materials & Methods. The trimer was firstly collected by an anti-Flag purification of the cell lysate against Flag-PPP2CA (the catalytic subunit) with M2 agarose, and then subjected to gel filtration followed by ion-exchange chromatography. Finally, the protein sample was concentrated by PEG for further *in vitro* assays.

The gel-filtration column separates protein molecules on the basis of their sizes. Indeed, The Flag-tag affinity purified protein sample of PPP2R3A was further separated into several peaks, of which a major peak emerged first in fractions 6-13 followed by several small peaks appearing later (Figure 4-3 A). The PPP2R3A trimer was eluted into fractions 6-13 where the big peak emerges, while the peaks that came out later turned out to be His-PPP2R1A/Flag-PPP2CA dimers as well as other impurities (Figure 4-3 B). However, the eluate still contains some unwanted proteins that cannot be separated by the gel-filtration columns. We therefore combined samples from fractions 7-9 in which the three PP2A subunits showed homogeneity and thus we tried to further improve the purity using anion-exchange chromatography. The combined sample resulted in several continuous peaks after purification on the anion-exchange column, where the PP2A trimer was enriched in fractions 35-38 eluted at a salt concentration of approximately 300 mM (Figure 4-4 A and B). Although the purification did not give a high yield, the purity was significantly improved (Figure 4-4 B). Fractions 35-38 were then combined and concentrated by dialysis using polyethylene glycerol (PEG), loaded on an SDS-PAGE gel and stained by Coomassie (Figure 4-4 C). Activity of the PEG concentrated PPP2R3A/PP2A trimer was subsequently tested *in vitro*, which is discussed in Chapter 4.3.

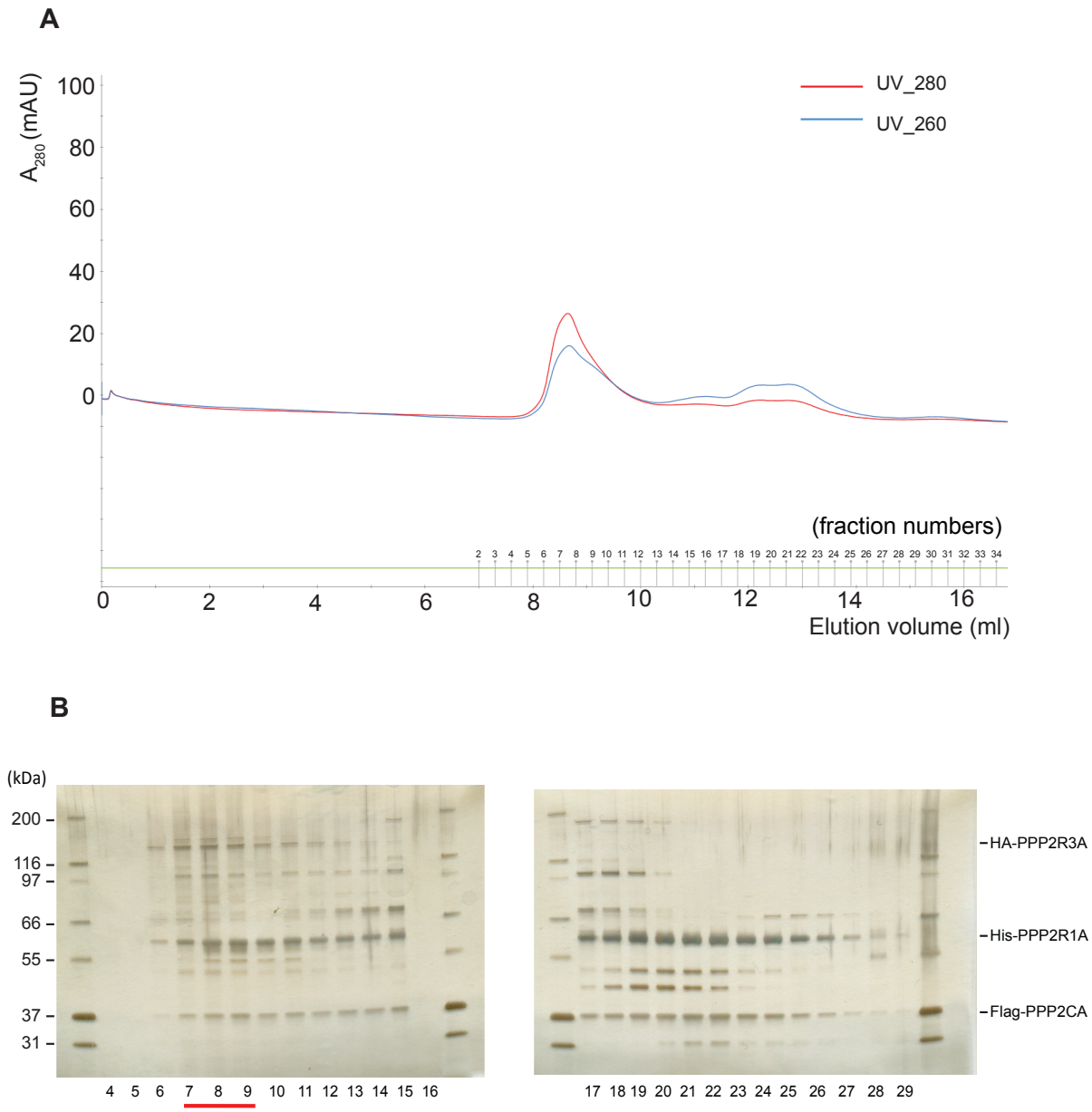

Figure 4-3 Gel filtration chromatography of the PPP2R3A/PP2A trimer. (A) Elution profile of the trimer after passing through the Superdex® 200 gel filtration column. 500 µl eluate in each fraction. UV 280 nm: trypsin absorbance. UV 260 nm: DNA absorbance. Y-axis: absorption at 280 nm (mAU). X-axis: elution volume. (B) Silver stain of protein fractions collected in (A). 20 µl out of 500 µl eluate was loaded in each well. The PPP2R3A/PP2A trimer was enriched in fraction numbers 7-9. Samples were combined and subsequently subjected to ion-exchange chromatography.

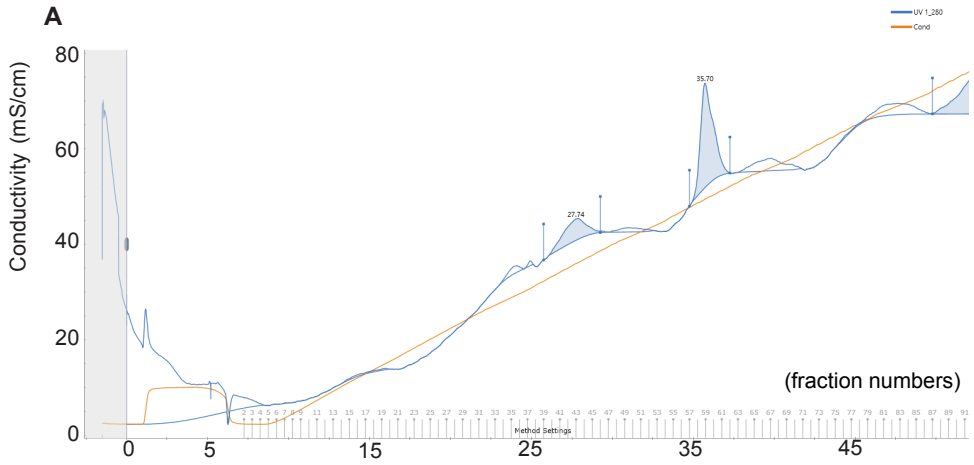
A
UV 1_280
Cond
Conductivity (mS/cm)
80
60
40
20
0
35.70
27.74
(fraction numbers)
0
5
15
25
35
45

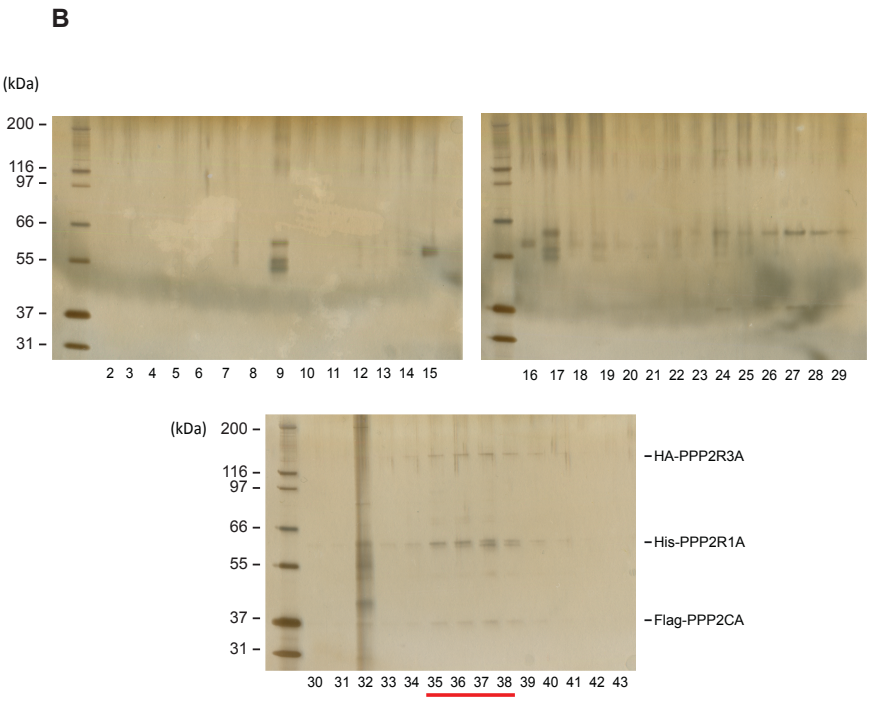
B
(kDa)
200
116
97
66
55
37
31
2 3 4 5 6 7 8 9 10 11 12 13 14 15
16 17 18 19 20 21 22 23 24 25 26 27 28 29
(kDa)
200
116
97
66
55
37
31
HA-PPP2R3A
His-PPP2R1A
Flag-PPP2CA
30 31 32 33 34 35 36 37 38 39 40 41 42 43

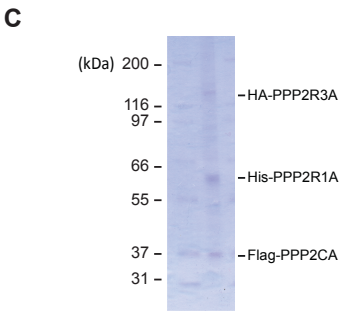
C
(kDa)
200
116
97
66
55
37
31
HA-PPP2R3A
His-PPP2R1A
Flag-PPP2CA

Figure 4-4 Ion-exchange chromatography of the PPP2R3A/PP2A trimer. (A) Elution profile of the gel filtration purified trimer after passing through the Mono Q™ anion-exchange column. 500 µl eluate in each fraction. UV 280 nm: trypsin absorbance. Conductivity: salt concentration (KCl) in the buffer. Y-axis: conductivity (salt conc., mS/cm). X-axis: elution volume. (B) Silver stain of protein fractions collected in (A). 20 µl out of 500 µl eluate was loaded to each well. The PPP2R3A/PP2A trimer was enriched in fraction numbers 35-38 eluted at around 300 mM KCl. Samples were subsequently combined and concentrated by PEG. (C) Coomassie stain of the PEG concentrated samples eluted in (B).

4.3 Effect of FANCD2 dephosphorylation by PPP2R3A/PP2A on its *in vitro* activity

In order to test whether the purified PPP2R3A trimer was fully active, we first purified the FANCD2/FANCI complex to homogeneity from Sf9 cells. Using affinity chromatography and gel filtration, a homogenous protein complex was purified (Figure 4-5 A). The complex could then be used for reconstitution of the phosphorylation and dephosphorylation reactions *in vitro*. The recombinant FANCD2/FANCI complex was phosphorylated *in vitro* by CK2 enzyme obtained from a commercial supplier, and its phosphorylation status assessed by Western blot analysis using a pan-phospho-serine/threonine antibody specific for CK2-mediated phosphorylation. Robust phosphorylation was observed (Figure 4-5 B, lane 2). We then subjected the phosphorylated substrate to a dephosphorylation reaction using the purified PPP2R3A/PP2A holoenzyme in the presence of other essential components (see Materials and Methods for detail). As expected, we observed a reduction in CK2 phosphorylated FANCD2 after PPP2R3A/PP2A treatment (Figure 4-5 B, lane 3), which was prevented by addition of the PP2A inhibitor OA (Figure 4-5 B, lane 4). We also dephosphorylated CK2 treated FANCD2 with a commercial lambda protein phosphatase (λPP) that has a broad activity towards phosphorylated residues by different kinases, which completely removed all the detectable phosphorylation signal of FANCD2 (Figure 4-5 B, lane 5). This raises the possibility that the residual signal of phosphorylated FANCD2 after PPP2R3A/PP2A treatment might come from other sites that are not phosphorylated by CK2. Meanwhile, the PPP2R3A trimer could not antagonise the phosphorylation catalysed by ATR (purified in our laboratory by a colleague, Figure 4-5 C, lanes 2 and 3), underscoring the specificity of the PPP2R3A/PP2A holoenzyme towards CK2 phosphorylated sites on FANCD2. These data indicate that the purified trimer is catalytically active *in vitro*, and that it can specifically dephosphorylate sites on FANCD2 that have been phosphorylated by CK2.

Next, we tested whether the dynamic CK2 phosphorylation and PPP2R3A dephosphorylation control the activity of the FANCD2/FANCI complex *in vitro*. We first reconstituted the monoubiquitination reaction by incubating purified recombinant E1/E2/E3 and ubiquitin proteins with the FANCD2/FANCI complex, in the presence of a double-stranded DNA plasmid (Lopez-Martinez & D., 2018; Lopez-Martinez et al, 2019). This set-up allows us to assess the propensity of the complex as substrate for ubiquitination before and after treatment of CK2 and PPP2R3A. FANCD2 was efficiently monoubiquitinated in the reaction (Figure 4-5 D, lanes 2 and 3). Under the same assay conditions, CK2 phosphorylation weakened the ubiquitination reaction (Figure 4-5 D, lanes 4 and 5, Figure 4-5 E). Strikingly, the CK2-mediated reduction in FANCD2 monoubiquitination could be rescued by subsequent PPP2R3A treatment (Figure 4-5 D, lanes 6 and 7), but not in the presence of OA (Figure 4-5 D, lane 8 and 9) (Figure 4-5 E). Taken together, our *in vitro* data demonstrate that the purified PPP2R3A/PP2A holoenzyme is catalytic active and that it can specifically dephosphorylate FANCD2 that is prior phosphorylated by CK2. Importantly, the PPP2R3A/PP2A holoenzyme is able to activate the FANCD2/FANCI complex, which has been previously inactivated by CK2. These data are in good agreement with the observations *in vivo*, presented in previous chapters.

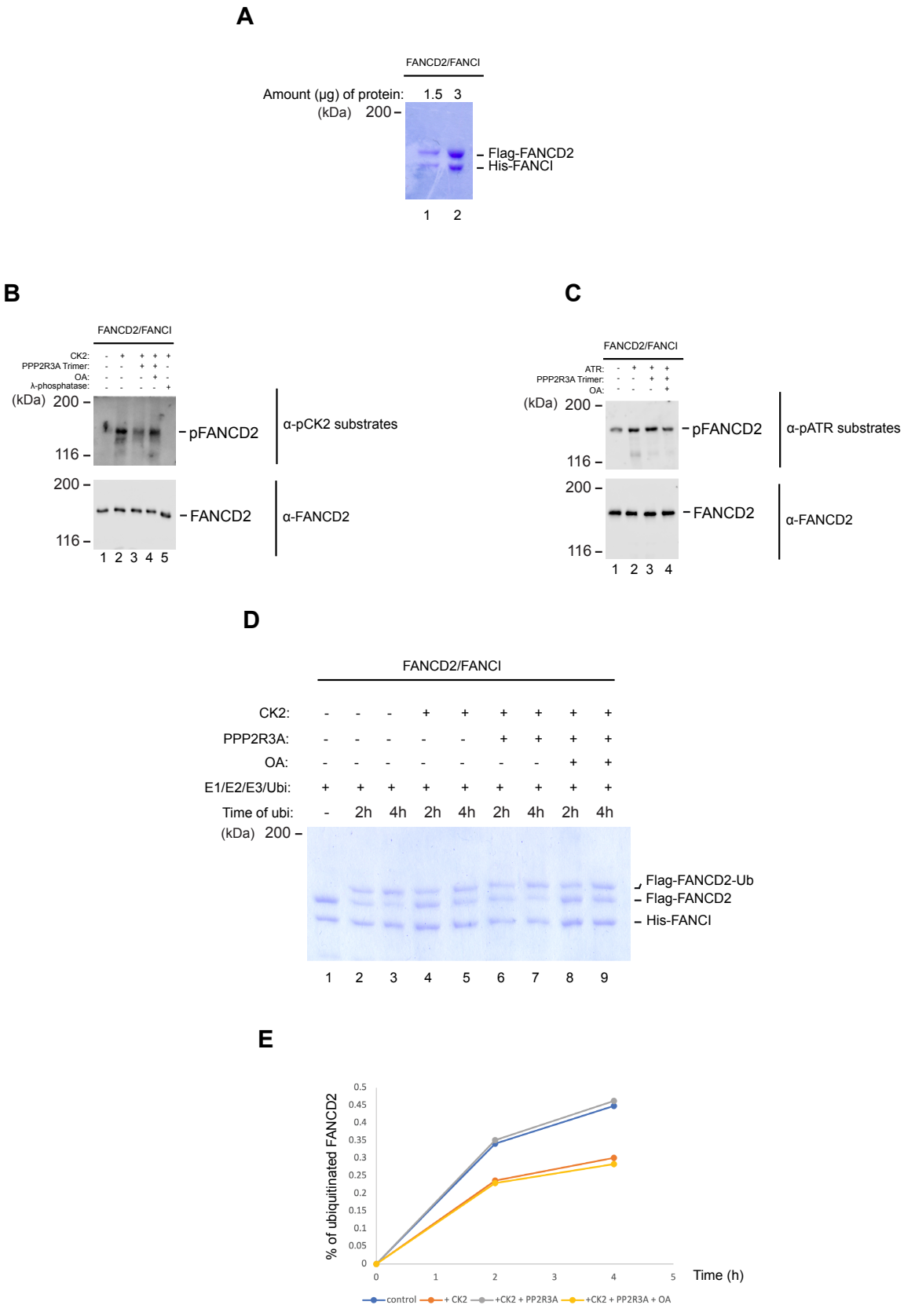
A
FANCD2/FANCI
Amount (μg) of protein: 1.5 3
(kDa) 200 –
– Flag-FANCD2
– His-FANCI
1 2
B
FANCD2/FANCI
CK2:
PPP2R3A Trimer:
OA:
λ-phosphatase:
(kDa) 200 –
116 –
– pFANCD2
α-pCK2 substrates
200 –
116 –
– FANCD2
α-FANCD2
1 2 3 4 5
C
FANCD2/FANCI
ATR:
PPP2R3A Trimer:
OA:
(kDa) 200 –
116 –
– pFANCD2
α-pATR substrates
200 –
116 –
– FANCD2
α-FANCD2
1 2 3 4
D
FANCD2/FANCI
CK2: - - - + + + + + +
PPP2R3A: - - - - - + + + +
OA: - - - - - - - + +
E1/E2/E3/Ubi: + + + + + + + + +
Time of ubi: - 2h 4h 2h 4h 2h 4h 2h 4h
(kDa) 200 –
– Flag-FANCD2-Ub
– Flag-FANCD2
– His-FANCI
1 2 3 4 5 6 7 8 9
E
% of ubiquitinated FANCD2
0.5
0.45
0.4
0.35
0.3
0.25
0.2
0.15
0.1
0.05
0
0 1 2 3 4 5
Time (h)
control
+ CK2
+CK2 + PP2R3A
+CK2 + PP2R3A + OA

Figure 4-5 PPP2R3A/PP2A holoenzyme dephosphorylates CK2 phosphorylated FANCD2 and promotes FANCD2 monoubiquitination *in vitro*. (A) Coomassie stain of recombinant FANCD2/FANCI complex obtained from Sf9 for the *in vitro* dephosphorylation assay. The complex was purified by anti-Flag purification followed by gel filtration. (B) Representative Western blot of *in vitro* dephosphorylation assay with CK2 phosphorylated FANCD2/FANCI complex by the recombinant PPP2R3A/PP2A phosphatase. A commercial λPP was used as a positive control. (C) Representative Western blot of *in vitro* dephosphorylation assay with lab purified ATR phosphorylated FANCD2/FANCI complex by the recombinant PPP2R3A/PP2A phosphatase. (D) Coomassie stain of *in vitro* ubiquitination assay of the WT FANCD2/FANCI complex treated with CK2 followed by PPP2R3A/PP2A dephosphorylation. (E) Quantification showing the ratio of Ub-FANCD2 to FANCD2 + FANCI.

4.4 Discussion

In this chapter, I have described an in vitro set-up that allowed us to successfully express and purify PPP2R3A/PP2A holoenzyme as a trimeric recombinant protein from Sf9 cells. PP2A acts on a wide range of substrates and is an important player in many crucial cellular functions from cell cycle regulation to cell transformation; this and other reasons make it challenging to overexpress and purify the complex from the whole organism-based purification systems (bacteria, yeast and insect cells), since it might lead to protein degradation when over expressed. Previously, PP2A with high yield and good purity was mostly obtained from animal tissue extraction (Tehrani et al, 1996; ZOLNIEROWICZ et al, 1996; Hendrix et al, 1993b). We took advantage of the MultiBac baculovirus expression system, and gel-filtration, as well as ion-exchange chromatography, to allow us to successfully obtain a stable, pure and catalytically active PPP2R3A holoenzyme for downstream experiments (Figures 4-1 to 4-4). The purified PPP2R3A holoenzyme was able to dephosphorylate FANCD2, and thereby activate the FANCD2/FANCI complex, which had previously been phosphorylated by CK2, and thereby inactivated. The dephosphorylation reaction was specific, since FANCD2 phosphorylated by ATR (Figure 4-5 B and C) was not dephosphorylated by PP2A. Notably, the yield of PP2A complex after the two chromatography columns was relatively low (Figure 4-4 B, silver stain). Limited by the final concentration obtained, we could only add PPP2R3A timer to a concentration of 3.2 nM (17.5 ng in 20 µl reaction) maximum, and this also may explain why residual CK2 phosphorylated FANCD2 is still observed after PPP2R3A treatment (Figure 4-5 B, lane 3).

The data from several *in vivo* settings shown in Chapter 2 demonstrate that FANCD2 is only weakly recruited to chromosomes in the absence of PPP2R3A, and therefore only very modestly monoubiquitinated. Our previous *in vitro* studies also confirmed that the general activity of the FANCD2/FANCI complex, including DNA binding affinity and monoubiquitination, was inhibited by CK2 phosphorylation at the 882-898 cluster (Lopez-Martinez et al, 2019; Lopez-Martinez & D., 2018). Here we could reverse the negative effect of CK2 phosphorylation

on FANCD2 monoubiquitination by PPP2R3A treatment (Figure 4-5 D), supporting our hypothesis that FANCD2 is subjected to a regulatory mechanism of dynamic phosphorylation/ dephosphorylation mediated by CK2 and PPP2R3A/PP2A. Since FANCD2 is monoubiquitinated on DNA (Liang et al, 2016; Lopez-Martinez & D., 2018; Sato et al, 2012; Longerich et al, 2014; Twest et al, 2017), electrophoretic mobility shift assay (EMSA) could be carried out in the future to confirm the potentially restored DNA affinity of CK2 treated FANCD2 after PPP2R3A dephosphorylation. The *in vivo* and *in vitro* data suggest that the FANCD2/FANCI complex needs to be dephosphorylated by PPP2R3A/PP2A before binding to chromatin where it is monoubiquitinated. We therefore propose that what happens in cells after ICL damage is that while the FANCD2/FANCI complex is kept at a low affinity for DNA by CK2 in the absence of DNA damage, PPP2R3A/PP2A activates the complex via dephosphorylating the CK2 cluster. This results in a facultative active FANCD2/FANCI complex with higher affinity for DNA, promoting the monoubiquitination that takes place in chromatin after recruitment. As has been discussed in the Introduction, it was previously proposed that monoubiquitination causes stabilization of the FANCD2/FANCI complex on DNA (Liang et al, 2016). Recent studies have confirmed this hypothesis, by demonstrating how the FANCD2/FANCI complex adapts a clamp-like conformation on DNA. The clamp can slide away from the initial site of ICL, allowing the action of downstream repair factors (Alcón et al, 2020; Wang et al, 2020). Eventually the complex is deubiquitinated by USP1/UAF1 and dissociated from DNA, which is essential for the completion of ICL repair. Although whether the CK2 phosphorylation on FANCD2 plays a role in promoting deubiquitination and unloading of the complex from DNA still remains to be investigated, data from a previous EMSA performed by our colleagues showing that phosphorylating the complex by CK2 before the USP1/UAF1 deubiquitination promotes further DNA dissociation than the non-phosphorylated control (Lopez-Martinez & D., 2018). More work is still needed to fully elucidate the role of CK2/PP2A mediated FANCD2 phosphorylation/dephosphorylation in the activation/deactivation of the FA pathway.

Chapter 5. Discussion

So far, we have characterised in this thesis that PPP2R3A/PP2A being a phosphatase that dephosphorylates CK2 phosphorylated FANCD2 on the 882-898 cluster in response to ICL damage, which is indispensable for the activation of the FA pathway. This licensing step is achieved by switching the FANCD2/FANCI complex from a "low DNA affinity" state to a "high DNA affinity" state due to the PPP2R3A/PP2A mediated dephosphorylation when ICLs are introduced into the chromosomes (Figure 5-1). The complex with higher affinity for DNA can therefore be recruited to chromatin where it undergoes further modifications, most importantly monoubiquitination by the FA core complex. Monoubiquitination converts the FANCD2/FANCI heterodimer into a sliding clamp, subsequently locking it on the DNA strand. We presume that the extra layer of regulation to the FANCD2/FANCI complex by phosphorylation/dephosphorylation before it gets monoubiquitinated on chromatin aims to protect the cell from unwanted DNA cleavage and spurious activation of the FA pathway when DNA damage is absent.

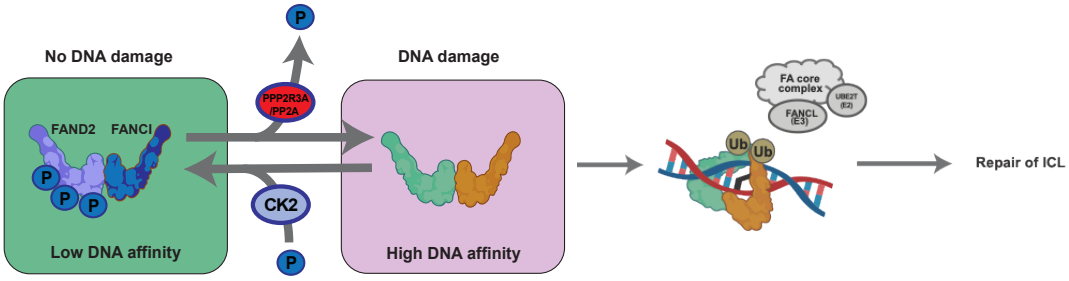

Figure 5-1 Model of activation of the FA pathway by PPP2R3A/PP2A dephosphorylation on FANCD2. In the absence of DNA damage, FANCD2 is constantly phosphorylated by CK2 and the FANCD2/FANCI complex is kept in a state with low DNA affinity to avoid spurious activation of the FA pathway. Upon ICL induction, FANCD2 gets dephosphorylated by the PPP2R3A/PP2A phosphatase and the complex is switched to a state with higher DNA affinity. This allows the complex to bind DNA where it undergoes further modifications, including monoubiquitination events by the FA core complex that converts the complex to a sliding clamp locked on DNA. The FA pathway is therefore fully activated, which promotes the downstream repair events to happen, leading to repair of the ICL lesion.

5.1 Potential Impact of PPP2R3A/PP2A dephosphorylation on the structure of FANCD2/FANCI complex

The structure of monoubiquitinated human FANCD2/FANCI bound to DNA has recently been resolved by cryo-electron microscopy (cyro-EM) (Liang *et al*, 2016; Alcón *et al*, 2020; Wang *et al*, 2020). Examination of the cryo-EM structures revealed that DNA is encircled by the FANCD2/FANCI complex, and that the interface of the dimer acts like a "hinge" which can close through the swing of FANCD2 and FANCI's C-termini (Figure 5-2, A and B). The two ubiquitin molecules are positioned at the interface of FANCD2 and FANCI, which are proposed to mimic functions of a "molecular pin" that keep the FANCD2/FANCI complex into the clamp conformation and lock onto DNA (Alcón *et al*, 2020). Unfortunately, the CK2 six-residue phosphorylation cluster as well as the sequence nearby (aa 842 to aa 915) are missing from the cryo-EM structures, likely because they locate on a potentially highly flexible loop region of the protein (Figure 5-2 C, black dash lines) (Wang *et al*, 2020). Nonetheless, it is likely that this flexible loop region containing the phosphorylation cluster lies in a close physical proximity with DNA. There is mounting evidence that protein phosphorylation and dephosphorylation regulate protein-protein and protein-DNA interactions. For example, Cys_2His_2 zinc finger proteins which make up the greatest family of transcription factors in higher eukaryotes, undergo cell-cycle dependent alternation in DNA association that is thought to be regulated by phosphorylation (Jantz & Berg, 2004). Fluorescence-based DNA-binding studies revealed that multisite phosphorylation of these transcription factors can reduce the DNA affinity for about 40-130 folds (Jantz & Berg, 2004). The most possible mechanism contributing to the reduction in DNA binding upon phosphorylation could be alternation in the direct electrostatic interactions between the conjugated phosphoryl group and the negatively charged DNA backbone. Similarly, we have shown that PPP2R3A/PP2A mediated dephosphorylation on the CK2 cluster on FANCD2 increases the binding affinity of the complex for DNA. This is possibly due to an increase in net charge of the FANCD2 flexible loop region after dephosphorylation, allowing it to better interact with the negatively charged DNA phosphate backbone.

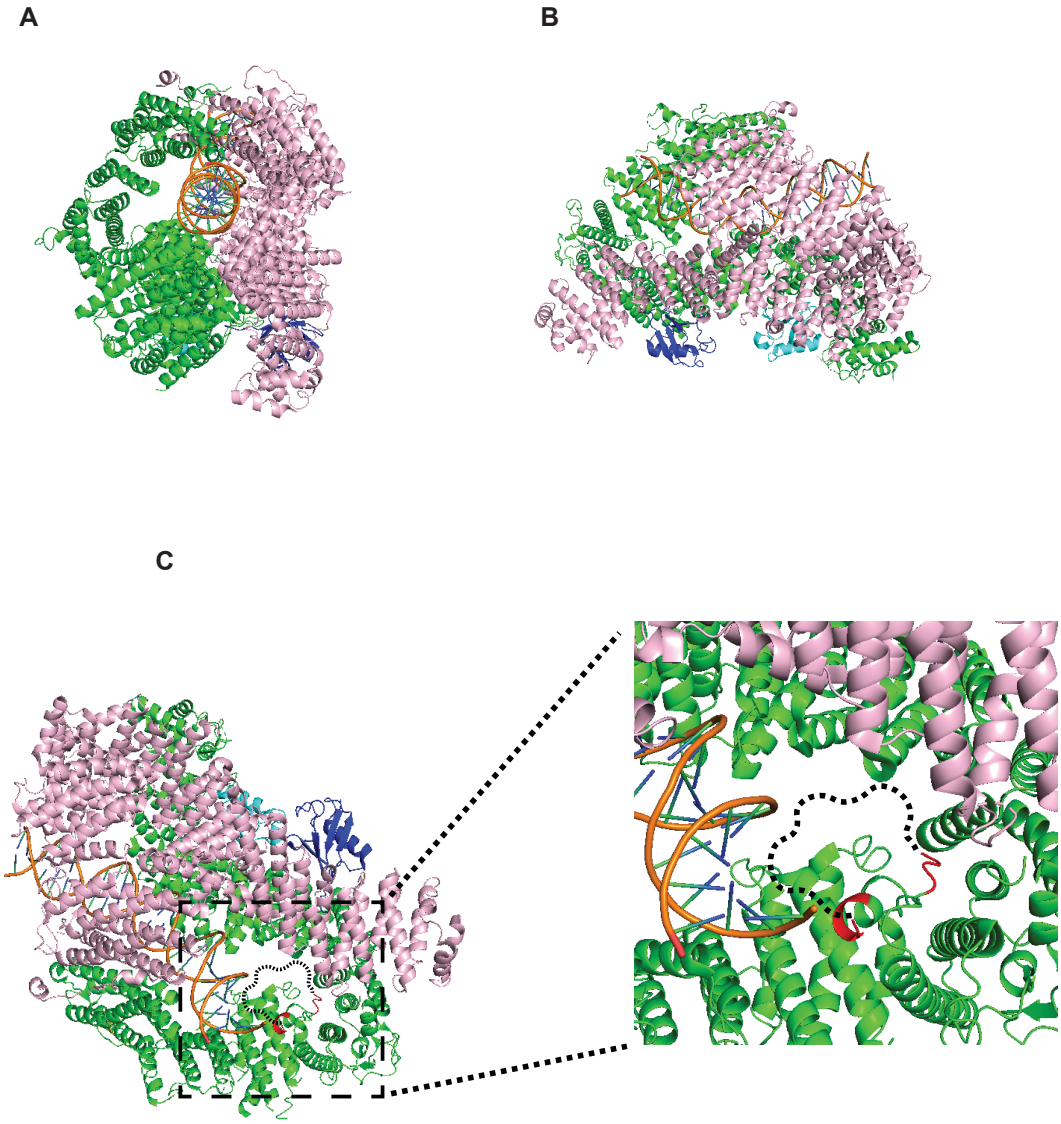

Figure 5-2 The location of the 882-898 CK2 cluster on FANCD2. (A) (B) Cyro-EM structure looked from different sides of the human monoubiquitinated FANCD2/FANCI complex bound to DNA (FANCD2 in green, FANCI in pink, ubiquitins in cyan and blue, DNA in orange, PDB 6VAE). (C) Zoom-in view of the area near the 882-898 CK2 cluster. Sequence aa 842 to aa 915 containing the CK2 cluster potentially lies on a highly flexible loop region of the protein (drawn in black dash lines), which is missing from the structure. Four amino acids at each end of the missing part are labelled in red. Adapted from (Wang *et al*, 2020).

Several studies have reported that FANCI is only inefficiently monoubiquitinated by either recombinant or by the native FA core complex in *in vitro* set-ups (Rajendra *et al*, 2014;

Shakeel *et al*, 2019; Twest *et al*, 2017). This is due to FANCI monoubiquitination on site K525 is only partially exposed upon DNA binding (Alcón *et al*, 2020). In mammalian cells, FANCI monoubiquitination is facilitated further by ATR mediated phosphorylation, though it is not compulsory for ICL repair by the FA pathway (Joo *et al*, 2011). While it is reported that DNA binding exposes the FANCD2 K563 monoubiquitination site that is buried at the FANCD2/FANCI dimer interface, hence allowing the subsequent ubiquitin conjugation (Alcón *et al*, 2020; Wang *et al*, 2020), PPP2R3A/PP2A mediated dephosphorylation could induce additional conformational change to FANCD2, which potentially further exposes the K563 monoubiquitination site that allow even better access of the FA core complex, hence facilitating FANCD2 monoubiquitination indirectly. This presumption could be validated by comparing the relative position of K563 on the cryo-EM structure of the DNA bound WT-FANCD2/FANCI with the non-phosphorylable 6A-FANCD2/FANCI and the phosphomimic 6D-FANCD2/FANCI heterodimers.

5.2 Regulation of the PPP2R3A/PP2A phosphatase

Historically, it is believed that protein phosphorylation is only responsible for activating DDR related pathways in response to DNA damage, while protein dephosphorylation is restricted to shutting off DDR pathways induced by phosphorylation when the repair is complete. However, several studies published recently, including our work demonstrate that protein kinases can inactivate DNA repair (such as FANCD2 inhibition by constitutive CK2 mediated phosphorylation). On the other hand, protein phosphatases are also not only required for shutting down but also for promoting DDR, such as the role of PPP2R3A/PP2A in the activation of ICL repair.

As discussed in Chapter 1.3.2, the enzymatic activity of PP2A depends upon the stability of the holoenzyme (Seshacharyulu *et al*, 2013), such as the half-life of each functional monomer and its ability of them to interact with another to form the intact holoenzyme. There are still several questions related to the regulation and function of PPP2R3A in promoting the FA pathway which remain to be investigated. Firstly, how PPP2R3A/PP2A recognises its substrate FANCD2 is not clear. It was reported that PPP2R3A interacts one of its substrates with a high specificity, the LIM protein lipoma-preferred partner (LPP), through the interaction between a well conserved cysteine rich Zn^{2+} finger like domain in the N terminus of PPP2R3A and the LIM domain of LPP (Janssens *et al*, 2016). Similarly, PPP2R3A might bind to FANCD2 through an unidentified specific interaction existing between the two proteins. FANCD2 mainly comprises of α-helices that are arranged into four α-solenoid structures (S1, S2, S3 and S4) and two helical domains (HD1, HD2) (Joo *et al*, 2011). *In vivo* or *in vitro* immunoprecipitations could be carried out to identify where and how PPP2R3A interacts with FANCD2 specifically.

Secondly, how PPP2R3A is activated after ICL induction to dephosphorylate FANCD2 and is inactivated after the completion of repair still remain to be investigated. The FA pathway is believed to take place in S phase in a replication dependent manner (Räschle *et al*, 2008; Amunugama *et al*, 2018; Zhang *et al*, 2015), therefore we firstly tested whether the cellular

protein level of PPP2R3A changes during the cell cycle. HeLa cells were synchronised in early S phase by double Thymidine block and harvested in every 1 h. They propagated through S phase and subsequently entered G2 phase in roughly 7 hours post-release, which can be told detected from the start of increase in cyclin A2 and the downregulation of cyclin E (Figure 5-3, lane 7). Indeed, FANCD2 in S phase cells was partially monoubiquitinated, but disappeared completely after 7 h when cells started to enter G2 (Figure 5-3). In fact, FANCD2 was found to be recruited to DNA during S phase even in the absence of exogenous ICL damage to stabilise replication forks (Wang *et al*, 2008; Mi & Kupfer, 2005). In this experiment, we did not introduce ICLs by treating cells with ICL inducing agents; thus FANCD2 activated in S phase should be mainly due to DNA replication rather than ICL repair. The protein level of PPP2R3A remained stable through the cell cycle under non-perturbed conditions (Figure 5-3), suggesting that the activation of the FA pathway in S phase is not regulated through the stability or the half-life of PPP2R3A phosphatase. Another potential mechanism is that PPP2R3A/PP2A is activated due to change in its ability to form the trimeric holoenzyme after ICL induction, i.e., the ability of PPP2R3A to be associated with the PP2A core-enzyme. This could be mediated by other regulatory proteins that affect the binding of PPP2R3A to the core enzyme, such as the case of the Greatwall-ENSA-PP2A/PR55 pathway regulating mitotic exit (see Chapter 1.3.2). To investigate this, one could purify PPP2R3A and compare its interaction partners with PPP2R3A before and after ICL induction, or from cells synchronised at different stages of the cell-cycle by mass spectrometry analysis, to validate if such regulatory proteins exist. Similarly, one could also purify epitope tagged PPP2R3A as a holoenzyme and perform *in vitro* dephosphorylation assays using FANCD2 as the substrate, to test if its enzymatic activity increase after ICL induction or in cells in S phase.

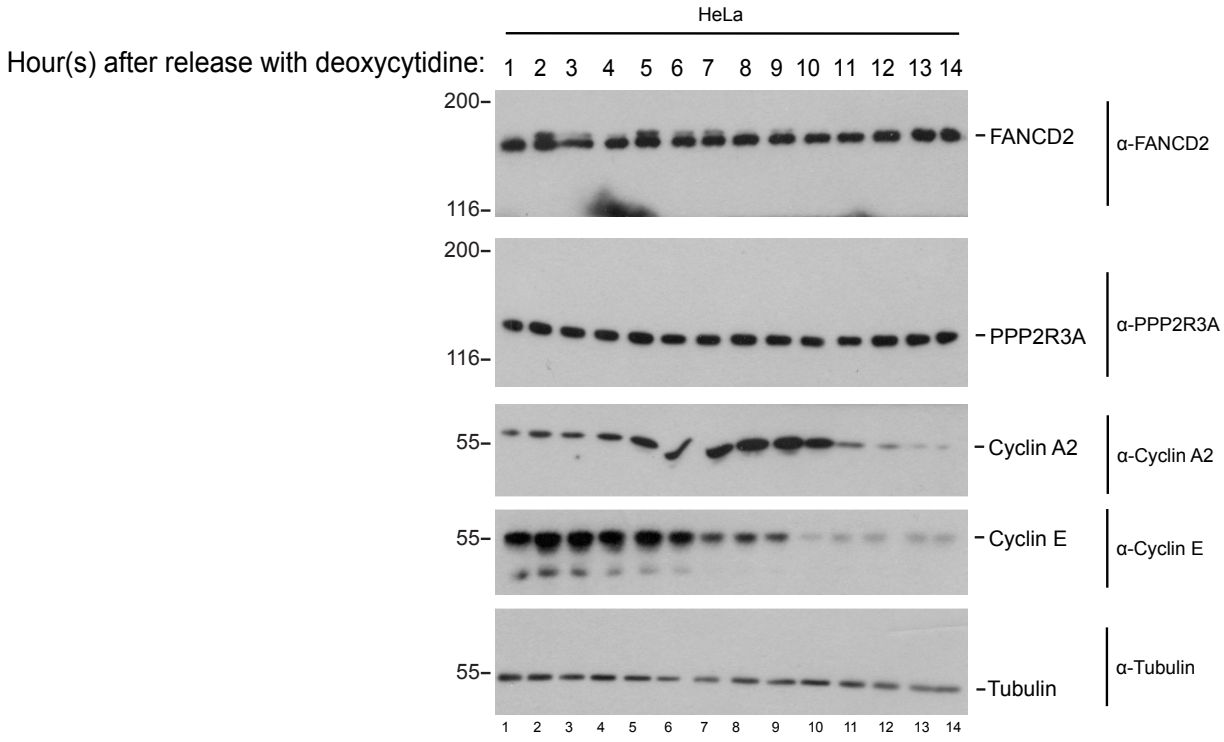

Figure 5-3 Protein level of PPP2R3A remains stable among the cell cycle in HeLa cells. Western blot of HeLa cells synchronised in early S phase by double Thymidine block.

Importantly, depletion of PPP2R3A has been connected to oncogenic transformation, likely because it is involved in regulating multiple tumour related pathways including cell proliferation, invasion and migration (Dzulko *et al*, 2020; Chen *et al*, 2019). Here we identified a novel role of PPP2R3A in activating the FA pathway during ICL repair, reinforcing the fact that it acts as an anti-carcinogenesis factor, as depletion of PPP2R3A leads to genome instability. On one hand, FA is a cancer-prone disease, so it would be interesting to see if PPP2R3A is highly mutated in FA patient populations. On the other hand, overactivation of the FA pathway and FANCD2 by monoubiquitination are responsible for unwanted cell survival and induced resistance of chemotherapeutic ICL inducing agents, such as cisplatin, in certain types of cancers (Sharp *et al*, 2020; Rocha *et al*, 2018). Therefore, targeting the inhibition of FANCD2 activation presents a possible therapeutic opportunity for combating cancers, which makes PPP2R3A a potential drug target. Further research needs to be carried out to

completely elucidate the mechanism of PPP2R3A activation upon ICL damage, and this could shine more lights on the development of small molecule inhibitors that target PPP2R3A and hence inactivating FANCD2 in cancer cells.

Last but not least, although we focused on PP2A in this study based on the results obtained from the siRNA screening (Figure 2-2), there might be functional redundancy between PP2A with other phosphatases. Indeed, cells without PPP2R3A were partially sensitive to MMC treatment, compared to the FANCD2 -/- cells (Figure 3-5 D). Interestingly, the core domain of PP2A's catalytic subunit is shared with PP1 (Ramos *et al*, 2019), and it is not surprising that PP1 also participates in regulating the FA pathway during ICL repair. PP1 holoenzyme comprises a catalytic subunit and at least one regulatory subunit. Similar to PP2A, the regulatory subunit determines its substrate specificity as well as localisation (Goldberg *et al*, 1995). In addition, it has also been implicated to play a role in facilitating DNA repair through dephosphorylating BRCA1 phosphorylated by Chk2, which is essential for the completion of the HR mediated DSB repair (Moorhead *et al*, 2007; Kurimchak & Grana, 2012). Further insight might be provided by testing whether PP1 is involved in activating the FA pathway upon ICL induction by analysing chromatin recruitment of FANCD2 and its monoubiquitination in PP1 deficient cells.

5.3 Limitations and Conclusions

Apart from questions discussed above, there are several limitations of techniques used in the project. Firstly, cell cycle profiles were analysed based on a FACS system where cell stages were determined by measuring the DNA content that was stained by propidium iodide. However, this method cannot distinguish between G2 and mitotic phase cells in PP2A deficient cells as they share similar DNA content. While PP2A has profound roles in regulating the mitosis entry and exit (discussed in Chapter 1.3.2), it was not clearly identified whether the cell population accumulated after MMC treatment was in G2 or mitosis in PP2A depleted cells. In fact, those cells were put under a light microscope before the FACS was carried out, and there was no significant increase in mitotic cells based on morphological observations. To fully address this problem, we could combine DNA content staining by propidium iodide together with mitotic marker staining. For example, cells can be stained with a fluorescent antibody against phosphorylated histone H3 (pH3), which is a well-known mitotic marker, together with propidium iodine and subsequently subjected to FACS to distinguish between G2 and mitotic cells.

Besides, siRNAs and CRISPR/Cas9 directed gene editing were used to remove the target protein in most of the functional assays involved in this study, involving the analysis of FANCD2 ubiquitination by Western blot and recruitment by live cell imaging, as well as the clonogenic survival assay. Nonetheless, both siRNA and CRISPR/Cas9 mediated gene silencing requires relatively long-term treatment (a few days to weeks), which might not the most optimum strategy in our case since PP2A has been associated with a broad range of cellular pathways. Instead, protein knockdown using a degradation TAG (dTAG) or the auxin-inducible degron (AID) system could be adopted to achieve fast and inducible protein degradation, while studying functions of PPP2R3A/PP2A in mediating the FA pathway during ICL repair.

Our study revealed an activating effect of PPP2R3A/PP2A on the FA pathway during ICL repair by mediating the DNA loading and hence monoubiquitination of FANCD2. Identifying the presence of such a new layer of regulation on FANCD2 activation not only helps us to better understand the repair mechanism of ICL by the FA pathway, but also the FA pathogenesis. PPP2R3A/PP2A might serve as a druggable target to combat chemotherapy resistance of ICL inducing agents, such as cisplatin that has been widely used to treat a wide range of cancers. Potential PPP2R3A inhibitors could be developed to prevent over activation of the FA pathway in cancer cells treated with ICL inducers, if the mechanism of how PPP2R3A/PP2A is triggered by ICL induction can be identified in the future.

Materials and Methods

Cell lines

HeLa (including gene-edited clones originated from Hela) and Phoenix A cells were cultured in DMEM (D5796; Sigma-Aldrich) supplemented with 10% Foetal Bovine Serum (FBS) (F7524; Sigma-Aldrich). Cells were detached using Trypsin-EDTA (T4049; Sigma-Aldrich) for passage. Cells were grown in a 37 ℃ incubator supplemented with 5% CO_2.

CRISPR/Cas9 gene editing

Hela FANCD2 -/- cells used in this study were previously generated by Lopez-Martinez *et al*., as described in the publication by Ran *et al*., 2013. PPP2R3A -/- cells were generated using pX459 plasmid (Addgene #48139) in Hela cells. The guide sequence before the PAM sequence is 5' TGTGAACCACTACAGCAGCG 3'. Primers (5' CACCGTGTGAACCACTACAGCAGCG 3' and 5' AAACCGCTGCTGTAGTGGTTCACAC 3') are annealed and phosphorylated before cloning into BbsI digested pX459. Hela cells were electroporated with 5 µg of pX459 containing sgRNA targeting PPP2R3A. After 24 h of electroporation, cells were transiently selected by 2 µg/ml puromycin for 24 h then plated at a low density (100 -300 cells) in 15-cm plates to grow single cell clones. After two weeks, single cell clones were isolated using 150 µl glass cloning cylinders (C1059-1EA, Merk) and transferred to 24-well plates. Protein expression was examined by Western blot using specific antibody (see western blot section) to confirm the deletion of PPP2R3A.

Preparation of whole cell lysate

3 X 10^6 cells of each sample were collected from a 6 cm dish using a plastic scrapper. Cell pellets were resuspended in 50 µl (volume added depends on the pellet size) Benzonase buffer (2 mM $MgCl_2$, 20 mM Tris pH 8.0, 10% glycerol, 1% Triton X-100 and 0.125 units/µl benzonase (E1014, Sigma)), and subsequently left on ice for 10 minutes. An equal volume of

2% SDS was added to the lysate before the sample was heated at 70°C for 5 minutes. The protein concentration was subsequently measured using the Bradford assay (500- 0006, Bio-Rad Life Science). Specifically, 2 µl lysate sample was mixed with 50 µl water and 1 ml Bradford reagent followed by incubation at room temperature for 5 min. The resultant blue colour was measure by a spectrometer at 595 nm.

Western blot (WB)

Whole cell lysate was mixed with 6X home-made SDS-PAGE loading buffer which results in samples containing 50 mM DTT (NP0009; Life Technologies), 62.5 mM Tris-HCl (pH 6.8), 1% SDS, 10% glycerol, and 0.01% bromophenol blue. Samples were boiled at 100 ^{o}C for 10 minutes. Undissolved precipitates were removed by centrifugation at 17000 x g for 5 min.

Protein samples were separated by polyacrylamide (PAA) gel with different percentages (4 % for viewing proteins greater than 100 kDa, such as FANCD2 and PPP2R3A, 12 % for viewing proteins at 30 – 70 kDa, such as α-tubulin). Mark12 protein ladder (100006637; Invitrogen) was used as a maker of protein molecular weights. The stacking and separating gel were cast by following the standard procedure described in Molecular Cloning (Sambrook, J. and Russel, D.W. 2001). Samples were run in 1X Tris-Glycine-SDS running buffer containing 25 mM Tris pH 8.3, 192 mM Glycine, and 0.1% SDS) at a constant voltage of 70 V for 30 min followed by 100V until the dye front reaches the edge of the gel. Proteins on the PAA gel were transferred onto a nitrocellulose membrane in a transfer buffer (192 mM Glycine, 24 mM Tris 8.3, 20% methanol) at a constant voltage of 25 V for 16 h at 4 °C. After transfer, the membrane was blocked with 5% milk (170-6404; Bio-Rad) in TBS-T (10 mM Tris 7.4, 150 mM NaCl, 0.05% Tween-20) for 1 h and followed by incubation with primary antibody at 4 ^{o}C overnight. The membrane was washed by TBST before incubating with corresponding secondary antibody for 1 h at room temperature. Excess secondary antibody was washed away using TBS (10 mM Tris 7.4, 150 mM NaCl). The membrane was finally developed by ECL (0RT2405 and 0RT2505; PerkinElmer) and X-ray films (28906837; GE Healthcare) in a dark room.

Used antibodies and their dilution: anti-FANCD2, 1:200 (sc-20022, Santa Cruz Biotechnology); anti-FANCI, 1:500 (G4270, Merck-Millipore); anti-α-Tubulin, 1:2000 (5829, Millipore); anti-Flag, 1:1000 (M5, F4042, Sigma-Aldrich); anti-cyclin A2 (E399, ab32498, Abcam); anti-cyclin E (HE12, sc-247, Santa Cruz Biotechnology); anti-PPP2CA/B (610555, BD Biosciences); anti-PPP2R3A (HPA035829, Sigma-Aldrich); anti-PPP2R1A (NBP2-19907, Novus).

Plasmids, transfection and transduction

EGFP-fused FANCD2, PPP2R3A and PTPA, mCherry-fused UHRF1 cDNAs were cloned into a derivative of the pOZ vector (Nakatani and Ogryzko, 2003; Sato et al., 2012b), amplified by DH5α competent *E. Coli* cells and purified by Midiprep (27106, Qiagen). The pOZ plasmid containing the gene of interest along with helper plasmids expressing the retroviral gene Pol, Gag, and Env proteins were transfected in proportion into 50 % confluent (for example, 4 X 10^6 cells for a 10 cm dish and etc.) Phoenix A cells by FuGENE6 (E2692, Promega) to generate the retrovirus for transduction. For every 1 µg plasmids used, 3 µl FuGENE6 was added. 72 h post transfection, the culture medium of Phoenix A cells was collected and filtered by a 0.45 µm filter (for 10 cm dish, 10 ml medium was collected). The transduction was subsequently carried out by mixing the retroviral medium with the culture medium supplemented with 4 µg/ml polybrene and added to a over 50 % confluent plate of target cells. Cells expressing the gene of interest were selected by either 2 µg/ml puromycin (P8833; Sigma-Aldrich) for 24 h or the lab made anti-IL2Rα antibody-conjugated beads (05-170, Millipore; 11033, Invitrogen).

For siRNA transfection of PP2A regulatory and catalytic subunits, a total number of 6 X 10^5 Hela cells are seeded in a 6-well plate a day before. On the day of transfection, siRNAs are mixed with Lipofectamine (13778100, Thermo Fisher Scientific) according to the manufacturer's procedure. Two siRNAs with different target sequences were used for each gene at a final concentration of 25 nM, except for the two PP2A catalytic subunits of which SMARTpools were used. After three days of incubation with siRNAs at the 37 ℃ incubator, cells were harvested for downstream experiments.

Table 6-1 List of siRNAs (Ambion Life Technology) and siRNA SMARTpool (Horizon Discovery Ltd) used in this study.

Gene	siRNA1	siRNA2
PPP2CA	5515 (SMARTpool)	-
PPP2CB	5516 (SMARTpool)	-
PPP2R2A	S608	S610
PPP2R2B	S10971	S10969
PPP2R2C	S10973	S10972
PPP2R2D	S224395	S31640
PPP2R3A	S10977	S10976
PPP2R3B	S26254	S26253
PPP2R3C	S29987	S29986
PPP2R5A	S10981	S10982
PPP2R5B	S10985	S10984
PPP2R5C	S10987	S10988
PPP2R5D	S10990	S10992
PPP2R5E	S10993	S10994
STRN	S13587	S13586
STRN3	S226265	S226266
PPP2R4 (PTPA)	S10980	S10978

shRNA mediated knock-down of PP2A catalytic and regulatory subunits was carried out by expressing the targeting sequences in the pSUPER.retro vector (Clontech). The targeting sequence of each gene was searched and selected in the RNAi Consortium shRNA Library from the Broad Institute. 5 X 10^6 cells in 10 cm dishes were transduced with 100% non-diluted retroviral medium supplemented with 4 μg/ml polybrene. Cells were slected with puromycin

at a high concentration of 10 μg/ml for 24 h. Primers used to generate shRNAs are listed below in Table 7-2:

Table 7-2 List of primers used for generating shRNAs.

Gene	Primers
PPP2CA	5'GATCCCCACCGGAATGTAGTAACGATTTTTCAAGAGAAAATCGTTACTACATTCCGGTTTTTTGGAAA3'
	5'AGCTTTTCCAAAAAACCGGAATGTAGTAACGATTTTCTCTTGAAAAATCGTTACTACATTCCGGTGGG3'
PPP2CB	5'GATCCCCTAGACACACTGGATCATATAATTCAAGAGATTATATGATCCAGTGTGTCTATTTTTGGAAA3'
	5'AGCTTTTCCAAAAATAGACACACTGGATCATATAATCTCTTGAATTATATGATCCAGTGTGTCTAGGG3'
PPP2R2A	5'GATCCCCGCAAGTGGCAAGCGAAAGAAATTCAAGAGATTTCTTTCGCTTGCCACTTGCTTTTTGGAAA3'
	5' AGCTTTTCCAAAAAGCAAGTGGCAAGCGAAAGAAATCTCTTGAATTTCTTTCGCTTGCCACTTGCGGG 3'
PPP2R2B	5' GATCCCCGCGGCTACAAATAACCTATATTTCAAGAGAATATAGGTTATTTGTAGCCGCTTTTTGGAAA 3'
	5' AGCTTTTCCAAAAAGCGGCTACAAATAACCTATATTCTCTTGAAATATAGGTTATTTGTAGCCGCGGG3'
PPP2R2C	5' GATCCCCCCGCTCATTCTTCTCGGAAATTTCAAGAGAATTTCCGAGAAGAATGAGCGGTTTTTGGAAA 3'
	5' AGCTTTTCCAAAAACCGCTCATTCTTCTCGGAAATTCTCTTGAAATTTCCGAGAAGAATGAGCGGGGG3'
PPP2R2D	5' GATCCCCGTCCTTCTTCTCAGAAATAATTTCAAGAGAATTATTTCTGAGAAGAAGGACTTTTTGGAAA3'
	5' AGCTTTTCCAAAAAGTCCTTCTTCTCAGAAATAATTCTCTTGAAATTATTTCTGAGAAGAAGGACGGG3'
PPP2R3A	5'GATCCCCCCACGGTTATTCAGAGAATATTTCAAGAGAATATTCTCTGAATAACCGTGGTTTTTGGAAA3'
	5'AGCTTTTCCAAAAACCACGGTTATTCAGAGAATATTCTCTTGAAATATTCTCTGAATAACCGTGGGGG3'
PPP2R3B	5'GATCCCCAGATCAGCTATGCCGACTTTGTTCAAGAGACAAAGTCGGCATAGCTGATCTTTTTTGGAAA3'
	5'AGCTTTTCCAAAAAAGATCAGCTATGCCGACTTTGTCTCTTGAACAAAGTCGGCATAGCTGATCTGGG3'
PPP2R3C	5'GATCCCCGCAGCTTCCTAGATGATTTATTTCAAGAGAATAAATCATCTAGGAAGCTGCTTTTTGGAAA3'
	5'AGCTTTTCCAAAAAGCAGCTTCCTAGATGATTTATTCTCTTGAAATAAATCATCTAGGAAGCTGCGGG3'
PPP2R5A	5'GATCCCCGCTAACATCTTCCGTACACTTTTCAAGAGAAAGTGTACGGAAGATGTTAGCTTTTTGGAAA3'
	5'AGCTTTTCCAAAAAGCTAACATCTTCCGTACACTTTCTCTTGAAAAGTGTACGGAAGATGTTAGCGGG3'
PPP2R5B	5'GATCCCCCCGCATGATCTCAGTGAATATTTCAAGAGAATATTCACTGAGATCATGCGGTTTTTGGAAA3'
	5'AGCTTTTCCAAAAACCGCATGATCTCAGTGAATATTCTCTTGAAATATTCACTGAGATCATGCGGGGG3'
PPP2R5C	5'GATCCCCCCAGAAGTAGTCCATATGTTTTTCAAGAGAAAACATATGGACTACTTCTGGTTTTTGGAAA3'
	5'AGCTTTTCCAAAAACCAGAAGTAGTCCATATGTTTTCTCTTGAAAAACATATGGACTACTTCTGGGGG3'
PPP2R5D	5'GATCCCCGAGTTCTTCTTACGTTTCCTTTTCAAGAGAAAGGAAACGTAAGAAGAACTCTTTTGGAAA3'
	5'AGCTTTTCCAAAAAGAGTTCTTCTTACGTTTCCTTTCTCTTGAAAAGGAAACGTAAGAAGAACTCGGG3'
PPP2R5E	5'GATCCCCCCTCCTAGTGACAGCAATGAATTCAAGAGATTCATTGCTGTCACTAGGAGGTTTTTGGAAA3'
	5' AGCTTTTCCAAAAACCTCCTAGTGACAGCAATGAATCTCTTGAATTCATTGCTGTCACTAGGAGGGGG 3'
STRN	5'GATCCCCGCAAGGGATATACAAGCATTTTTCAAGAGAAAATGCTTGTATATCCCTTGCTTTTTGGAAA3'
	5'AGCTTTTCCAAAAAGCAAGGGATATACAAGCATTTTCTCTTGAAAAATGCTTGTATATCCCTTGCGGG3'
STRN3	5'GATCCCCGCTGGCACTTTAGTTGGTCATTTCAAGAGAATGACCAACTAAAGTGCCAGCTTTTTGGAAA3'
	5'AGCTTTTCCAAAAAGCTGGCACTTTAGTTGGTCATTCTCTTGAAATGACCAACTAAAGTGCCAGCGGG3'
PTPA	5'GATCCCCCCGTTTGATGAGAGGCTGTTT TTCAAGAGAAAACAGCCTCTCATCAAACGGTTTTTGGAAA3'
	5'AGCTTTTCCAAAAACCGTTTGATGAGAGGCTGTTTTCTCTTGAAAAACAGCCTCTCATCAAACGGGGG3'

Protein purification

The PPP2R3A/PP2A holoenzyme was purified by employing the MultiBac™ expression system. Flag-PPP2CA, His-PPP2R1A and HA-PPP2R3A were cloned into the pACEBac1 as a combined vector and transformed into DH10Bac^{TM} competent *E. coli* cells for generation of the bacmid. Specifically, DH10Bac^{TM} competent cells were thawed on ice and incubated with 500 ng purified pACEBac1 plasmid at 4 ℃ for 25 min, followed by heat shock for 40 sec at 42 ℃. Cells were immediately transferred back on ice to cool down for 2 min and were subsequently recovered by shaking with 1 ml LB medium at 37 °C at 225 rpm for 4 hours. After that, the medium was removed by centrifugation at 17000 x g for 2 min while the pellet was resuspended and plated to an agar plate containing 50 μg/mL kanamycin, 7 μg/mL gentamicin, 10 μg/mL tetracycline, 100 μg/mL Bluo-gal, and 40 μg/mL IPTG. The plate was incubated in a 37 °C incubator overnight, positive colonies were selected by blue/white selection. The positive bacmid was then transfected into Sf9 cells to produce baculovirus. 1 μg bacmid was transfected into 5 X 10^5 Sf9 cells by mixing the bacmid with 2 ml Grace's Insect Cell Culture Medium (11595030, Gibco^{TM}) and 6 μl Cellfectin® II (10362100, Gibco^{TM}). Cells were incubated at a 27 °C incubate for 5 h before the medium was replaced with 2 ml Sf-900™ III SFM medium (12659017, Gibco). Five days post transfection, the baculovirus was harvested by collecting the 2 ml culture medium. The virus was passaged twice before being used for the transduction of sf9 cells. 200 μl virus (the value depended on the virus titer) was added to 15 million Sf9 cells in 20 ml Sf-900™ III SFM medium in a 15 cm dish. Cells were harvested three days after infection by scraping with lysis buffer (20 mM Tris-HCl pH 8.0, 100mM KCl, 10% glycerol and 2 mM β-mercaptoethanol and 0.2 mM PMSF) followed by sonication (4 X 10 s bursts on ice). After centrifugation at 17000 x g for 5 min, the supernatants were incubated with 50 μl M2 anti-Flag agarose resin for 2 h at 4 ℃. After extensive washes, the proteins were eluted from the resin in 0.5 mg/ml Flag peptide in the same lysis buffer. The eluate was firstly run on a Superdex® 200 26/60 column (GE Healthcare Life Sciences) in 20 mM Tris-HCl pH 8.0, 100mM KCl, 10% glycerol and 2 mM β-mercaptoethanol and 0.2 mM PMSF. Fractions containing the complex were combined and subsequently passed through a Mono Q^{TM} anion exchange chromatography column (GE

Healthcare Life Sciences) to further remove impurities. Proteins were eluted by a salt gradient of KCl from 10 mM to 1M. Finally, elutes were combined and concentrated by PEG for subsequent *in vitro* assays.

In vitro phosphorylation and dephosphorylation assays

Purification of FANCD2/FANCI complex was carried out according to the protocol in Lopez-Martinez *et al*., 2019. Phosphorylation of FANCD2/FANCI complex was done by mixing FANCD2/FANCI with either CK2 (P6010, NEB) or lab purified ATR at a final concentration of 7.32nM (CK2, estimated) and 131 nM (CK2, estimated) respectively, and incubated at 30°C for 30 min in 50 mM Tris pH 7.5, 10 mM $MgCl_2$, 2 mM DTT, 0.1 mM EDTA and 2mM ATP. The dephosphorylation reaction was carried out by mixing FANCD2/FANCI with either the λPP (P0753, NEB) or the purified PPP2R3A/PP2A holoenzyme at final a concentration 3.2 nM, followed by incubation at 30°C for 60 min in 50 mM HEPES pH 7.5, 100 mM NaCl, 2 mM DTT, 1mM $MnCl_2$ and 0.5 μM CX-4549 (CK2 inhibitor).

In vitro ubiquitination assay

The ubiquitination reaction was performed in reaction buffer (50 mM Tris pH 7.5, 100 mM KCl, 2 mM $MgCl_2$, 0.5 mM DTT and 2 mM ATP) in the presence of 22 nM UBA1, 1.16 μM UBE2T, 4.66 μM His-Ub, 0.285 μM FANCD2/FANCI complex and 1.02 μM FANCL. The reaction was incubated at RT for the indicated period of time (2-4 h, Figure 4-5) with 0.13 μM pBlueScript SKII (+) plasmid. After incubation, reactions were stopped by 6X SDS loading buffer containing 2-mercaptoethanol. Samples were analysed by SDS-PAGE gel electrophoresis and subjected to Coomassie blue staining to analyse.

Clonogenic survival assay

HeLa cells were plated in 6-well plates (seeding number varies from 200 to 1,000 depending on the genetic background) the day before MMC treatment. After 24 hours, cells

were treated with indicated concentration of MMC and left for 14 days, and the number of colonies formed was manually counted after staining with 1% (w/v) crystal violet in methanol.

Live-cell imaging

Cells expressing fluorophore-tagged proteins were imaged using an OLYMPUS IX81 microscope in connection with the PerkinElmer UltraView Vox spinning disk system conjugated with a Plan-Apochromat 60x/1.4 oil objective. Volocity software 6.3 was used for image capturing and ImageJ was used to quantify the strip intensity. To record the EGFP and mCherry signal, 488 nm and 561 nm laser channels were used, respectively. To be more specific, cells were seeded at 40 % confluency in a 35 mm glass bottom dish (P35G-1.5-14-C, MatTek) in DMEM supplemented with 10% FBS the day before imaging. Right before imaging, the regular growth medium was replaced with 20 μg/ml TMP in a colourless medium containing DMEM without phenol red (D1145; Sigma-Aldrich) followed by incubation at 37 ℃ for 30 min. During the recording, cells were kept in a live cell environmental chamber (Tokai hit) supplemented with 5% CO_2 and maintained at 37 ℃ constantly. To micro-irradiate the cell, a localized fully powered 405 nm laser was used to irradiate a selected stripe region (40 x 3 pixels) in the nucleus for 60 times, under the FRAP mode of the Volocity software. Intensities of EGFP and mCherry fluorescence at the micro-irradiated area were quantified using ImageJ and normalized to signals in the surrounding nuclear and extracellular background. Briefly, the background signal from the field between cells was measured (denoted signal A) by selecting the area to be measured using the freehand tool followed by using the Ctrl+M function within ImageJ. The Ctrl+M function allows the measurement of the mean gray value, which represents fluorescent intensity of the area interested. The fluorescent intensity from the strip (denoted signal B) and the other area within the nucleus excluding the strip (denoted signal C) were measured subsequently by the same Ctrl+M function. The background signal A was subtracted from signals B (denoted B') and C (denoted C'). The recruitment of target protein for each time point post irradiation was represented as the ratio of fluorescent intensity of the strip to the nuclear background, which was calculated based on equation B'/C' (relative

intensity in the chart). The value of relative intensity at 0 minutes post irradiation was normalised to 1.

Cell synchronization

To synchronize cells in early S phase, cells were firstly plated at 50-70% confluency. Thymidine (T9250; Sigma-Aldrich) was used at 2 mM for 14-18 hours for the first round of synchronization. Cells were then washed with PBS and cultured in DMEM containing 24 μM 2'-deoxycytidine (D3897; Sigma-Aldrich) for 10 h to release the cell cycle. After that, they were washed again with PBS and incubated with 2 mM Thymidine for another 14-18 hours for the second Thymidine block. Finally, they were washed in PBS and released again into DMEM containing 24 μM 2'-deoxycytidine, and were harvested at indicated time intervals.

Cell cycle analysis by flow cytometry

HeLa cells depleted with the gene of interest were incubated with 20 ng/mL MMC for 2 hours before recovering in DMEM for 24 hours. Cells were harvested and washed by cold PBS containing 1 mM EDTA. Cells were collected and the concentration was adjusted to 2 x 10^6 cells/mL, then 1 ml of the suspension was added dropwise into 9 ml of 70% cold ethanol and incubated for at least 48 hours at 4 ^{o}C. Samples were then centrifuged at 200 xg for 10 min. The pellet was then washed three times with cold PBS supplemented with 1 mM EDTA before stained with 20 mg/mL propidium iodide (P4170; Sigma-Aldrich) in PBS containing 1 mM EDTA, 0.1% Triton X-100 and 0.2 mg/mL RNase A (R5503; Sigma-Aldrich) at RT for 30 min. The cell cycle profile was recorded using a FACSCalibur flow cytometer and the data were analysed by BD CellQuest.

Separate Research conducted

During my D. Phil study, I have also conducted another research project which is not incorporated into this thesis. The results of the project have been published at the time of writing this thesis and I was one of the co-first authors. The citation (Socha *et al*, 2020) below marks part of my time spent during D. Phil study.

References

Ahn J-Y, Li X, Davis HL & Canman CE (2002) Phosphorylation of Threonine 68 Promotes Oligomerization and Autophosphorylation of the Chk2 Protein Kinase via the Forkhead-associated Domain*. *J Biol Chem* 277: 19389–19395

Ahnesorg P, Smith P & Jackson SP (2006) XLF Interacts with the XRCC4-DNA Ligase IV Complex to Promote DNA Nonhomologous End-Joining. *Cell* 124: 301–313

Alcón P, Shakeel S, Chen ZA, Rappsilber J, Patel KJ & Passmore LA (2020) FANCD2–FANCI is a clamp stabilized on DNA by monoubiquitination of FANCD2 during DNA repair. *Nat Struct Mol Biol* 27: 240–248

Allen JB, Zhou Z, Siede W, Friedberg EC & Elledge SJ (1994) The SAD1/RAD53 protein kinase controls multiple checkpoints and DNA damage-induced transcription in yeast. *Gene Dev* 8: 2401–2415

Amunugama R & Walter JC (2020) A new varietal of DNA interstrand crosslink repair. *Cell Res* 30: 459–460

Amunugama R, Willcox S, Wu RA, Abdullah UB, El-Sagheer AH, Brown T, McHugh PJ, Griffith JD & Walter JC (2018) Replication Fork Reversal during DNA Interstrand Crosslink Repair Requires CMG Unloading. *Cell Reports* 23: 3419–3428

Andreassen PR, D'Andrea AD & Taniguchi T (2004) ATR couples FANCD2 monoubiquitination to the DNA-damage response. *Gene Dev* 18: 1958–1963

Auerbach AD (2009) Fanconi anemia and its diagnosis. *Mutat Res Fundam Mol Mech Mutagen* 668: 4–10

Balcome S, Park S, Dorr DRQ, Hafner L, Phillips L & Tretyakova N (2004) Adenine-Containing DNA−DNA Cross-Links of Antitumor Nitrogen Mustards. *Chem Res Toxicol* 17: 950–962

Banerjee AK, Read CA, Griffiths MH, George PJ & Rabbitts PH (2007) Clonal divergence in lung cancer development is associated with allelic loss on chromosome 4. *Genes Chromosomes Cancer* 46: 852–860

Basbous J & Constantinou A (2019) A tumor suppressive DNA translocase named FANCM. *Crit Rev Biochem Mol* 54: 1–14

Beard WA, Horton JK, Prasad R & Wilson SH (2019) Eukaryotic Base Excision Repair: New Approaches Shine Light on Mechanism. *Annu Rev Biochem* 88: 137–162

Becker JR, Clifford G, Bonnet C, Groth A, Wilson MD & Chapman JR (2021) BARD1 reads H2A lysine 15 ubiquitination to direct homologous recombination. *Nature* 596: 433–437

Bensimon A, Schmidt A, Ziv Y, Elkon R, Wang S-Y, Chen DJ, Aebersold R & Shiloh Y (2010) ATM-Dependent and -Independent Dynamics of the Nuclear Phosphoproteome After DNA Damage. *Sci Signal* 3: rs3

Bessho T, Mu D & Sancar A (1997) Initiation of DNA interstrand cross-link repair in humans: the nucleotide excision repair system makes dual incisions 5' to the cross-linked base and removes a 22- to 28-nucleotide-long damage-free strand. *Mol Cell Biol* 17: 6822–6830

Bezalel-Buch R, Cheun YK, Roy U, Schärer OD & Burgers PM (2020) Bypass of DNA interstrand crosslinks by a Rev1–DNA polymerase ζ complex. *Nucleic Acids Res* 48: gkaa580-

Bhargava R, Onyango DO & Stark JM (2016) Regulation of Single-Strand Annealing and its Role in Genome Maintenance. *Trends Genet* 32: 566–575

Bhattacharyya A, Chattopadhyay R, Mitra S & Crowe SE (2014) Oxidative Stress: An Essential Factor in the Pathogenesis of Gastrointestinal Mucosal Diseases. *Physiol Rev* 94: 329–354

Bjelland S & Seeberg E (2003) Mutagenicity, toxicity and repair of DNA base damage induced by oxidation. *Mutat Res Fundam Mol Mech Mutagen* 531: 37–80

Blackford AN & Jackson SP (2017) ATM, ATR, and DNA-PK: The Trinity at the Heart of the DNA Damage Response. *Mol Cell* 66: 801–817

Bont RD & Larebeke N van (2004) Endogenous DNA damage in humans: a review of quantitative data. *Mutagenesis* 19: 169–185

Breslin C, Hornyak P, Ridley A, Rulten SL, Hanzlikova H, Oliver AW & Caldecott KW (2015) The XRCC1 phosphate-binding pocket binds poly (ADP-ribose) and is required for XRCC1 function. *Nucleic Acids Res* 43: 6934–6944

Brown MW, Kim Y, Williams GM, Huck JD, Surtees JA & Finkelstein IJ (2016) Dynamic DNA binding licenses a repair factor to bypass roadblocks in search of DNA lesions. *Nat Commun* 7: 10607

Budzowska M, Graham TG, Sobeck A, Waga S & Walter JC (2015) Regulation of the Rev1–pol ζ complex during bypass of a DNA interstrand cross-link. *Embo J* 34: 1971–1985

Cadet J, Douki T & Ravanat J-L (2010) Oxidatively generated base damage to cellular DNA. *Free Radical Bio Med* 49: 9–21

Calin GA, Iasio MG di, Caprini E, Vorechovsky I, Natali PG, Sozzi G, Croce CM, Barbanti-Brodano G, Russo G & Negrini M (2000) Low frequency of alterations of the α (PPP2R1A) and β (PPP2R1B) isoforms of the subunit A of the serine-threonine phosphatase 2A in human neoplasms. *Oncogene* 19: 1191–1195

Carr AM (1995) DNA structure checkpoints in fission yeast. *Semin Cell Biol* 6: 65–72

Castor D, Nair N, Déclais A-C, Lachaud C, Toth R, Macartney TJ, Lilley DMJ, Arthur JSC & Rouse J (2013) Cooperative Control of Holliday Junction Resolution and DNA Repair by the SLX1 and MUS81-EME1 Nucleases. *Mol Cell* 52: 221–233

Cathcart R, Schwiers E, Saul RL & Ames BN (1984) Thymine glycol and thymidine glycol in human and rat urine: a possible assay for oxidative DNA damage. *Proc National Acad Sci* 81: 5633–5637

Centurion SA, Kuo H-R & Lambert WC (2000) Damage-Resistant DNA Synthesis in Fanconi Anemia Cells Treated with a DNA Cross-Linking Agent. *Exp Cell Res* 260: 216–221

Chatterjee N & Walker GC (2017) Mechanisms of DNA damage, repair, and mutagenesis. *Environ Mol Mutagen* 58: 235–263

Chen DS, Herman T & Demple B (1991) Two distinct human DNA diesterases that hydrolyze 3'-blocking deoxyribose fragments from oxidized DNA. *Nucleic Acids Res* 19: 5907–5914

Chen H, Xu J, Wang P, Shu Q, Huang L, Guo J, Zhang X, Zhang H, Wang Y, Shen Z, *et al* (2019) Protein phosphatase 2 regulatory subunit B''Alpha silencing inhibits tumor cell proliferation in liver cancer. *Cancer Med-us* 8: 7741–7753

Cheng KC, Cahill DS, Kasai H, Nishimura S & Loeb LA (1992) 8-Hydroxyguanine, an abundant form of oxidative DNA damage, causes G-T and A-C substitutions. *J Biol Chem* 267: 166–172

Cheung RS, Castella M, Abeyta A, Gafken PR, Tucker N & Taniguchi T (2017) Ubiquitination-Linked Phosphorylation of the FANCI S/TQ Cluster Contributes to Activation of the Fanconi Anemia I/D2 Complex. *Cell Reports* 19: 2432–2440

Cho Y-J, Kozekov ID, Harris TM, Rizzo CJ & Stone MP (2007) Stereochemistry modulates the stability of reduced interstrand cross-links arising from R- and S-alpha-CH3-gamma-OH-1,N2-propano-2'-deoxyguanosine in the 5'-CpG-3' DNA sequence. *Biochemistry-us* 46: 2608–21

Chowdhury D, Keogh M-C, Ishii H, Peterson CL, Buratowski S & Lieberman J (2005) γ-H2AX Dephosphorylation by Protein Phosphatase 2A Facilitates DNA Double-Strand Break Repair. *Mol Cell* 20: 801–809

Chowdhury D, Xu X, Zhong X, Ahmed F, Zhong J, Liao J, Dykxhoorn DM, Weinstock DM, Pfeifer GP & Lieberman J (2008) A PP4-Phosphatase Complex Dephosphorylates γ-H2AX Generated during DNA Replication. *Mol Cell* 31: 33–46

Ciccia A & Elledge SJ (2010) The DNA Damage Response: Making It Safe to Play with Knives. *Mol Cell* 40: 179–204

Ciccia A, Ling C, Coulthard R, Yan Z, Xue Y, Meetei AR, Laghmani EH, Joenje H, McDonald N, Winter JP de, *et al* (2007) Identification of FAAP24, a Fanconi Anemia Core Complex Protein that Interacts with FANCM. *Mol Cell* 25: 331–343

Cimino GD, Gamper HB, Isaacs ST & Hearst JE (1985) Psoralens as Photoactive Probes of Nucleic Acid Structure and Function: Organic Chemistry, Photochemistry, and Biochemistry. *Annu Rev Biochem* 54: 1151–1193

Cohn MA, Kowal P, Yang K, Haas W, Huang TT, Gygi SP & D'Andrea AD (2007) A UAF1-Containing Multisubunit Protein Complex Regulates the Fanconi Anemia Pathway. *Mol Cell* 28: 786–797

Coste F, Malinge J-M, Serre L, Leng M, Zelwer C, Shepard W & Roth M (1999) Crystal structure of a double-stranded DNA containing a cisplatin interstrand cross-link at 1.63 Å resolution: Hydration at the platinated site. *Nucleic Acids Res* 27: 1837–1846

Creyghton MP, Roël G, Eichhorn PJA, Vredeveld LC, Destrée O & Bernards R (2006) PR130 is a modulator of the Wnt-signaling cascade that counters repression of the antagonist Naked cuticle. *Proc National Acad Sci* 103: 5397–5402

Daley JM, Jimenez-Sainz J, Wang W, Miller AS, Xue X, Nguyen KA, Jensen RB & Sung P (2017) Enhancement of BLM-DNA2-Mediated Long-Range DNA End Resection by CtIP. *Cell Reports* 21: 324–332

Demin AA, Hirota K, Tsuda M, Adamowicz M, Hailstone R, Brazina J, Gittens W, Kalasova I, Shao Z, Zha S, *et al* (2021) XRCC1 prevents toxic PARP1 trapping during DNA base excision repair. *Mol Cell* 81: 3018-3030.e5

Demple B, Herman T & Chen DS (1991) Cloning and expression of APE, the cDNA encoding the major human apurinic endonuclease: definition of a family of DNA repair enzymes. *Proc National Acad Sci* 88: 11450–11454

Ding Q, Reddy YVR, Wang W, Woods T, Douglas P, Ramsden DA, Lees-Miller SP & Meek K (2003) Autophosphorylation of the catalytic subunit of the DNA-dependent protein kinase is required for efficient end processing during DNA double-strand break repair. *Mol Cell Biol* 23: 5836–48

Dizdaroglu M, Coskun E & Jaruga P (2017) Repair of oxidatively induced DNA damage by DNA glycosylases: Mechanisms of action, substrate specificities and excision kinetics. *Mutat Res Rev Mutat Res* 771: 99–127

Dong H, Nebert DW, Bruford EA, Thompson DC, Joenje H & Vasiliou V (2015) Update of the human and mouse Fanconi anemia genes. *Hum Genomics* 9: 32

Douglas P, Moorhead GBG, Ye R & Lees-Miller SP (2001) Protein Phosphatases Regulate DNA-dependent Protein Kinase Activity*. *J Biol Chem* 276: 18992–18998

Douwel DK, Hoogenboom WS, Boonen RA & Knipscheer P (2017) Recruitment and positioning determine the specific role of the XPF-ERCC1 endonuclease in interstrand crosslink repair. *Embo J* 36: 2034–2046

Dupont WD, Breyer JP, Bradley KM, Schuyler PA, Plummer WD, Sanders ME, Page DL & Smith JR (2010) Protein phosphatase 2A subunit gene haplotypes and proliferative breast disease modify breast cancer risk. *Cancer* 116: 8–19

Durocher D, Henckel J, Fersht AR & Jackson SP (1999) The FHA Domain Is a Modular Phosphopeptide Recognition Motif. *Mol Cell* 4: 387–394

Dutertre S, Sekhri R, Tintignac LA, Onclercq-Delic R, Chatton B, Jaulin C & Amor-Guéret M (2002) Dephosphorylation and Subcellular Compartment Change of the Mitotic Bloom's Syndrome DNA Helicase in Response to Ionizing Radiation*. *J Biol Chem* 277: 6280–6286

Dutrillaux B, Aurias A, Dutrillaux A-M, Buriot D & Prieur M (1982) The cell cycle of lymphocytes in Fanconi anemia. *Hum Genet* 62: 327–332

Dzulko M, Pons M, Henke A, Schneider G & Krämer OH (2020) The PP2A subunit PR130 is a key regulator of cell development and oncogenic transformation. *Biochimica Et Biophysica Acta Bba - Rev Cancer* 1874: 188453

Eichhorn PJA, Creyghton MP & Bernards R (2009) Protein phosphatase 2A regulatory subunits and cancer. *Biochimica Et Biophysica Acta Bba - Rev Cancer* 1795: 1–15

Eustermann S, Videler H, Yang J-C, Cole PT, Gruszka D, Veprintsev D & Neuhaus D (2011) The DNA-Binding Domain of Human PARP-1 Interacts with DNA Single-Strand Breaks as a Monomer through Its Second Zinc Finger. *J Mol Biol* 407: 149–170

Fellner T, Lackner DH, Hombauer H, Piribauer P, Mudrak I, Zaragoza K, Juno C & Ogris E (2003) A novel and essential mechanism determining specificity and activity of protein phosphatase 2A (PP2A) in vivo. *Gene Dev* 17: 2138–2150

Feng J, Wakeman T, Yong S, Wu X, Kornbluth S & Wang X-F (2009) Protein Phosphatase 2A-Dependent Dephosphorylation of Replication Protein A Is Required for the Repair of DNA Breaks Induced by Replication Stress. *Mol Cell Biol* 29: 5696–5709

Fishel R & Lee J-B (2016) DNA Replication, Recombination, and Repair, Molecular Mechanisms and Pathology. 305–339

Flegg CP, Sharma M, Medina-Palazon C, Jamieson C, Galea M, Brocardo MG, Mills K & Henderson BR (2010) Nuclear export and centrosome targeting of the protein phosphatase 2A subunit B56alpha: role of B56alpha in nuclear export of the catalytic subunit. *J Biological Chem* 285: 18144–54

Forester CM, Maddox J, Louis JV, Goris J & Virshup DM (2007) Control of mitotic exit by PP2A regulation of Cdc25C and Cdk1. *Proc National Acad Sci* 104: 19867–19872

Fortini P, Parlanti E, Sidorkina OM, Laval J & Dogliotti E (1999) The Type of DNA Glycosylase Determines the Base Excision Repair Pathway in Mammalian Cells*. *J Biol Chem* 274: 15230–15236

Fousteri M & Mullenders LH (2008) Transcription-coupled nucleotide excision repair in mammalian cells: molecular mechanisms and biological effects. *Cell Res* 18: 73–84

Freeman AK & Monteiro AN (2010) Phosphatases in the cellular response to DNA damage. *Cell Commun Signal* 8: 27

Fujiki H & Suganuma M (1993) Tumor promotion by inhibitors of protein phosphatases 1 and 2A: the okadaic acid class of compounds. *Adv Cancer Res* 61: 143–94

Fullbright G, Rycenga HB, Gruber JD & Long DT (2016) p97 Promotes a Conserved Mechanism of Helicase Unloading during DNA Cross-Link Repair. *Mol Cell Biol* 36: 2983–2994

Garaycoechea JI, Crossan GP, Langevin F, Daly M, Arends MJ & Patel KJ (2012) Genotoxic consequences of endogenous aldehydes on mouse haematopoietic stem cell function. *Nature* 489: 571–575

Garcia L, Garcia F, Llorens F, Unzeta M, Itarte E & Gómez N (2002) PP1/PP2A phosphatases inhibitors okadaic acid and calyculin A block ERK5 activation by growth factors and oxidative stress. *Febs Lett* 523: 90–94

Garcia-Higuera I, Taniguchi T, Ganesan S, Meyn MS, Timmers C, Hejna J, Grompe M & D'Andrea AD (2001) Interaction of the Fanconi Anemia Proteins and BRCA1 in a Common Pathway. *Mol Cell* 7: 249–262

Gari K, Décaillet C, Delannoy M, Wu L & Constantinou A (2008a) Remodeling of DNA replication structures by the branch point translocase FANCM. *Proc National Acad Sci* 105: 16107–16112

Gari K, Décaillet C, Stasiak AZ, Stasiak A & Constantinou A (2008b) The Fanconi Anemia Protein FANCM Can Promote Branch Migration of Holliday Junctions and Replication Forks. *Mol Cell* 29: 141–148

Gharbi-Ayachi A, Labbé J-C, Burgess A, Vigneron S, Strub J-M, Brioudes E, Van-Dorsselaer A, Castro A & Lorca T (2010) The Substrate of Greatwall Kinase, Arpp19, Controls Mitosis by Inhibiting Protein Phosphatase 2A. *Science* 330: 1673–1677

Ghezraoui H, Piganeau M, Renouf B, Renaud J-B, Sallmyr A, Ruis B, Oh S, Tomkinson AE, Hendrickson EA, Giovannangeli C, *et al* (2014) Chromosomal Translocations in Human Cells Are Generated by Canonical Nonhomologous End-Joining. *Mol Cell* 55: 829–842

Ghosh S (2019) Cisplatin: The First Metal Based Anticancer Drug. *Bioorg Chem* 88: 102925

Göder A, Emmerich C, Nikolova T, Kiweler N, Schreiber M, Kühl T, Imhof D, Christmann M, Heinzel T, Schneider G, *et al* (2018) HDAC1 and HDAC2 integrate checkpoint kinase phosphorylation and cell fate through the phosphatase-2A subunit PR130. *Nat Commun* 9: 764

Goldberg J, Huang H, Kwon Y, Greengard P, Nairn AC & Kuriyan J (1995) Three-dimensional structure of the catalytic subunit of protein serine/threonine phosphatase-1. *Nature* 376: 745–753

Götz J, Probst A, Ehler E, Hemmings B & Kues W (1998) Delayed embryonic lethality in mice lacking protein phosphatase 2A catalytic subunit Cα. *Proc National Acad Sci* 95: 12370–12375

Grompe M & D'Andrea A (2001) Fanconi anemia and DNA repair. *Hum Mol Genet* 10: 2253–2259

Grundmann-Kollmann M, Ludwig R, Zollner TM, Ochsendorf F, Thaci D, Boehncke W-H, Krutmann J, Kaufmann R & Podda M (2004) Narrowband UVB and cream psoralen-UVA combination therapy for plaque-type psoriasis. *J Am Acad Dermatol* 50: 734–739

Grundy GJ & Parsons JL (2020) Base excision repair and its implications to cancer therapy. *Essays Biochem* 64: 831–843

Guo F, Stanevich V, Wlodarchak N, Sengupta R, Jiang L, Satyshur KA & Xing Y (2014) Structural basis of PP2A activation by PTPA, an ATP-dependent activation chaperone. *Cell Res* 24: 190–203

Harper JW & Elledge SJ (2007) The DNA Damage Response: Ten Years After. *Mol Cell* 28: 739–745

Heijden T van der, Modesti M, Hage S, Kanaar R, Wyman C & Dekker C (2008) Homologous Recombination in Real Time: DNA Strand Exchange by RecA. *Mol Cell* 30: 530–538

Hendrix P, Mayer-Jackel RE, Cron P, Goris J, Hofsteenge J, Merlevede W & Hemmings BA (1993) Structure and expression of a 72-kDa regulatory subunit of protein phosphatase 2A. Evidence for different size forms produced by alternative splicing. *J Biological Chem* 268: 15267–76

Hira A, Yabe H, Yoshida K, Okuno Y, Shiraishi Y, Chiba K, Tanaka H, Miyano S, Nakamura J, Kojima S, *et al* (2013) Variant ALDH2 is associated with accelerated progression of bone marrow failure in Japanese Fanconi anemia patients. *Blood* 122: 3206–3209

Hodskinson MR, Bolner A, Sato K, Kamimae-Lanning AN, Rooijers K, Witte M, Mahesh M, Silhan J, Petek M, Williams DM, *et al* (2020) Alcohol-derived DNA crosslinks are repaired by two distinct mechanisms. *Nature* 579: 603–608

Hombauer H, Weismann D, Mudrak I, Stanzel C, Fellner T, Lackner DH & Ogris E (2007) Generation of Active Protein Phosphatase 2A Is Coupled to Holoenzyme Assembly. *Plos Biol* 5: e155

Hoogenboom WS, Douwel DK & Knipscheer P (2017) Xenopus egg extract: A powerful tool to study genome maintenance mechanisms. *Dev Biol* 428: 300–309

Huang J, Liu S, Bellani MA, Thazhathveetil AK, Ling C, de Winter JP, Wang Y, Wang W & Seidman MM (2013) The DNA Translocase FANCM/MHF Promotes Replication Traverse of DNA Interstrand Crosslinks. *Mol Cell* 52: 434–446

Huen MS & Chen J (2008) The DNA damage response pathways: at the crossroad of protein modifications. *Cell Res* 18: 8–16

Hunt T (2013) On the regulation of protein phosphatase 2A and its role in controlling entry into and exit from mitosis. *Adv Biological Regul* 53: 173–178

Ijsselsteijn R, Jansen JG & Wind N de (2020) DNA mismatch repair-dependent DNA damage responses and cancer. *Dna Repair* 93: 102923

Ishiai M, Kitao H, Smogorzewska A, Tomida J, Kinomura A, Uchida E, Saberi A, Kinoshita E, Kinoshita-Kikuta E, Koike T, *et al* (2008) FANCI phosphorylation functions as a molecular switch to turn on the Fanconi anemia pathway. *Nat Struct Mol Biol* 15: 1138–1146

Ishihara H, Martin BL, Brautigan DL, Karaki H, Ozaki H, Kato Y, Fusetani N, Watabe S, Hashimoto K, Uemura D, *et al* (1989) Calyculin A and okadaic acid: Inhibitors of protein phosphatase activity. *Biochem Bioph Res Co* 159: 871–877

Jacobs AL & Schär P (2012) DNA glycosylases: in DNA repair and beyond. *Chromosoma* 121: 1–20

Jamieson ER & Lippard SJ (1999) Structure, Recognition, and Processing of Cisplatin−DNA Adducts. *Chem Rev* 99: 2467–2498

Janssens V & Goris J (2001) Protein phosphatase 2A: a highly regulated family of serine/threonine phosphatases implicated in cell growth and signalling. *Biochem J* 353: 417–39

Janssens V, Zwaenepoel K, Rossé C, Petit MMR, Goris J & Parker PJ (2016) PP2A binds to the LIM domains of lipoma-preferred partner through its PR130/B″ subunit to regulate cell adhesion and migration. *J Cell Sci* 129: 1605–1618

Jantz D & Berg JM (2004) Reduction in DNA-binding affinity of Cys2His2 zinc finger proteins by linker phosphorylation. *Proc National Acad Sci* 101: 7589–7593

Jeong AL & Yang Y (2013) PP2A function toward mitotic kinases and substrates during the cell cycle. *Bmb Rep* 46: 289–294

Joo W, Xu G, Persky NS, Smogorzewska A, Rudge DG, Buzovetsky O, Elledge SJ & Pavletich NP (2011) Structure of the FANCI-FANCD2 Complex: Insights into the Fanconi Anemia DNA Repair Pathway. *Science* 333: 312–316

Jordens J, Janssens V, Longin S, Stevens I, Martens E, Bultynck G, Engelborghs Y, Lescrinier E, Waelkens E, Goris J, *et al* (2006) The Protein Phosphatase 2A Phosphatase Activator Is a Novel Peptidyl-Prolyl cis/trans-Isomerase*. *J Biol Chem* 281: 6349–6357

Kaiser TN, Lojewski A, Dougherty C, Juergens L, Sahar E & Latt SA (1982) Flow cytometric characterization of the response of Fanconi's anemia cells to mitomycin C treatment. *Cytometry* 2: 291–297

Kato N, Kawasoe Y, Williams H, Coates E, Roy U, Shi Y, Beese LS, Schärer OD, Yan H, Gottesman ME, *et al* (2017) Sensing and Processing of DNA Interstrand Crosslinks by the Mismatch Repair Pathway. *Cell Reports* 21: 1375–1385

Khew-Goodall Y & Hemmings BA (1988) Tissue-specific expression of mRNAs encoding alpha- and beta-catalytic subunits of protein phosphatase 2A. *Febs Lett* 238: 265–8

Kim H, Huang J & Chen J (2007) CCDC98 is a BRCA1-BRCT domain–binding protein involved in the DNA damage response. *Nat Struct Mol Biol* 14: 710–715

Klein Douwel D, Boonen RACM, Long DT, Szypowska AA, Räschle M, Walter JC & Knipscheer P (2014) XPF-ERCC1 Acts in Unhooking DNA Interstrand Crosslinks in Cooperation with FANCD2 and FANCP/SLX4. *Mol Cell* 54: 460–471

Knipscheer P, Räschle M, Schärer OD & Walter JC (2012) Replication-coupled DNA interstrand cross-link repair in Xenopus egg extracts. *Methods Mol Biology Clifton N J* 920: 221–43

Kolodner R (1996) Biochemistry and genetics of eukaryotic mismatch repair. *Gene Dev* 10: 1433–1442

Kolupaeva V & Janssens V (2013) PP1 and PP2A phosphatases – cooperating partners in modulating retinoblastoma protein activation. *Febs J* 280: 627–643

Kumar V, Alt FW & Frock RL (2016) PAXX and XLF DNA repair factors are functionally redundant in joining DNA breaks in a G1-arrested progenitor B-cell line. *Proc National Acad Sci* 113: 10619–10624

Kunkel TA (2004) DNA Replication Fidelity*. *J Biol Chem* 279: 16895–16898

Kuraoka I, Kobertz WR, Ariza RR, Biggerstaff M, Essigmann JM & Wood RD (2000) Repair of an Interstrand DNA Cross-link Initiated by ERCC1-XPF Repair/Recombination Nuclease*. *J Biol Chem* 275: 26632–26636

Kurimchak A & Grana X (2012) PP2A Counterbalances Phosphorylation of pRB and Mitotic Proteins by Multiple CDKs: Potential Implications for PP2A Disruption in Cancer. *Genes Cancer* 3: 739–748

Kusakabe M, Onishi Y, Tada H, Kurihara F, Kusao K, Furukawa M, Iwai S, Yokoi M, Sakai W & Sugasawa K (2019) Mechanism and regulation of DNA damage recognition in nucleotide excision repair. *Genes Environ* 41: 2

Lai C, Cao H, Hearst JE, Corash L, Luo H & Wang Y (2008) Quantitative Analysis of DNA Interstrand Cross-Links and Monoadducts Formed in Human Cells Induced by Psoralens and UVA Irradiation. *Anal Chem* 80: 8790–8798

Langerak P, Mejia-Ramirez E, Limbo O & Russell P (2011) Release of Ku and MRN from DNA Ends by Mre11 Nuclease Activity and Ctp1 Is Required for Homologous Recombination Repair of Double-Strand Breaks. *Plos Genet* 7: e1002271

Langevin F, Crossan GP, Rosado IV, Arends MJ & Patel KJ (2011) Fancd2 counteracts the toxic effects of naturally produced aldehydes in mice. *Nature* 475: 53–58

Lans H, Hoeijmakers JHJ, Vermeulen W & Marteijn JA (2019) The DNA damage response to transcription stress. *Nat Rev Mol Cell Bio* 20: 766–784

Lee D-H, Pan Y, Kanner S, Sung P, Borowiec JA & Chowdhury D (2010) A PP4 phosphatase complex dephosphorylates RPA2 to facilitate DNA repair via homologous recombination. *Nat Struct Mol Biol* 17: 365–372

Lee Y, Choi I, Kim J & Kim K (2016) DNA damage to human genetic disorders with neurodevelopmental defects. *J Genetic Medicine* 13: 1–13

Lempiäinen H & Halazonetis TD (2009) Emerging common themes in regulation of PIKKs and PI3Ks. *Embo J* 28: 3067–3073

Lescale C, Hasse HL, Blackford AN, Balmus G, Bianchi JJ, Yu W, Bacoccina L, Jarade A, Clouin C, Sivapalan R, *et al* (2016) Specific Roles of XRCC4 Paralogs PAXX and XLF during V(D)J Recombination. *Cell Reports* 16: 2967–2979

Leyns L & Gonzalez L (2012) Embryogenesis.

Li G-M (2008) Mechanisms and functions of DNA mismatch repair. *Cell Res* 18: 85–98

Li N, Wang J, Wallace SS, Chen J, Zhou J & D'Andrea AD (2020) Cooperation of the NEIL3 and Fanconi anemia/BRCA pathways in interstrand crosslink repair. *Nucleic Acids Res* 48: 3014–3028

Liang C-C, Li Z, Lopez-Martinez D, Nicholson WV, Vénien-Bryan C & Cohn MA (2016) The FANCD2–FANCI complex is recruited to DNA interstrand crosslinks before monoubiquitination of FANCD2. *Nat Commun* 7: 12124

Liang C-C, Zhan B, Yoshikawa Y, Haas W, Gygi SP & Cohn MA (2015) UHRF1 Is a Sensor for DNA Interstrand Crosslinks and Recruits FANCD2 to Initiate the Fanconi Anemia Pathway. *Cell Reports* 10: 1947–1956

Lieber MR (1997) The FEN-1 family of structure-specific nucleases in eukaryotic dna replication, recombination and repair. *Bioessays* 19: 233–240

Limbo O, Chahwan C, Yamada Y, Bruin RAM de, Wittenberg C & Russell P (2007) Ctp1 Is a Cell-Cycle-Regulated Protein that Functions with Mre11 Complex to Control Double-Strand Break Repair by Homologous Recombination. *Mol Cell* 28: 134–146

Lin L-S, Wang J-F, Song J, Liu Y, Zhu G, Dai Y, Shen Z, Tian R, Song J, Wang Z, *et al* (2019) Cooperation of endogenous and exogenous reactive oxygen species induced by zinc peroxide nanoparticles to enhance oxidative stress-based cancer therapy. *Theranostics* 9: 7200–7209

Litchfield DW (2002) Protein kinase CK2: structure, regulation and role in cellular decisions of life and death. *Biochem J* 369: 1–15

Liu D, Keijzers G & Rasmussen LJ (2017) DNA mismatch repair and its many roles in eukaryotic cells. *Mutat Res Rev Mutat Res* 773: 174–187

Long DT, Joukov V, Budzowska M & Walter JC (2014) BRCA1 Promotes Unloading of the CMG Helicase from a Stalled DNA Replication Fork. *Mol Cell* 56: 174–185

Longerich S, Kwon Y, Tsai M-S, Hlaing AS, Kupfer GM & Sung P (2014) Regulation of FANCD2 and FANCI monoubiquitination by their interaction and by DNA. *Nucleic Acids Res* 42: 5657–5670

LONGIN S, JORDENS J, MARTENS E, STEVENS I, JANSSENS V, RONDELEZ E, BAERE ID, DERUA R, WAELKENS E, GORIS J, *et al* (2004) An inactive protein phosphatase 2A population is associated with methylesterase and can be re-activated by the phosphotyrosyl phosphatase activator. *Biochem J* 380: 111–119

Lopez-Martinez (2018) Characterisation of novel phosphorylation sites on FANCD2 and their role in the Fanconi anaemia pathway.

Lopez-Martinez D, Kupculak M, Yang D, Yoshikawa Y, Liang C-C, Wu R, Gygi SP & Cohn MA (2019) Phosphorylation of FANCD2 Inhibits the FANCD2/FANCI Complex and Suppresses the Fanconi Anemia Pathway in the Absence of DNA Damage. *Cell Reports* 27: 2990-3005.e5

Lopez-Martinez D, Liang C-C & Cohn MA (2016) Cellular response to DNA interstrand crosslinks: the Fanconi anemia pathway. *Cell Mol Life Sci* 73: 3097–3114

Lovejoy CA & Cortez D (2009) Common mechanisms of PIKK regulation. *Dna Repair* 8: 1004–1008

Lu K, Collins LB, Ru H, Bermudez E & Swenberg JA (2010) Distribution of DNA Adducts Caused by Inhaled Formaldehyde Is Consistent with Induction of Nasal Carcinoma but Not Leukemia. *Toxicol Sci* 116: 441–451

Malinge J-M, Pérez C & Leng M (1994) Base sequence-independent distortions induced by interstrand cross-links in cis -diamminedichloroplatinum (ll)-modified DNA. *Nucleic Acids Res* 22: 3834–3839

Manke IA, Lowery DM, Nguyen A & Yaffe MB (2003) BRCT Repeats As Phosphopeptide-Binding Modules Involved in Protein Targeting. *Science* 302: 636–639

Maréchal A & Zou L (2013) DNA Damage Sensing by the ATM and ATR Kinases. *Csh Perspect Biol* 5: a012716

Marnett LJ, Riggins JN & West JD (2003) Endogenous generation of reactive oxidants and electrophiles and their reactions with DNA and protein. *J Clin Invest* 111: 583–593

Marteijn JA, Lans H, Vermeulen W & Hoeijmakers JHJ (2014) Understanding nucleotide excision repair and its roles in cancer and ageing. *Nat Rev Mol Cell Bio* 15: 465–481

Martín-López JV & Fishel R (2013) The mechanism of mismatch repair and the functional analysis of mismatch repair defects in Lynch syndrome. *Fam Cancer* 12: 159–168

Matsumoto Y & Kim K (1995) Excision of Deoxyribose Phosphate Residues by DNA Polymerase β During DNA Repair. *Science* 269: 699–702

Matsuoka S, Ballif BA, Smogorzewska A, III ERM, Hurov KE, Luo J, Bakalarski CE, Zhao Z, Solimini N, Lerenthal Y, *et al* (2007) ATM and ATR Substrate Analysis Reveals Extensive Protein Networks Responsive to DNA Damage. *Science* 316: 1160–1166

Matsuoka S, Huang M & Elledge SJ (1998) Linkage of ATM to Cell Cycle Regulation by the Chk2 Protein Kinase. *Science* 282: 1893–1897

McElhinny SAN, Snowden CM, McCarville J & Ramsden DA (2000) Ku Recruits the XRCC4-Ligase IV Complex to DNA Ends. *Mol Cell Biol* 20: 2996–3003

Meetei AR, Winter JP de, Medhurst AL, Wallisch M, Waisfisz Q, Vrugt HJ van de, Oostra AB, Yan Z, Ling C, Bishop CE, *et al* (2003) A novel ubiquitin ligase is deficient in Fanconi anemia. *Nat Genet* 35: 165–170

Menolfi D & Zha S (2020) ATM, ATR and DNA-PKcs kinases—the lessons from the mouse models: inhibition ≠ deletion. *Cell Biosci* 10: 8

Mi J & Kupfer GM (2005) The Fanconi anemia core complex associates with chromatin during S phase. *Blood* 105: 759–766

Mimitou EP & Symington LS (2008) Sae2, Exo1 and Sgs1 collaborate in DNA double-strand break processing. *Nature* 455: 770–774

Mochida S, Ikeo S, Gannon J & Hunt T (2009) Regulated activity of PP2A-B55 delta is crucial for controlling entry into and exit from mitosis in Xenopus egg extracts. *Embo J* 28: 2777–85

Mochida S, Maslen SL, Skehel M & Hunt T (2010) Greatwall phosphorylates an inhibitor of protein phosphatase 2A that is essential for mitosis. *Sci New York N Y* 330: 1670–3

Modrich P & Lahue R (1996) Mismatch Repair in Replication Fidelity, Genetic Recombination, and Cancer Biology. *Annu Rev Biochem* 65: 101–133

Moorhead GBG, Trinkle-Mulcahy L & Ulke-Lemée A (2007) Emerging roles of nuclear protein phosphatases. *Nat Rev Mol Cell Bio* 8: 234–244

Moreno OM, Paredes AC, Suarez-Obando F & Rojas A (2021) An update on Fanconi anemia: Clinical, cytogenetic and molecular approaches (Review). *Biomed Reports* 15: 74

Motnenko A, Liang C-C, Yang D, Lopez-Martinez D, Yoshikawa Y, Zhan B, Ward KE, Tian J, Haas W, Spingardi P, *et al* (2018) Identification of UHRF2 as a novel DNA interstrand crosslink sensor protein. *Plos Genet* 14: e1007643

Mouw KW & D'Andrea AD (2014) Crosstalk between the nucleotide excision repair and Fanconi anemia/BRCA pathways. *Dna Repair* 19: 130–134

Muniandy PA, Liu J, Majumdar A, Liu S & Seidman MM (2009) DNA interstrand crosslink repair in mammalian cells: step by step. *Crit Rev Biochem Mol* 45: 23–49

Murina O, von Aesch C, Karakus U, Ferretti LP, Bolck HA, Hänggi K & Sartori AA (2014) FANCD2 and CtIP Cooperate to Repair DNA Interstrand Crosslinks. *Cell Reports* 7: 1030–1038

Nakamura K, Saredi G, Becker JR, Foster BM, Nguyen NV, Beyer TE, Cesa LC, Faull PA, Lukauskas S, Frimurer T, *et al* (2019) H4K20me0 recognition by BRCA1–BARD1 directs homologous recombination to sister chromatids. *Nat Cell Biol* 21: 311–318

Nematullah M, Hoda MN & Khan F (2018) Protein Phosphatase 2A: a Double-Faced Phosphatase of Cellular System and Its Role in Neurodegenerative Disorders. *Mol Neurobiol* 55: 1750–1761

Nijman SMB, Huang TT, Dirac AMG, Brummelkamp TR, Kerkhoven RM, D'Andrea AD & Bernards R (2005) The Deubiquitinating Enzyme USP1 Regulates the Fanconi Anemia Pathway. *Mol Cell* 17: 331–339

Nimonkar AV, Genschel J, Kinoshita E, Polaczek P, Campbell JL, Wyman C, Modrich P & Kowalczykowski SC (2011) BLM–DNA2–RPA–MRN and EXO1–BLM–RPA–MRN constitute two DNA end resection machineries for human DNA break repair. *Gene Dev* 25: 350–362

Oestergaard VH, Langevin F, Kuiken HJ, Pace P, Niedzwiedz W, Simpson LJ, Ohzeki M, Takata M, Sale JE & Patel KJ (2007) Deubiquitination of FANCD2 Is Required for DNA Crosslink Repair. *Mol Cell* 28: 798–809

Pang Q & Andreassen PR (2009) Fanconi anemia proteins and endogenous stresses. *Mutat Res Fundam Mol Mech Mutagen* 668: 42–53

Park W-H, Margossian S, Horwitz AA, Simons AM, D'Andrea AD & Parvin JD (2005) Direct DNA Binding Activity of the Fanconi Anemia D2 Protein*. *J Biol Chem* 280: 23593–23598

Parsons JL & Dianov GL (2013) Co-ordination of base excision repair and genome stability. *Dna Repair* 12: 326–333

Pećina-Šlaus N, Kafka A, Salamon I & Bukovac A (2020) Mismatch Repair Pathway, Genome Stability and Cancer. *Frontiers Mol Biosci* 7: 122

Pichierri P & Rosselli F (2004) The DNA crosslink-induced S-phase checkpoint depends on ATR–CHK1 and ATR–NBS1–FANCD2 pathways. *Embo J* 23: 1178–1187

Prasad R, Dianov GL, Bohr VA & Wilson SH (2000) FEN1 Stimulation of DNA Polymerase β Mediates an Excision Step in Mammalian Long Patch Base Excision Repair*. *J Biol Chem* 275: 4460–4466

Prindle MJ & Loeb LA (2012) DNA polymerase delta in dna replication and genome maintenance. *Environ Mol Mutagen* 53: 666–682

Punatar RS, Martin MJ, Wyatt HDM, Chan YW & West SC (2017) Resolution of single and double Holliday junction recombination intermediates by GEN1. *Proc National Acad Sci* 114: 443–450

Rajendra E, Oestergaard VH, Langevin F, Wang M, Dornan GL, Patel KJ & Passmore LA (2014) The Genetic and Biochemical Basis of FANCD2 Monoubiquitination. *Mol Cell* 54: 858–869

Ramos F, Villoria MT, Alonso-Rodríguez E & Clemente-Blanco A (2019) Role of protein phosphatases PP1, PP2A, PP4 and Cdc14 in the DNA damage response. *Cell Stress* 3: 70

Ranjha L, Howard SM & Cejka P (2018) Main steps in DNA double-strand break repair: an introduction to homologous recombination and related processes. *Chromosoma* 127: 187–214

Räschle M, Knipscheer P, Knipsheer P, Enoiu M, Angelov T, Sun J, Griffith JD, Ellenberger TE, Schärer OD & Walter JC (2008) Mechanism of Replication-Coupled DNA Interstrand Crosslink Repair. *Cell* 134: 969–980

Reinhardt HC, Aslanian AS, Lees JA & Yaffe MB (2007) p53-Deficient Cells Rely on ATM- and ATR-Mediated Checkpoint Signaling through the p38MAPK/MK2 Pathway for Survival after DNA Damage. *Cancer Cell* 11: 175–189

Rennie ML, Lemonidis K, Arkinson C, Chaugule VK, Clarke M, Streetley J, Spagnolo L & Walden H (2020) Differential functions of FANCI and FANCD2 ubiquitination stabilize ID2 complex on DNA. *Embo Rep* 21: e50133

Resjö S, Oknianska A, Zolnierowicz S, Manganiello V & Degerman E (1999) Phosphorylation and activation of phosphodiesterase type 3B (PDE3B) in adipocytes in response to serine/threonine phosphatase inhibitors: deactivation of PDE3B in vitro by protein phosphatase type 2A. *Biochem J* 341 (Pt 3): 839–45

Reyes GX, Schmidt TT, Kolodner RD & Hombauer H (2015) New insights into the mechanism of DNA mismatch repair. *Chromosoma* 124: 443–462

Rink SM, Lipman R, Alley SC, Hopkins PB & Tomasz M (1996) Bending of DNA by the Mitomycin C-Induced, GpG Intrastrand Cross-Link. *Chem Res Toxicol* 9: 382–389

Robson CN & Hickson ID (1991) Isolation of cDNA clones encoding a human apurinic/apyrimidinic endonuclease that corrects DNA repair and mutagenesis defects in E. coli xth (exonuclease III) mutants. *Nucleic Acids Res* 19: 5519–23

Rocha CRR, Silva MM, Quinet A, Cabral-Neto JB & Menck CFM (2018) DNA repair pathways and cisplatin resistance: an intimate relationship. *Clinics* 73: e478s

Roques C, Coulombe Y, Delannoy M, Vignard J, Grossi S, Brodeur I, Rodrigue A, Gautier J, Stasiak AZ, Stasiak A, *et al* (2009) MRE11–RAD50–NBS1 is a critical regulator of FANCD2 stability and function during DNA double-strand break repair. *Embo J* 28: 2400–2413

Rothkamm K, Krüger I, Thompson LH & Löbrich M (2003) Pathways of DNA Double-Strand Break Repair during the Mammalian Cell Cycle. *Mol Cell Biol* 23: 5706–5715

Roy U & Schärer OD (2016) Involvement of translesion synthesis DNA polymerases in DNA interstrand crosslink repair. *Dna Repair* 44: 33–41

Sala-Trepat M, Rouillard D, Escarceller M, Laquerbe A, Moustacchi E & Papadopoulo D (2000) Arrest of S-Phase Progression Is Impaired in Fanconi Anemia Cells. *Exp Cell Res* 260: 208–215

Sancar A (2016) Mechanisms of DNA Repair by Photolyase and Excision Nuclease (Nobel Lecture). *Angewandte Chemie Int Ed* 55: 8502–8527

Saredi G, Huang H, Hammond CM, Alabert C, Bekker-Jensen S, Forne I, Reverón-Gómez N, Foster BM, Mlejnkova L, Bartke T, *et al* (2016) H4K20me0 marks post-replicative chromatin and recruits the TONSL–MMS22L DNA repair complex. *Nature* 534: 714–718

Sartorelli AC, Hodnick WF, Belcourt MF, Tomasz M, Haffty B, Fischer JJ & Rockwell S (1994) Mitomycin C: a prototype bioreductive agent. *Oncol Res* 6: 501–8

Sartori AA, Lukas C, Coates J, Mistrik M, Fu S, Bartek J, Baer R, Lukas J & Jackson SP (2007) Human CtIP promotes DNA end resection. *Nature* 450: 509–514

Sato K, Toda K, Ishiai M, Takata M & Kurumizaka H (2012) DNA robustly stimulates FANCD2 monoubiquitylation in the complex with FANCI. *Nucleic Acids Res* 40: 4553–4561

Sattler U, Frit P, Salles B & Calsou P (2003) Long-patch DNA repair synthesis during base excision repair in mammalian cells. *Embo Rep* 4: 363–367

Savitsky K, Bar-Shira A, Gilad S, Rotman G, Ziv Y, Vanagaite L, Tagle DA, Smith S, Uziel T, Sfez S, *et al* (1995) A Single Ataxia Telangiectasia Gene with a Product Similar to PI-3 Kinase. *Science* 268: 1749–1753

Schärer OD (2013) Nucleotide Excision Repair in Eukaryotes. *Csh Perspect Biol* 5: a012609

Schönthal AH (2001) Role of serine/threonine protein phosphatase 2A in cancer. *Cancer Lett* 170: 1–13

Schwarz JK, Lovly CM & Piwnica-Worms H (2003) Regulation of the Chk2 protein kinase by oligomerization-mediated cis- and trans-phosphorylation. *Mol Cancer Res Mcr* 1: 598–609

Scully R, Panday A, Elango R & Willis NA (2019) DNA double-strand break repair-pathway choice in somatic mammalian cells. *Nature Reviews Molecular Cell Biology* 20

Scully R & Xie A (2013) Double strand break repair functions of histone H2AX. *Mutat Res Fundam Mol Mech Mutagen* 750: 5–14

Semlow DR & Walter JC (2021) Mechanisms of Vertebrate DNA Interstrand Cross-Link Repair. *Annu Rev Biochem* 90: 1–29

Semlow DR, Zhang J, Budzowska M, Drohat AC & Walter JC (2016) Replication-Dependent Unhooking of DNA Interstrand Cross-Links by the NEIL3 Glycosylase. *Cell* 167: 498-511.e14

Sents W, Ivanova E, Lambrecht C, Haesen D & Janssens V (2013) The biogenesis of active protein phosphatase 2A holoenzymes: a tightly regulated process creating phosphatase specificity. *Febs J* 280: 644–661

Seshacharyulu P, Pandey P, Datta K & Batra SK (2013) Phosphatase: PP2A structural importance, regulation and its aberrant expression in cancer. *Cancer Lett* 335: 9–18

Shakeel S, Rajendra E, Alcón P, O'Reilly F, Chorev DS, Maslen S, Degliesposti G, Russo CJ, He S, Hill CH, *et al* (2019) Structure of the Fanconi anaemia monoubiquitin ligase complex. *Nature* 575: 234–237

Sharp MF, Murphy VJ, Twest SV, Tan W, Lui J, Simpson KJ, Deans AJ & Crismani W (2020) Methodology for the identification of small molecule inhibitors of the Fanconi Anaemia ubiquitin E3 ligase complex. *Sci Rep-uk* 10: 7959

Shimada M & Nakanishi M (2013) Response to DNA damage: why do we need to focus on protein phosphatases? *Frontiers Oncol* 3: 8

Singh TR, Saro D, Ali AM, Zheng X-F, Du C, Killen MW, Sachpatzidis A, Wahengbam K, Pierce AJ, Xiong Y, *et al* (2010) MHF1-MHF2, a Histone-Fold-Containing Protein Complex, Participates in the Fanconi Anemia Pathway via FANCM. *Mol Cell* 37: 879–886

Slyskova J, Sabatella M, Ribeiro-Silva C, Stok C, Theil AF, Vermeulen W & Lans H (2018) Base and nucleotide excision repair facilitate resolution of platinum drugs-induced transcription blockage. *Nucleic Acids Res* 46: 9537–9549

Sobol RW, Horton JK, Kühn R, Gu H, Singhal RK, Prasad R, Rajewsky K & Wilson SH (1996) Requirement of mammalian DNA polymerase-beta in base-excision repair. *Nature* 379: 183–6

Socha A, Yang D, Bulsiewicz A, Yaprianto K, Kupculak M, Liang C-C, Hadjicharalambous A, Wu R, Gygi SP & Cohn MA (2020) WRNIP1 Is Recruited to DNA Interstrand Crosslinks and Promotes Repair. *Cell Reports* 32: 107850

Spivak G (2015) Nucleotide excision repair in humans. *Dna Repair* 36: 13–18

Stinson BM, Moreno AT, Walter JC & Loparo JJ (2020) A Mechanism to Minimize Errors during Non-homologous End Joining. *Mol Cell* 77: 1080-1091.e8

Suganuma M, Fujiki H, Furuya-Suguri H, Yoshizawa S, Yasumoto S, Kato Y, Fusetani N & Sugimura T (1990) Calyculin A, an inhibitor of protein phosphatases, a potent tumor promoter on CD-1 mouse skin. *Cancer Res* 50: 3521–5

Suganuma M, Fujiki H, Suguri H, Yoshizawa S, Hirota M, Nakayasu M, Ojika M, Wakamatsu K, Yamada K & Sugimura T (1988) Okadaic acid: an additional non-phorbol-12-tetradecanoate-13-acetate-type tumor promoter. *Proc National Acad Sci* 85: 1768–1771

Tan W, Twest S van, Leis A, Bythell-Douglas R, Murphy VJ, Sharp M, Parker MW, Crismani W & Deans AJ (2020) Monoubiquitination by the human Fanconi anemia core complex clamps FANCI:FANCD2 on DNA in filamentous arrays. *Elife* 9: e54128

Tian Y, Paramasivam M, Ghosal G, Chen D, Shen X, Huang Y, Akhter S, Legerski R, Chen J, Seidman MM, *et al* (2015) UHRF1 Contributes to DNA Damage Repair as a Lesion Recognition Factor and Nuclease Scaffold. *Cell Reports* 10: 1957–1966

Trenner A & Sartori AA (2019) Harnessing DNA Double-Strand Break Repair for Cancer Treatment. *Frontiers Oncol* 9: 1388

Tseng L-M, Liu C-Y, Chang K-C, Chu P-Y, Shiau C-W & Chen K-F (2012) CIP2A is a target of bortezomib in human triple negative breast cancer cells. *Breast Cancer Res Bcr* 14: R68–R68

Twest S van, Murphy VJ, Hodson C, Tan W, Swuec P, O'Rourke JJ, Heierhorst J, Crismani W & Deans AJ (2017) Mechanism of Ubiquitination and Deubiquitination in the Fanconi Anemia Pathway. *Mol Cell* 65: 247–259

Unno J, Itaya A, Taoka M, Sato K, Tomida J, Sakai W, Sugasawa K, Ishiai M, Ikura T, Isobe T, *et al* (2014) FANCD2 Binds CtIP and Regulates DNA-End Resection during DNA Interstrand Crosslink Repair. *Cell Reports* 7: 1039–1047

Vaughn CM & Sancar A (2020) DNA Damage, DNA Repair and Disease: Volume 2. *Chem Biology*: 1–23

Vítor AC, Huertas P, Legube G & Almeida SF de (2020) Studying DNA Double-Strand Break Repair: An Ever-Growing Toolbox. *Frontiers Mol Biosci* 7: 24

Wallace SS (2013) DNA glycosylases search for and remove oxidized DNA bases. *Environ Mol Mutagen* 54: 691–704

Wallace SS (2014) Base excision repair: A critical player in many games. *Dna Repair* 19: 14–26

Wang AT & Smogorzewska A (2015) SnapShot: Fanconi Anemia and Associated Proteins. *Cell* 160: 354-354.e1

Wang LC, Stone S, Hoatlin ME & Gautier J (2008) Fanconi anemia proteins stabilize replication forks. *Dna Repair* 7: 1973–1981

Wang R, Wang S, Dhar A, Peralta C & Pavletich NP (2020) DNA clamp function of the monoubiquitinated Fanconi anaemia ID complex. *Nature* 580: 278–282

Wang S, Wang R, Peralta C, Yaseen A & Pavletich NP (2021) Structure of the FA core ubiquitin ligase closing the ID clamp on DNA. *Nat Struct Mol Biol* 28: 300–309

Wang Y, Leung JW, Jiang Y, Lowery MG, Do H, Vasquez KM, Chen J, Wang W & Li L (2013) FANCM and FAAP24 Maintain Genome Stability via Cooperative as Well as Unique Functions. *Mol Cell* 49: 997–1009

Warren AJ, Maccubbin AE & Hamilton JW (1998) Detection of mitomycin C-DNA adducts in vivo by 32P-postlabeling: time course for formation and removal of adducts and biochemical modulation. *Cancer Res* 58: 453–61

Wiederhold L, Leppard JB, Kedar P, Karimi-Busheri F, Rasouli-Nia A, Weinfeld M, Tomkinson AE, Izumi T, Prasad R, Wilson SH, *et al* (2003) AP endonuclease-independent DNA base excision repair in human cells. *Mol Cell* 15: 209–20

Williams HL, Gottesman ME & Gautier J (2012) Replication-Independent Repair of DNA Interstrand Crosslinks. *Mol Cell* 47: 140–147

Wlodarchak N & Xing Y (2016) PP2A as a master regulator of the cell cycle. *Crit Rev Biochem Mol* 51: 162–184

Wood RD (2010) Mammalian nucleotide excision repair proteins and interstrand crosslink repair. *Environ Mol Mutagen* 51: 520–526

Woodhouse BC, Dianova II, Parsons JL & Dianov GL (2008) Poly(ADP-ribose) polymerase-1 modulates DNA repair capacity and prevents formation of DNA double strand breaks. *Dna Repair* 7: 932–940

Wu RA, Semlow DR, Kamimae-Lanning AN, Kochenova OV, Chistol G, Hodskinson MR, Amunugama R, Sparks JL, Wang M, Deng L, *et al* (2019) TRAIP is a master regulator of DNA interstrand crosslink repair. *Nature* 567: 267–272

Wyatt HDM, Sarbajna S, Matos J & West SC (2013) Coordinated Actions of SLX1-SLX4 and MUS81-EME1 for Holliday Junction Resolution in Human Cells. *Mol Cell* 52: 234–247

Yamamoto KN, Kobayashi S, Tsuda M, Kurumizaka H, Takata M, Kono K, Jiricny J, Takeda S & Hirota K (2011) Involvement of SLX4 in interstrand cross-link repair is regulated by the Fanconi anemia pathway. *Proc National Acad Sci* 108: 6492–6496

Yan CT, Boboila C, Souza EK, Franco S, Hickernell TR, Murphy M, Gumaste S, Geyer M, Zarrin AA, Manis JP, *et al* (2007) IgH class switching and translocations use a robust non-classical end-joining pathway. *Nature* 449: 478–482

Yan Y, Cao PT, Greer PM, Nagengast ES, Kolb RH, Mumby MC & Cowan KH (2010a) Protein phosphatase 2A has an essential role in the activation of γ-irradiation-induced G2/M checkpoint response. *Oncogene* 29: 4317–4329

Yan Z, Delannoy M, Ling C, Daee D, Osman F, Muniandy PA, Shen X, Oostra AB, Du H, Steltenpool J, *et al* (2010b) A Histone-Fold Complex and FANCM Form a Conserved DNA-Remodeling Complex to Maintain Genome Stability. *Mol Cell* 37: 865–878

Yang H, Li Q, Fan J, Holloman WK & Pavletich NP (2005) The BRCA2 homologue Brh2 nucleates RAD51 filament formation at a dsDNA–ssDNA junction. *Nature* 433: 653–657

Yu X & Chen J (2004) DNA Damage-Induced Cell Cycle Checkpoint Control Requires CtIP, a Phosphorylation-Dependent Binding Partner of BRCA1 C-Terminal Domains. *Mol Cell Biol* 24: 9478–9486

Yu X, Chini CCS, He M, Mer G & Chen J (2003) The BRCT Domain Is a Phospho-Protein Binding Domain. *Science* 302: 639–642

Yuan F, Hokayem JE, Zhou W & Zhang Y (2009) FANCI Protein Binds to DNA and Interacts with FANCD2 to Recognize Branched Structures*. *J Biol Chem* 284: 24443–24452

Zha S, Guo C, Boboila C, Oksenych V, Cheng H-L, Zhang Y, Wesemann DR, Yuen G, Patel H, Goff PH, *et al* (2011) ATM damage response and XLF repair factor are functionally redundant in joining DNA breaks. *Nature* 469: 250–254

Zhang J, Dewar JM, Budzowska M, Motnenko A, Cohn MA & Walter JC (2015) DNA interstrand cross-link repair requires replication fork convergence. *Nat Struct Mol Biol* 22: 242–247

Zhang W, Yang J, Liu Y, Chen X, Yu T, Jia J & Liu C (2009) PR55 alpha, a regulatory subunit of PP2A, specifically regulates PP2A-mediated beta-catenin dephosphorylation. *J Biological Chem* 284: 22649–56

Zhao Q, Saro D, Sachpatzidis A, Singh TR, Schlingman D, Zheng X-F, Mack A, Tsai M-S, Mochrie S, Regan L, *et al* (2014) The MHF complex senses branched DNA by binding a pair of crossover DNA duplexes. *Nat Commun* 5: 2987

Zheng H, Wang X, Warren AJ, Legerski RJ, Nairn RS, Hamilton JW & Li L (2003) Nucleotide excision repair- and polymerase eta-mediated error-prone removal of mitomycin C interstrand cross-links. *Mol Cell Biol* 23: 754–61

Zheng X-F, Kalev P & Chowdhury D (2015) Emerging role of protein phosphatases changes the landscape of phospho-signaling in DNA damage response. *Dna Repair* 32: 58–65

Zhi G, Wilson JB, Chen X, Krause DS, Xiao Y, Jones NJ & Kupfer GM (2009) Fanconi Anemia Complementation Group FANCD2 Protein Serine 331 Phosphorylation Is Important for Fanconi Anemia Pathway Function and BRCA2 Interaction. *Cancer Res* 69: 8775–8783

Zwaenepoel K, Louis JV, Goris J & Janssens V (2008) Diversity in genomic organisation, developmental regulation and distribution of the murine PR72/B" subunits of protein phosphatase 2A. *Bmc Genomics* 9: 393